Defining the Essential Function of Yeast Hsf1 Reveals a Compact Transcriptional Program for Maintaining Eukaryotic Proteostasis

Defining the essential function of yeast Hsf1 reveals a compact transcriptional program for maintaining eukaryotic proteostasis

A dissertation presented

by

Eric John Solis

to

The Committee on Higher Degrees in Systems Biology

in partial fulfillment of the requirements

for the degree of

Doctor of Philosophy

in the subject of

Systems Biology

Harvard University

Cambridge, Massachusetts

February 2016

Dissertation Advisors: Vladimir Denic and Edoardo Airoldi Eric John Solis

Defining the essential function of yeast Hsf1 reveals a compact transcriptional program for maintaining eukaryotic proteostasis

Abstract

Despite its eponymous association with proteotoxic stress, heat shock factor 1 (Hsf1 in yeast and HSF1 in mammals) is required for viability of yeast and many human cancer cells, yet its essential role remains undefined. Here we show that rapid nuclear export of Hsf1 achieved in a matter of minutes by a chemical genetics approach results in cell growth arrest in a matter of hours, which was associated with massive protein aggregation and eventual cell death. Genome-wide analyses of immediate gene expression changes induced by Hsf1 nuclear export revealed a basal transcriptional program comprising 18 genes, predominately encoding chaperones and other proteostasis factors. During heat shock, Hsf1 increases the magnitude of its transcriptional program without expanding its breadth. Strikingly, engineered Hsf1-independent co-expression of just Hsp70 and Hsp90 chaperones enabled robust cell growth in the complete absence of Hsf1. A comparative genomic analysis of mammalian fibroblasts and embryonic stem cells revealed that HSF1 lacks a basal transcriptional program but still regulates a similar set of chaperone genes during heat shock. Our work demonstrates that basal chaperone gene expression is a housekeeping mechanism controlled by Hsf1 in yeast and serves as a roadmap for defining the housekeeping

function of HSF1 in many cancers. Finally, we investigate the mechanism causing age-associated inactivation of Hsf1 during replicative aging in budding yeast. Using classic and chemical-genetic tools, we demonstrate that inactivation is due to constitutive activation of the distinct General Stress Response. These experiments reveal that stress pathway crosstalk inhibits Hsf1 activation during replicative aging and under physiological stress in young cells.

Table of Contents

List of figures and tables

Acknowledgments

I would not have made it through my PhD without the help, love and support of my family, friends and colleagues.

I am especially thankful to my mom, dad and brother, all of whom were critical for getting me to grad school in the first place. I'm also forever thankful that they were always there to support and listen to me through my many struggles, even when the problems I was describing were unrelatable or unintelligibly described.

I am also unbelievably thankful for the love and support of my brilliant and sassy partner Patricia Rogers. She is without any doubt the best thing to come out of my time at Harvard and has made my life immeasurably better. She is both a match and a counter to my own ridiculousness, and her drive and perseverance push me to be a better scientist and person every day. I'm so looking forward to living and growing together, now as I crash head-on into adulthood and for the rest of our lives.

I can also say definitively that Patrick Stoddard is the second best thing to come out of my time at Harvard. Patrick is a great friend, a talented scientist and an absolutely ridiculous person. Patrick understands me and my intricacies like no other friend I have ever had, and this makes him an invaluable part of my life. I know my time in graduate school would have been so much less fun, interesting and rewarding if it weren't for him. Also, I know it would have been significantly less silly, ludicrous and off-putting to everyone else

on the periphery if Patrick weren't down the hall from me, but I'm so glad I didn't have to live in that counterfactual universe. We have spent countless hours talking about science, politics, our personal lives, and many other things that I hope never get repeated, and I have enjoyed it all so very much.

I have also been extremely fortunate for my academic advisors Vlad Denic and Edo Airoldi, along with my mentor and friend David Pincus. The three of them put an incredible amount of time into helping and guiding me as I grew as a scientist. When I reflect on the progress I've made since I started graduate school, I know that it would not have been possible without them constantly pushing me to be better. While it wasn't always fun or easy, I am so thankful for the time, energy and effort they put into me personally. They all went so far beyond what could reasonably be expected from an advisor, and even though all three were at challenging early stages of their own careers, they made an exceptional effort to help me as I started my own. I will always be thankful and grateful to Edo, Vlad and Dave for molding me into the scientist that I am today.

Finally, I'd like to thank my colleagues. First, to the amazing scientists and labmates in the Denic Lab, thank you for welcoming in a statistician who had never pipetted anything before and supporting me as I learned to do experiments and think about science rigorously. It has been an amazing experience to be surrounded by such incredible and talented scientists on a daily basis. Beyond my home lab, the O'Shea, Murray and other labs in Northwest, as well as my Systems Biology programmates, have provided an

incredible broader environment to do science in, it has been a pleasure be surrounded by such a diverse group of talented scientists during my time at Harvard.

Chapter 1: Introduction to proteostasis and the conserved Heat shock transcription factor.

Protein folding information is contained within each protein's amino acid sequence, and because of this many proteins spontaneously fold into their functional conformation *in vitro* (Anfinsen, 1973). However, in the crowded and chaotic environment of a cell, newly synthesized proteins must traverse a series of unstable intermediate folds that are prone to aggregation and therefore rely on complex chaperoning mechanisms to assist them to adopt their native fold (Dobson, 2003). Even under ideal conditions many nascent proteins randomly misfold into unstable conformations that must be rapidly cleared to prevent them from aggregating (Buchberger et al., 2010). If left unchecked, protein aggregates will precipitate toxic co-aggregation with unfolded nascent polypeptides and cellular proteins with unstructured regions causing proteotoxic collapse and cell death (Olzscha et al., 2011). Further, proteostasis must be maintained when cells are challenged by transient environmental perturbations, such as high temperature, which cause protein unfolding and acutely increase the demand for chaperones and other protein quality control factors (Richter et al., 2010).

In order to adapt when stress causes the folding environment to deteriorate, cells need a mechanism to adjust the availability of chaperones according to need. One simple mechanism employed by some bacteria to regulate expression of chaperones during heat shock involves RNA secondary structure that occludes the ribosome binding site at low

temperatures, but melts at high temperature de-repressing translation during thermal stress (Cimdins et al., 2014). However, rather than regulating each chaperone gene individually, eukaryotic cells have evolved a highly conserved feedback mechanism that coordinates up-regulation of many proteostasis factors in response to stress. The first indication of this mechanism were made by Ferruccio Ritossa in 1962 when he noticed a novel pattern of “puffs” on the polytene salivary gland chromosomes of Drosophila larvae that were subjected to a serendipitous heat shock when a co-worker increased their incubator’s temperature (Ritossa, 1996). Subsequent controlled experiments revealed that shifting larvae from 25°C to 30°C caused puffs that were stable at the lower temperature to rapidly dissipate and induced the appearance of novel, reproducible puffs (Ritossa, 1962). It was soon revealed that the temperature stress caused by the actions of an unwitting co-worker has spurred the first observation of the dramatic changes in gene expression that comprise the heat shock response.

It was subsequently revealed that chromosomal puffs, including those that Ritossa observed following heat shock, were sites of significant RNA synthesis (Ellgaard and Clever, 1971). Additionally, it was shown that heat shock caused dramatic changes in protein synthesis: most proteins that were translated pre-shock were no longer synthesized, while translation of a small set of proteins was highly induced (Tissiéres et al., 1974). Importantly, this work also noted a rough correspondence between the increase in synthesis for some proteins with the level of RNA synthesis induced at particular puff loci following heat shock. A satisfying denouement was reached when

Susan Lindquist and colleagues analyzed heat shock polysomes and found that a single mRNA accounted for the majority of post-shock translation in Drosophila, which was transcribed at the site of the major heat-induced chromosomal puff (McKenzie et al., 1975) and coded for the most strongly induced heat shock protein (the 70kD heat shock protein, or Hsp70) (McKenzie and Meselson, 1977). Together, these results demonstrated that heat shock causes a rapid reallocation of cellular gene expression and protein translation capacity to enable the preferential synthesis of a small set of Hsps over all other proteins.

Characterization of the heat shock response in a variety of model organisms has revealed that homologous heat shock proteins (HSPs) are up-regulated following temperature increase in highly diverged species (Richter et al., 2010). For example, members of the Hsp70 family are among the most strongly heat-induced proteins in bacteria, yeast and flies (Parsell and Lindquist, 1993). Biochemical analysis has reveled that HSPs primarily function as molecular chaperones. The function of some non-ATPase HSPs, including the Hsp40 family and other small HSPs, consists of binding to unfolded substrate proteins with exposed hydrophobic residues in order to shield them from the aqueous cytosol and prevent non-specific hydrophobic interactions that can cause other proteins to misfold and aggregate (Hartl et al., 2011). Alternatively, some chaperones (*e.g.*, members of the Hsp70 and Hsp90 families) are ATPases for which rounds of nucleotide binding and hydrolysis drive conformational changes in the chaperone that facilitate the folding of bound substrates (Buchberger et al., 2010; Taipale et al., 2010). Finally, many HSPs are

auxiliary factors known as co-chaperones whose diverse functions include delivering specific substrates to other HSPs, modifying chaperone activity, or scaffolding the assembly of large multi-chaperone complexes (Abrams et al., 2014; Fan et al., 2004; Lee et al., 2004; Lu and Cyr, 1998; Richter et al., 2003; Taipale et al., 2014; Terasawa et al., 2005; Wegele et al., 2003). In addition to their roles during stress, some chaperones have critical non-stress functions. For example, Hsp90 is required for the function of mammalian steroid receptors (Grad and Picard, 2007) and yeast kinases involved in the pheromone response (Louvion et al., 1998) in the absence of any extrinsic stress. In general the function of many chaperones appears to be highly conserved as, for example, expression of human Hsp90 can rescue growth of an inviable yeast mutant lacking endogenous Hsp90 (Millson et al., 2007), and function of heterologously expressed human glucocorticoid receptor (GR) in yeast is enabled by yeast Hsp90 even though there are no GR homologs in yeast (Picard et al., 1990). Taken together, these observations strongly support that the notion that the conserved function of the heat shock response that enables survival at high temperatures is to increase cellular folding capacity by coordinated up-regulation of folding chaperones.

As it became clear that the components of the heat shock response were conserved across diverse organisms, there was great interest in understanding the regulatory mechanisms that coordinated HSPs expression during stress. Intriguingly, repeats of common DNA motif, called heat shock elements (HSEs), were found in the promoter of HSP genes in diverse organisms (Morimoto, 1998; Pirkkala et al., 2001; Wu, 1995).

These motifs had a clear regulatory function as mutating the HSEs in the promoters of many heat shock protein genes prevented their up-regulation following stress, and conversely engineering HSEs into a gene's promoter was sufficient to render it heat-inducible (Bienz and Pelham, 1986). As these results held in a variety of organisms, the favored hypothesis was that a conserved HSE-binding factor regulated expression of many HSPs during heat shock. Heat shock factor (Hsf) was first purified from budding yeast using a HSE affinity purification strategy (Sorger and Pelham, 1987), against which antibodies were raised then used to isolate the *S. cerevisiae HSF* gene by screening a lambda phage yeast cDNA library (Sorger and Pelham, 1988; Wiederrecht et al., 1988). The close sequence similarity of the *S. cerevisiae* and *Kluyveromyces lactis HSF* genes facilitate facile subsequent isolation of *HSF* from this yeast species (Jakobsen and Pelham, 1991). Shortly thereafter, the Drosophila *HSF* gene was independently cloned (Clos et al., 1990), and sequence comparison of yeast and fly Hsf enabled generation of degenerate oligonucleotides against conserved residues to spur cloning of *HSF* from diverse higher eukaryotes including humans (Rabindran et al., 1991). Thus, it appeared that homologs of a single transcription factor regulate the heat shock response in diverse organisms.

Since its initial isolation, there has been intense interest in elucidating the mechanisms that regulate Hsf activity. Given that the threshold temperature for Hsf activation differed between organisms, it was unclear if this implied divergent regulatory mechanisms amongst Hsf homologs. However, the conservation of Hsf regulation was elegantly

demonstrated by showing that when human Hsf1 was transgenic expressed in Drosophila its activation temperature was reset to match endogenous Hsf (Clos et al., 1993). There are some *bona fide* differences between Hsf regulation in yeast and higher eukaryotes (Sorger et al., 1987). In yeast, Hsf is constitutively trimeric and bound to target gene promoters, and its function is essential for viability even in the absence of any stress (Jakobsen and Pelham, 1988; Sorger and Pelham, 1988). By contrast Hsf in unstressed drosophila and mammalian cells is cytoplasmic and monomeric, but becomes competent for nuclear entry, trimerization and DNA binding following stress (Sarge et al., 1993; Westwood et al., 1991). However, in spite of these differences, the core of Hsf function is conserved even between distantly related yeast and humans, as unmodified human HSF2 or a constitutively trimerized mutant of human HSF1 expressed in yeast complement the essential basal function of yeast Hsf and activate expression of yeast HSPs at a similar temperature to the endogenous homolog (Liu et al., 1997). These observations strongly suggest that Hsf is not a simpler thermometer with a set activation temperature, but rather it becomes activated in response to conserved cellular cues that are generated by stress in diverse eukaryotic species.

What are the inputs that regulate Hsf activity? The signals that lead to Hsf activation are a ubiquitous consequence of many environmental stresses, as heat shock, amino acid analogs, heavy metals, ethanol and oxidative stress cause Hsf to become activated (Sarge et al., 1993; Sorger and Pelham, 1988; Trotter et al., 2002). Misfolded proteins are a common consequence of stresses that activate Hsf, and in yeast expression of a single

misfolded mutant protein was sufficient to cause up-regulation of many putative Hsf targets (Geiler-Samerotte et al., 2011). However, rather than directly sensing misfolding, Hsf binding by client-free chaperones, in particular Hsp70 and Hsp90, has been proposed as the feedback mechanism that signals the state of protein folding to Hsf. Under this model, in unstressed cells misfolded proteins are rare and therefore client-free HSPs are available to bind to Hsf restraining its activity; stress-induced protein misfolding titrates HSPs away from Hsf derepressing it and leading to up-regulation of HSP expression until their concentration is sufficient to refold misfolding proteins and bind to Hsf attenuating its activity (Mosser et al., 1993; Zou et al., 1998). Additionally, posttranslational modification of Hsf, in particular phosphorylation and acetylation, has been found to correlate with Hsf activity and been proposed as both an excitatory and inhibitory signal (Kline and Morimoto, 1997; Sorger and Pelham, 1988; Westerheide et al., 2009). However, phosphorylation is likely not essential for Hsf activity, as induction by a toxic proline analog in mammalian cells is phosphorylation-independent (Sarge et al., 1993). Further, a genome wide screen for modifiers of mammalian Hsf function suggested that acetylation tunes Hsf attenuation following stress by altering the rate at which active Hsf is degraded by the proteasome (Raychaudhuri et al., 2014). Finally, a compelling study found that activation of mammalian Hsf requires the presence of a complex between a non-coding RNA and the translation elongation factor eEF1A, although the broader significance of this observation has yet to be elucidated (Shamovsky et al., 2006). Thus, while many biochemical changes that occur contemporaneously with Hsf activity changes have been catalogued, a complete mechanistic description of Hsf regulation is still outstanding.

In yeast, the existence of an essential basal Hsf function adds an additional complication to understanding its function and regulation, nonetheless the powerful genetic tools available in this organism have enabled a number of important insights to be made. Genetic analysis of Hsf has identified mutants that separate Hsf basal and stress-activated functions. For example, an N-terminal truncation mutant of Hsf is constitutively active to a similar extent in the absence of stress as the wild type during heat shock, while truncation from the C-terminus results in a mutant that is viable at low temperatures but not at elevated temperatures due to compromised stress-activated transcription (Sorger, 1990). It is well established that the presence of a potent transcriptional activation domain (AD) and a DNA binding domain bound to DNA is generally sufficient to stimulate transcription of down-stream genes. However, while the C-terminal AD from yeast Hsf is sufficient to strongly drive gene expression when fused to a heterologous DNA binding domain, this activator is repressed at low temperatures in the native context of Hsf in spite of constitutive DNA binding (Sorger, 1990). Further, even when the Hsf C-terminal AD is replaced with a heterologous AD, this HsfΔC-AD fusion retains near wild type activity under basal and heat shock conditions, though intergenic mutants can bypass basal repression of this fusion (Bonner et al., 1992). These observations suggest that inter-domain interactions restrain Hsf activity in the absence of stress. However, a comprehensive analysis of Hsf activity changes in all viable yeast deletion mutants revealed that Hsf activity in the absence of stress was up-regulated by multiple orthogonal genetic perturbations (Brandman et al., 2012). Further, comparative analysis of the effect

of deletions on the general stress response (GSR)—an independent yeast stress pathway also activated by heat shock—demonstrated that many Hsf activators are unique to it, but showed that independent activation of the GSR was associated with attenuated of Hsf stress-induction. This later observation raises the possibility that Hsf may be further tuned by the activity of distinct stress responses with independent inputs, thus deploying Hsf alongside other evolutionary divergent stress pathways may cause speciation of Hsf regulation. In support of this notion, while the GSR is not conserved in mammals, activity of the mammalian metabolic stress sensor AMPK has recently been shown to have an analogous antagonistic effect on Hsf activation by proteotoxic stress (Dai et al., 2015).

In addition to the challenge of studying Hsf regulation, additional issues have hampered efforts to systematically define genes under Hsf control. One complication in mammalian cells is the presence of multiple heat shock factor homologs (e.g., HSF1, 2, 4, 5, X and Y in the human genome), which are differentially deployed during development and across tissues (Akerfelt et al., 2010). Further, other-cell type specific transcription factors co-regulate expression of some Hsf targets (Zhang et al., 2002). Thus, while deletion of HSF1, the primary stress-induced Hsf homolog, in mouse embryonic fibroblasts abolished heat-activation of hundreds of genes (Trinklein et al., 2004), a comparative analysis of HSF1-dependent transcription in different cell types to define the core mammalian Hsf regulon is lacking. In yeast, the challenge of isolating the role of Hsf in the heat sock response is that thermal stress activates both Hsf and Msn2/4, two non-essential transcription factors that regulated the general stress response, and the prevalence of co-

regulation amongst their targets is not well defined (Boy-Marcotte et al., 1999; Gasch et al., 2000; Treger et al., 1998). Additionally, the essential function of Hsf in unstressed yeast cells has not been elucidated, however it is likely to involve expression of a basal transcriptional program since mutations that disrupt either the Hsf1 DNA binding or transcriptional activation are lethal (Jakobsen and Pelham, 1991; Torres and Bonner, 1995). Further, viable yeast Hsf mutants that disrupt heat-induced transcription can not determine whether heat shock expands the scope of Hsf target genes, or if Hsf simply up-regulates expression of its basal targets during stress (Eastmond and Nelson, 2006; Morano et al., 1999; Zarzov et al., 1997). The former model is favored by studies of yeast Hsf DNA binding using chromatin immunoprecipitation (ChIP), which suggest that Hsf binds an expanded set of gene promoters during heat shock (Hahn et al., 2004; Lee et al., 2002). Similar to the expansive target list obtained by deletion analysis in mammalian cells, intersecting yeast Hsf ChIP data with stress-induced expression changes has defined a list of over 160 Hsf target genes, which is partially comprised of proteostasis factors, but also encoding proteins involved in other disparate functions such as carbon metabolism and vesicle transport (Hahn et al., 2004). However, one major shortfall of previous studies is that even if their target gene lists are accurate, the fail to elucidate the critical components of the Hsf regulon that enable survival under basal or stress conditions.

Beyond its well-established role during stress, aberrant non-stress activation of Hsf has recently been implicated in oncogenesis and malignancy. In many human cancers cells,

Hsf is constitutively active in the absence of extrinsic stress, similar to Hsf in unstressed yeast cells (Dai et al., 2012). Further, Hsf loss-of-function ablates *in vitro* proliferation of many human cancer cell lines and HSF null mice are protected from tumors induced by treatment with carcinogens (Dai et al., 2007). Constitutive activation of Hsf has also been observed in stromal cells surrounding patient tumors which has been proposed to support malignancy, and increased stromal Hsf activity is associated with poor patient prognosis (Scherz-Shouval et al., 2014). However, the essential function of Hsf is in cancer has yet to be determined. Analysis of changes in Hsf DNA binding in transformed cells has suggested Hsf's target repertoire is expanded in cancer cells to include many genes not activated during heat shock and with functional roles outside of protein folding (Mendillo et al., 2012). However, it is also that case that Hsf is required to prevent proteostasis collapse in transformed cells (Tang et al., 2015). It has yet to be determined if the additional targets assigned to Hsf in cancer with non-protein folding functions comprise an additional essential role for Hsf besides preventing proteostasis collapse. However, the fact that oncogenesis renders Hsf essential in mammal cells raises the possibility that a better understanding of the essential targets of yeast Hsf could highlight therapeutic targets to combat Hsf-dependent cancers.

By contrast to Hsf hyperactivation in cancer, age-associated Hsf loss-of-function has been implicated as a cause of proteostasis collapse during cell aging (Balch et al., 2008). Beyond the well-established connection between protein aggregation and human neurodegenerative disease (Chiti and Dobson, 2006), the establishment of model

organisms to study the biology of aging has revealed that protein aggregation is a conserved age-associated phenotype observed in the nematode *C. elegans* (Ben-Zvi et al., 2009), the budding yeast *S. cerevisiae* (Aguilaniu et al., 2003), and many others. Concomitant with proteostasis collapse, aging has been shown to impinge upon Hsf stress-activation in worms and mammalian cells (Heydari et al., 2000; Kern et al., 2010), and additional worm studies have shown that Hsf over-expression suppresses age-induced aggregation of a meta-stable model protein (Ben-Zvi et al., 2009). Further linking Hsf to longevity, lifespan extension by a number of long-lived worm mutants is Hsf-dependent (Hsu et al., 2003), although a recent study has implicated a role outside of HSP expression in Hsf-mediated longevity (Baird et al., 2014). Given these observations, it is unsurprising that pharmacological activation of Hsf has been proposed as a therapeutic strategy to combat age-associated proteopathies in humans (Neef et al., 2011; 2010). However, a better understanding of the mechanisms causing Hsf inactivation during aging, as well as the resulting consequences on gene expression should expand the range of therapeutic targets available to counter the effects of Hsf loss-of-function during aging.

The following chapters will build on previous observations and address a number of outstanding questions related to Hsf biology:

Chapter 2, entitled “Defining the essential function of yeast Hsf1 reveals a compact transcriptional program for maintaining eukaryotic proteostasis”, presents a systematic

characterization of Hsf function in yeast and mammalian cells. Using a novel chemical genetics approach to rapidly inactivate Hsf function in yeast, we reveal that Hsf is essential to prevent lethal proteostasis collapse in unstressed yeast cells. Further, systematic analysis of Hsf-dependent gene expression reveals that Hsf's basal transcriptional program is much more compact that previously anticipated. Additionally, we demonstrate that during heat shock, Hsf mediates over-expression of its limited set of target genes, without expanding its breadth. Rather, we used chemical genetics to show that the vast majority of the yeast heat shock response is Hsf-independent, with most heat-induced gene expression driven by Msn2/4. In a comparative mammalian study, we systematically define the expression program of mammalian HSF, which we found is comprised of network of proteostasis factors that have a remarkably similar functional organization to yeast Hsf targets. We then turn to defining the essential function of Hsf in unstressed cells using a synthetic transcriptional program. Strikingly, we show that expression of two genes, encoding the Hsp70 and Hsp90 chaperones, are necessary and minimally sufficient for viability without Hsf and to prevent proteostasis collapse. Finally, we demonstrate that while the Hsf regulon comprises a minority of the heat shock response, coordinated up-regulation of this compact gene set is critical for fitness at elevated temperatures.

Chapter 3, entitled "Stress pathway cross-talk mediates attenuation of Hsf1 activity during stress and replicative aging in yeast", presents work on changes in Hsf function during yeast replicative aging. We first demonstrate that age-associated inactivation of Hsf is a

phenotype conserved in budding yeast. We then use genetic and cell biological tools to demonstrate that Hsf is inactivated during replicative aging by constitutive activation of the general stress response (GSR). Building on these observations, we show that engineered activation of the GSR in young cells is sufficient to prevent Hsf activation by stress. Further, we show that inhibition of Hsf by the GSR extends beyond aging to stress conditions that activate both Hsf and the GSR in young cells. Finally, we explore the mechanism by which the GSR suppresses Hsf activation and show that inhibition can be genetically bypassed.

Finally, Chapter 4, entitled “Future directions” presents additional lines of inquiry suggested by the previous chapters that should be addressed in future studies. In particular, our work suggests that the contribution of Hsf to cancer and cell aging may be limited to changes in expression of a very small set of genes. Additionally, we propose experiments that build on our synthetic transcriptional program to obviate the role of Hsf in proteostasis to better understand the consequences and mechanisms of survival for various proteotoxic stresses.

References

Abrams, J.L., Verghese, J., Gibney, P.A., and Morano, K.A. (2014). Hierarchical functional specificity of cytosolic heat shock protein 70 (Hsp70) nucleotide exchange factors in yeast. Journal of Biological Chemistry *289*, 13155–13167.

Aguilaniu, H., Gustafsson, L., Rigoulet, M., and Nyström, T. (2003). Asymmetric inheritance of oxidatively damaged proteins during cytokinesis. Science *299*, 1751–1753.

Akerfelt, M., Morimoto, R.I., and Sistonen, L. (2010). Heat shock factors: integrators of cell stress, development and lifespan. Nat Rev Mol Cell Biol *11*, 545–555.

Anfinsen, C.B. (1973). Principles that govern the folding of protein chains. Science *181*, 223–230.

Baird, N.A., Douglas, P.M., Simic, M.S., Grant, A.R., Moresco, J.J., Wolff, S.C., Yates, J.R.I., Manning, G., and Dillin, A. (2014). HSF-1-mediated cytoskeletal integrity determines thermotolerance and life span. Science *346*, 360–363.

Balch, W., Morimoto, R., and Dillin, A. (2008). Adapting Proteostasis for Disease Intervention. Science.

Ben-Zvi, A., Miller, E.A., and Morimoto, R.I. (2009). Collapse of proteostasis represents an early molecular event in Caenorhabditis elegans aging. Proc Natl Acad Sci USA *106*, 14914–14919.

Bienz, M., and Pelham, H.R. (1986). Heat shock regulatory elements function as an inducible enhancer in the Xenopus hsp70 gene and when linked to a heterologous promoter. Cell *45*, 753–760.

Bonner, J.J., Heyward, S., and Fackenthal, D.L. (1992). Temperature-dependent regulation of a heterologous transcriptional activation domain fused to yeast heat shock transcription factor. Mol Cell Biol *12*, 1021–1030.

Boy-Marcotte, E., Lagniel, G., Perrot, M., Bussereau, F., Boudsocq, A., Jacquet, M., and Labarre, J. (1999). The heat shock response in yeast: differential regulations and

contributions of the Msn2p/Msn4p and Hsf1p regulons. Molecular Microbiology *33*, 274–283.

Brandman, O., Stewart-Ornstein, J., Wong, D., Larson, A., Williams, C.C., Li, G.-W., Zhou, S., King, D., Shen, P.S., Weibezahn, J., et al. (2012). A ribosome-bound quality control complex triggers degradation of nascent peptides and signals translation stress. Cell *151*, 1042–1054.

Buchberger, A., Bukau, B., and Sommer, T. (2010). Protein quality control in the cytosol and the endoplasmic reticulum: brothers in arms. Mol Cell *40*, 238–252.

Chiti, F., and Dobson, C. (2006). Protein misfolding, functional amyloid, and human disease. Annu Rev Biochem.

Cimdins, A., Klinkert, B., Aschke-Sonnenborn, U., Kaiser, F.M., Kortmann, J., and Narberhaus, F. (2014). Translational control of small heat shock genes in mesophilic and thermophilic cyanobacteria by RNA thermometers. RNA Biol *11*, 594–608.

Clos, J., Rabindran, S., Wisniewski, J., and Wu, C. (1993). Induction temperature of human heat shock factor is reprogrammed in a Drosophila cell environment. Nature *364*, 252–255.

Clos, J., Westwood, J.T., Becker, P.B., Wilson, S., Lambert, K., and Wu, C. (1990). Molecular cloning and expression of a hexameric Drosophila heat shock factor subject to negative regulation. Cell *63*, 1085–1097.

Dai, C., Santagata, S., Tang, Z., Shi, J., Cao, J., Kwon, H., Bronson, R.T., Whitesell, L., and Lindquist, S. (2012). Loss of tumor suppressor NF1 activates HSF1 to promote carcinogenesis. The Journal of Clinical Investigation *122*, 3742–3754.

Dai, C., Whitesell, L., Rogers, A.B., and Lindquist, S. (2007). Heat Shock Factor 1 Is a Powerful Multifaceted Modifier of Carcinogenesis. Cell *130*, 1005–1018.

Dai, S., Tang, Z., Cao, J., Zhou, W., Li, H., Sampson, S., and Dai, C. (2015). Suppression of the HSF1-mediated proteotoxic stress response by the metabolic stress sensor AMPK. - PubMed - NCBI. Embo J *34*, 275–293.

Dobson, C. (2003). Protein folding and misfolding. Nature.

Eastmond, D.L., and Nelson, H.C.M. (2006). Genome-wide analysis reveals new roles for the activation domains of the Saccharomyces cerevisiae heat shock transcription factor (Hsf1) during the transient heat shock response. J Biol Chem *281*, 32909–32921.

Ellgaard, E.G., and Clever, U. (1971). RNA metabolism during puff induction in Drosophila melanogaster. Chromosoma *36*, 60–78.

Fan, C.-Y., Lee, S., Ren, H.-Y., and Cyr, D.M. (2004). Exchangeable chaperone modules contribute to specification of type I and type II Hsp40 cellular function. Mol Biol Cell *15*, 761–773.

Gasch, A.P., Spellman, P.T., Kao, C.M., Carmel-Harel, O., Eisen, M.B., Storz, G., Botstein, D., and Brown, P.O. (2000). Genomic expression programs in the response of yeast cells to environmental changes. Mol Biol Cell *11*, 4241–4257.

Geiler-Samerotte, K.A., Dion, M.F., Budnik, B.A., Wang, S.M., Hartl, D.L., and Drummond, D.A. (2011). Misfolded proteins impose a dosage-dependent fitness cost and trigger a cytosolic unfolded protein response in yeast. Proc Natl Acad Sci USA *108*, 680–685.

Grad, W., and Picard, D. (2007). The glucocorticoid responses are shaped by molecular

chaperones. Mol. Cell. Endocrinol. *275*, 2–12.

Hahn, J.-S., Hu, Z., Thiele, D.J., and Iyer, V.R. (2004). Genome-wide analysis of the biology of stress responses through heat shock transcription factor. Mol Cell Biol *24*, 5249–5256.

Hartl, F.U., Bracher, A., and Hayer-Hartl, M. (2011). Molecular chaperones in protein folding and proteostasis. Nature *475*, 324–332.

Heydari, A.R., You, S., Takahashi, R., Gutsmann-Conrad, A., Sarge, K.D., and Richardson, A. (2000). Age-related alterations in the activation of heat shock transcription factor 1 in rat hepatocytes. Exp. Cell Res. *256*, 83–93.

Hsu, A.-L., Murphy, C.T., and Kenyon, C. (2003). Regulation of aging and age-related disease by DAF-16 and heat-shock factor. Science *300*, 1142–1145.

Jakobsen, B.K., and Pelham, H.R. (1988). Constitutive binding of yeast heat shock factor to DNA in vivo. Mol Cell Biol *8*, 5040–5042.

Jakobsen, B.K., and Pelham, H.R. (1991). A conserved heptapeptide restrains the activity of the yeast heat shock transcription factor. Embo J *10*, 369–375.

Kern, A., Ackermann, B., Clement, A.M., Duerk, H., and Behl, C. (2010). HSF1-controlled and age-associated chaperone capacity in neurons and muscle cells of C. elegans. PLoS ONE *5*, e8568.

Kline, M.P., and Morimoto, R.I. (1997). Repression of the heat shock factor 1 transcriptional activation domain is modulated by constitutive phosphorylation. Mol Cell Biol.

Lee, P., Shabbir, A., Cardozo, C., and Caplan, A.J. (2004). Sti1 and Cdc37 can stabilize Hsp90 in chaperone complexes with a protein kinase. Mol Biol Cell *15*, 1785–1792.

Lee, T.I., Rinaldi, N.J., Robert, F., Odom, D.T., and Bar-Joseph, Z. (2002). Transcriptional regulatory networks in Saccharomyces cerevisiae. Science.

Liu, X.D., Liu, P.C.C., Santoro, N., and Thiele, D.J. (1997). Conservation of a stress response: human heat shock transcription factors functionally substitute for yeast HSF. Embo J *16*, 6466–6477.

Louvion, J.F., Abbas-Terki, T., and Picard, D. (1998). Hsp90 is required for pheromone signaling in yeast. Mol Biol Cell *9*, 3071–3083.

Lu, Z., and Cyr, D.M. (1998). Protein folding activity of Hsp70 is modified differentially by the hsp40 co-chaperones Sis1 and Ydj1. J Biol Chem *273*, 27824–27830.

McKenzie, S.L., and Meselson, M. (1977). Translation in vitro of Drosophila heat-shock messages. J Mol Biol *117*, 279–283.

McKenzie, S.L., Henikoff, S., and Meselson, M. (1975). Localization of RNA from heat-induced polysomes at puff sites in Drosophila melanogaster. Proc Natl Acad Sci USA *72*, 1117–1121.

Mendillo, M.L., Santagata, S., Koeva, M., Bell, G.W., Hu, R., Tamimi, R.M., Fraenkel, E., Ince, T.A., Whitesell, L., and Lindquist, S. (2012). HSF1 drives a transcriptional program distinct from heat shock to support highly malignant human cancers. Cell *150*, 549–562.

Millson, S.H., Truman, A.W., Rácz, A., Hu, B., Panaretou, B., Nuttall, J., Mollapour, M.,

Söti, C., and Piper, P.W. (2007). Expressed as the sole Hsp90 of yeast, the α and β isoforms of human Hsp90 differ with regard to their capacities for activation of certain client proteins, whereas only Hsp90β generates sensitivity to the Hsp90 inhibitor radicicol. FEBS Journal *274*, 4453–4463.

Morano, K.A., Santoro, N., Koch, K.A., and Thiele, D.J. (1999). A trans-activation domain in yeast heat shock transcription factor is essential for cell cycle progression during stress. Mol Cell Biol *19*, 402–411.

Morimoto, R.I. (1998). Regulation of the heat shock transcriptional response: cross talk between a family of heat shock factors, molecular chaperones, and negative regulators.

Mosser, D.D., Duchaine, J., and Massie, B. (1993). The DNA-binding activity of the human heat shock transcription factor is regulated in vivo by hsp70. Mol Cell Biol *13*, 5427–5438.

Neef, D.W., Jaeger, A.M., and Thiele, D.J. (2011). Heat shock transcription factor 1 as a therapeutic target in neurodegenerative diseases. Nat Rev Drug Discov *10*, 930–944.

Neef, D.W., Turski, M.L., and Thiele, D.J. (2010). Modulation of heat shock transcription factor 1 as a therapeutic target for small molecule intervention in neurodegenerative disease. PLoS Biol *8*, e1000291.

Olzscha, H., Schermann, S.M., Woerner, A.C., Pinkert, S., Hecht, M.H., Tartaglia, G.G., Vendruscolo, M., Hayer-Hartl, M., Hartl, F.U., and Vabulas, R.M. (2011). Amyloid-like aggregates sequester numerous metastable proteins with essential cellular functions. Cell *144*, 67–78.

Parsell, D.A., and Lindquist, S. (1993). The Function of Heat-Shock Proteins in Stress Tolerance - Degradation and Reactivation of Damaged Proteins. Annu. Rev. Genet. *27*, 437–496.

Picard, D., Khursheed, B., Garabedian, M.J., Fortin, M.G., Lindquist, S., and Yamamoto, K.R. (1990). Reduced levels of hsp90 compromise steroid receptor action in vivo. Nature *348*, 166–168.

Pirkkala, L., Nykanen, P., and Sistonen, L. (2001). Roles of the heat shock transcription factors in regulation of the heat shock response and beyond. The FASEB Journal *15*, 1118–1131.

Rabindran, S.K., Giorgi, G., Clos, J., and Wu, C. (1991). Molecular cloning and expression of a human heat shock factor, HSF1. Proc Natl Acad Sci USA *88*, 6906–6910.

Raychaudhuri, S., Loew, C., Körner, R., Pinkert, S., Theis, M., Hayer-Hartl, M., Buchholz, F., and Hartl, F.U. (2014). Interplay of Acetyltransferase EP300 and the Proteasome System in Regulating Heat Shock Transcription Factor 1. Cell *156*, 975–985.

Richter, K., Haslbeck, M., and Buchner, J. (2010). The Heat Shock Response: Life on the Verge of Death. Mol Cell *40*, 253–266.

Richter, K., Muschler, P., Hainzl, O., Reinstein, J., and Buchner, J. (2003). Sti1 is a non-competitive inhibitor of the Hsp90 ATPase. Binding prevents the N-terminal dimerization reaction during the atpase cycle. J Biol Chem *278*, 10328–10333.

Ritossa, F. (1962). A new puffing pattern induced by temperature shock and DNP in Drosophila. Experientia.

Ritossa, F. (1996). Discovery of the heat shock response. Cell Stress Chaperones *1*, 97–98.

Sarge, K.D., Murphy, S.P., and Morimoto, R.I. (1993). Activation of heat shock gene transcription by heat shock factor 1 involves oligomerization, acquisition of DNA-binding activity, and nuclear localization and can occur in the absence of stress. Mol Cell Biol *13*, 1392–1407.

Scherz-Shouval, R., Santagata, S., Mendillo, M.L., Sholl, L.M., Ben-Aharon, I., Beck, A.H., Dias-Santagata, D., Koeva, M., Stemmer, S.M., Whitesell, L., et al. (2014). The Reprogramming of Tumor Stroma by HSF1 Is a Potent Enabler of Malignancy. Cell *158*, 564–578.

Shamovsky, I., Ivannikov, M., Kandel, E.S., Gershon, D., and Nudler, E. (2006). RNA-mediated response to heat shock in mammalian cells. Nature *440*, 556–560.

Sorger, P.K. (1990). Yeast heat shock factor contains separable transient and sustained response transcriptional activators. Cell *62*, 793–805.

Sorger, P.K., and Pelham, H.R. (1987). Purification and characterization of a heat-shock element binding protein from yeast. Embo J *6*, 3035–3041.

Sorger, P.K., and Pelham, H.R. (1988). Yeast heat shock factor is an essential DNA-binding protein that exhibits temperature-dependent phosphorylation. Cell *54*, 855–864.

Sorger, P.K., Lewis, M.J., and Pelham, H.R. (1987). Heat shock factor is regulated differently in yeast and HeLa cells. Nature *329*, 81–84.

Taipale, M., Jarosz, D.F., and Lindquist, S. (2010). HSP90 at the hub of protein homeostasis: emerging mechanistic insights. Nat Rev Mol Cell Biol *11*, 515–528.

Taipale, M., Tucker, G., Peng, J., Krykbaeva, I., Lin, Z.-Y., Larsen, B., Choi, H., Berger, B., Gingras, A.-C., and Lindquist, S. (2014). A Quantitative Chaperone Interaction

Network Reveals the Architecture of Cellular Protein Homeostasis Pathways. Cell *158*, 434–448.

Tang, Z., Dai, S., He, Y., Doty, R.A., Shultz, L.D., Sampson, S.B., and Dai, C. (2015). MEK Guards Proteome Stability and Inhibits Tumor-Suppressive Amyloidogenesis via HSF1. Cell *160*, 729–744.

Terasawa, K., Minami, M., and Minami, Y. (2005). Constantly updated knowledge of Hsp90. J. Biochem. *137*, 443–447.

Tissiéres, A., Mitchell, H.K., and Tracy, U.M. (1974). Protein synthesis in salivary glands of Drosophila melanogaster: Relation to chromosome puffs. Journal of Molecular Biology *84*, 389–398.

Torres, F.A.G., and Bonner, J.J. (1995). Genetic Identification of the Site of Dna Contact in the Yeast Heat-Shock Transcription Factor. Mol Cell Biol *15*, 5063–5070.

Treger, J.M., Schmitt, A.P., Simon, J.R., and McEntee, K. (1998). Transcriptional factor mutations reveal regulatory complexities of heat shock and newly identified stress genes in Saccharomyces cerevisiae. J Biol Chem *273*, 26875–26879.

Trinklein, N.D., Murray, J.I., Hartman, S.J., Botstein, D., and Myers, R.M. (2004). The role of heat shock transcription factor 1 in the genome-wide regulation of the mammalian heat shock response. Mol Biol Cell *15*, 1254–1261.

Trotter, E.W., Kao, C.M.-F., Berenfeld, L., Botstein, D., Petsko, G.A., and Gray, J.V. (2002). Misfolded proteins are competent to mediate a subset of the responses to heat shock in Saccharomyces cerevisiae. Journal of Biological Chemistry *277*, 44817–44825.

Wegele, H., Haslbeck, M., Reinstein, J., and Buchner, J. (2003). Sti1 is a novel activator

of the Ssa proteins. J Biol Chem *278*, 25970–25976.

Westerheide, S.D., Anckar, J., Stevens, S.M., Sistonen, L., and Morimoto, R.I. (2009). Stress-inducible regulation of heat shock factor 1 by the deacetylase SIRT1. Science *323*, 1063–1066.

Westwood, J.T., Clos, J., and Wu, C. (1991). Stress-Induced Oligomerization and Chromosomal Relocalization of Heat-Shock Factor. Nature *353*, 822–823.

Wiederrecht, G., Seto, D., and Parker, C.S. (1988). Isolation of the gene encoding the S. cerevisiae heat shock transcription factor. Cell *54*, 841–853.

Wu, C. (1995). Heat Shock Transcription Factors: Structure and Regulation. Annu. Rev. Cell Dev. Biol. *11*, 441–469.

Zarzov, P., Boucherie, H., and Mann, C. (1997). A yeast heat shock transcription factor (Hsf1) mutant is defective in both Hsc82/Hsp82 synthesis and spindle pole body duplication. J. Cell. Sci.

Zhang, Y., Huang, L., Zhang, J., Moskophidis, D., and Mivechi, N.F. (2002). Targeted disruption of hsf1 leads to lack of thermotolerance and defines tissue-specific regulation for stress-inducible Hsp molecular chaperones. J. Cell. Biochem. *86*, 376–393.

Zou, J., Guo, Y., Guettouche, T., Smith, D.F., and Voellmy, R. (1998). Repression of heat shock transcription factor HSF1 activation by HSP90 (HSP90 complex) that forms a stress-sensitive complex with HSF1. Cell *94*, 471–480.

Chapter 2: Defining the essential function of yeast Hsf1 reveals a compact transcriptional program for maintaining eukaryotic proteostasis

Introduction

Cells maintain protein homeostasis (proteostasis) in the face of proteotoxic stresses, such as heat shock, by inducing expression of genes encoding factors for protein folding and degradation (Hartl et al., 2011; Richter et al., 2010). Failure to maintain proteostasis by regulating gene expression has been linked to aging and neurodegenerative diseases (Balch et al., 2008), while many cancers are associated with elevated expression of proteostasis factors (Tang et al., 2015). Yeast heat shock factor 1 (Hsf1) was the first eukaryotic proteostasis transcription factor to be discovered (Sorger and Pelham, 1987), which in turn enabled identification of homologous transcription factors across the eukaryotic lineage (Clos et al., 1990; Jakobsen and Pelham, 1991; Rabindran et al., 1991; Scharf et al., 1990). Hsf1 is constitutively nuclear and essential for yeast cell growth under all conditions (Jakobsen and Pelham, 1988; Sorger and Pelham, 1988). By contrast, the mammalian homolog HSF1 is normally dispensable for cell growth absent stress and resides in a repressed, cytoplasmically-localized state under physiological conditions (Sarge et al., 1993). Following heat shock, however, HSF1 undergoes activation associated with nuclear import to enable thermotolerance by inducing gene expression of proteostasis factors (McMillan et al., 1998; Zhang et al., 2002). Despite these species differences, the core function of mammalian HSF1 appears to be extremely conserved because a constitutively active version of it can enable yeast cells to live

without Hsf1 (Liu et al., 1997). Another interesting point of similarity between yeast and mammalian systems is that human HSF1 is constitutively active and essential for growth of many cancer cell types even in the absence of heat stress (Dai et al., 2007).

Efforts to systematically define genes whose stress-induced expression is dependent on either yeast Hsf1 or mammalian HSF1 have been challenging (Akerfelt et al., 2010). Part of the difficulty comes from gene co-regulation by other transcription factors with cell type-specific expression (Zhang et al., 2002). For example, deletion of the mouse *HSF1* gene abolished heat-induced expression of hundreds of genes in mouse embryonic fibroblasts (Trinklein et al., 2004). Heat induction of genes varies significantly between cell types and a comparative analysis of other mouse cell lines has yet to be performed to define the core HSF1 transcriptional program. Similarly, in yeast, it has been difficult to pinpoint the role of Hsf1 in heat-induced gene expression because many genes, including several that encode heat shock proteins (HSPs), are heat-activated by Msn2 and Msn4, two non-essential transcription factors (Boy-Marcotte et al., 1999a; Gasch et al., 2000; Treger et al., 1998). There is also the additional challenge in yeast of defining Hsf1's basal transcriptional program, which is presumed to be essential for cell viability because mutations that disrupt either the Hsf1 DNA binding or transcriptional activation domains are lethal (Jakobsen and Pelham, 1991; Torres and Bonner, 1995). Viable partial loss-of-function mutants of Hsf1 that disrupt heat shock-induced gene expression (Eastmond and Nelson, 2006; Morano et al., 1999; Zarzov et al., 1997) cannot resolve whether the basal and heat-induced transcriptional programs are qualitatively distinct or if heat primarily

tunes the magnitude of Hsf1's basal transcriptional program. Chromatin immunoprecipitation combined with DNA microarray (ChIP-chip) studies have favored the former possibility by showing that Hsf1 associates with additional promoters under heat stress (Hahn et al., 2004; Lee et al., 2002) . By intersecting these data with heat-induced changes in mRNA abundance detected using DNA microarrays, a list of >160 Hsf1-dependent genes has emerged that is partly devoted to proteostasis and partly to disparate cellular functions such as energy generation, carbon metabolism and vesicle transport (Eastmond and Nelson, 2006; Hahn et al., 2004).

Hsf1's essential function in the absence of stress is presumably to drive basal gene expression of essential proteostasis factors. However, closer inspection of the Hsf1 target genes challenges this simple conclusion in several ways. First, among Hsf1 gene targets not involved in protein folding, some are individually essential, while pairwise deletions of many non-essential ones result in synthetic lethality (Hahn et al., 2004). Second, it is not known to what extent other basal transcription factors would maintain expression of Hsf1 gene targets involved in protein folding were Hsf1 to be acutely inhibited. Finally, deletion of many non-essential Hsf1 targets results in elevated basal Hsf1 activity (Brandman et al., 2012), suggesting that overexpression of some targets can compensate for the loss of others. One unbiased strategy for defining essential Hsf1 targets would be to systematically place all targets under the control of Hsf1-independent promoters and find which among them are minimally required for life without Hsf1. This synthetic biology

approach is conceptually simple but the lengthiness of the target list renders the prospect of its execution fanciful.

Our starting point was to develop a chemical genetics tool for inducing Hsf1 nuclear export in a matter of minutes. This enabled us to measure immediate changes in genome-wide basal transcription before Hsf1 nuclear export caused protein aggregation, which was associated with cell cycle arrest and eventual cell lysis. From this analysis emerged a compact list of 18 genes—all but one of which encodes a chaperone—that are strongly dependent on Hsf1 for their basal expression. In addition, we find that Hsf1's repertoire of gene targets is not significantly expanded by heat shock; instead, Hsf1 drives heat-induced chaperone overexpression. With a greatly reduced list of Hsf1-dependent genes, we implemented the synthetic biology approach described in concept above to define Hsp70 and Hsp90 as the two critical chaperones on the list. Cells engineered to live robustly without Hsf1 were thermosensitive arguing that survival under severe proteotoxic stress necessitates chaperone overexpression by Hsf1. Lastly, we used CRISPR/Cas9 to create two distinct *hsf1*$^{-/-}$ mouse cell lines, which enabled us to define HSF1's core transcriptional program: a set of nine genes—eight of which encode chaperones—that are functionally akin to Hsf1-dependent genes in yeast. However, in mammalian cells basal chaperone expression is independent of HSF1; rather, HSF1 induced chaperone overexpression following heat shock.

Results

A chemical genetics approach enables acute Hsf1 inactivation at the physiological temperature.

To develop a tool that acutely inactivates Hsf1 in the absence of stress we used the "Anchor Away" (AA) approach (Haruki et al., 2008). Briefly, we created a yeast strain (Hsf1-AA) that is resistant to Tor1 inhibition by rapamycin (*TOR1-1, fpr1*) and co-expresses an Hsf1-FRB (FKBP rapamycin-binding domain) fusion and a ribosomal protein L13a-FKBP12 fusion (Rpl13A-FKBP12). In this strain, rapamycin should induce FRB-FKBP12 heterodimerization, thus tethering Hsf1 to nascent ribosome subunits prior to their nuclear export to the cytoplasm (Figure 2.1A). Indeed, real-time imaging of cells by fluorescence microscopy revealed that rapamycin treatment induced rapid nuclear export of Hsf1-FRB-GFP (within ~10 minutes, Figure S2.1A), which rendered a reporter of Hsf1-dependent transcription (Brandman et al., 2012) unresponsive to heat shock (Figure S2.1B). Importantly, rapamycin prevented growth of Hsf1-AA cells (Figure 2.1B) dependent on Hsf1-Rpl13a heterodimerization (Figure S2.1C), while a second copy of Hsf1 not fused to FRB was able to rescue growth (Figures 2.1B and S2.1C).

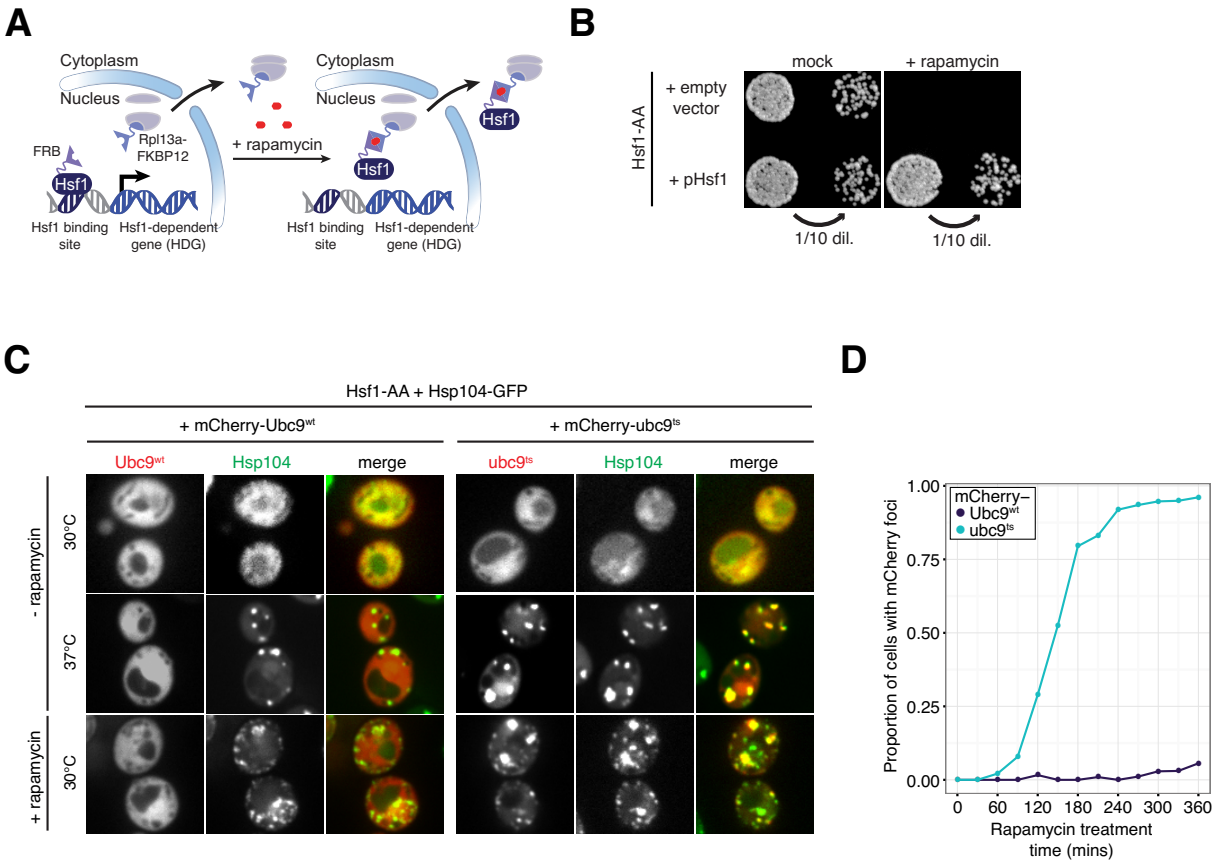

Figure 2.1: Acute inactivation of Hsf1 induces proteotoxicity even in the absence of stress.

(A) Schematic of Hsf1 Anchor Away (Hsf1-AA). **(B)** Hsf1-AA cells with indicated plasmids were spotted at two concentrations onto rapamycin or mock (carrier-only) plates. Shown are images of plates incubated for 3 days at 30°C. **(C)** Representative confocal micrographs of Hsf1-AA cells expressing endogenous Hsp104-GFP and plasmid-borne mCherry-Ubc9^{wt} or -ubc9^{ts} taken after logarithmic growth at 30°C, after treatment with heat shock (20' at 37°C), and after treatment with rapamycin (360' at 30°C). **(D)** Hsf1-AA cells described in part (C) were treated with rapamycin for indicated times at 30°C and imaged by epifluorescence microscopy. Blinded images containing at least 100 cells were scored for cells containing mCherry foci and the fraction of scored cells plotted.

Hsf1 prevents protein aggregation at the physiological temperature.

Even though rapamycin treatment of Hsf1-AA cells induced Hsf1 export in a matter of minutes, it took another ~2.5 hours before cells became arrested at various stages of the cell cycle (measured by budding index). After more extended treatment (>13 hours) some cells lysed asynchronously (Figure S2.1D), and removal of rapamycin failed to restore cell growth, arguing that we were observing irreversible cytotoxicity. Since constitutive expression of several chaperone genes is dependent on Hsf1 binding sites in their promoters (Erkine et al., 1996; Gross et al., 1993; Nicholls et al., 2009; Sakurai and Ota, 2011), we reasoned that rapid Hsf1 nuclear export is followed by a slower decrease in chaperone concentration leading to global protein misfolding associated with growth arrest and cytotoxicity. To test this, we used mCherry fused to a metastable, temperature-sensitive (ts) allele of the small ubiquitin-like modifier (SUMO) ligase Ubc9, an established reporter of protein misfolding in yeast that forms cytosolic protein aggregates visible as fluorescent puncta by microscopy (Kaganovich et al., 2008). In a control experiment, we confirmed that heat shock at 37ºC induced mCherry-ubc9^{ts}—but not stable mCherry-Ubc9^{wt}—to form puncta that co-localized with Hsp104-GFP, a protein disaggregase that localizes to misfolded protein aggregates (Glover and Lindquist, 1998) (Figure 2.1C). Consistent with the idea that delayed Hsf1-AA growth arrest is associated with proteostasis collapse, we observed mCherry-ubc9^{ts} aggregation at the physiological temperature in the majority of cells within 2.5 hours of rapamycin addition (Figure 2.1D). Importantly, mCherry-Ubc9^{wt} remained apparently soluble even after extended rapamycin treatment (Figure 2.1C, D) despite the appearance of Hsp104-GFP puncta in the same

cells, which likely mark aggregates of endogenous metastable proteins with similar folding requirements to ubc9^{ts} (Figure 2.1C).

Yeast Hsf1 drives basal expression of 18 genes.

To define the immediate transcriptional effects of Hsf1 nuclear export prior to any secondary effects of proteostasis collapse, we used native elongating transcript sequencing (NET-seq) (Churchman and Weissman, 2011) to globally track RNA polymerase II transcription of individual genes in Hsf1-AA cells during a rapamycin treatment time course (15, 30, and 60 minutes). Statistical analysis (see Experimental Procedures) defined 25 genes that were transcriptionally repressed and 5 that were induced by 15 minutes of drug treatment (p-value < 10^{-4}) (Figure S2.2A, left panel), and these changes persisted in the later time points (Figure S2.2A, middle and right panels). To substantiate that the transcriptional changes identified by the NET-seq analysis resulted in *bona fide* changes in mRNA abundance, we analyzed Hsf1-AA cells treated for 60 minutes with rapamycin by RNA-seq. We observed statistically significant changes in mRNA abundance for 18/25 transcriptionally-repressed genes and none of the induced genes (Figures 2.2A and S2.2B,C; see Experimental Procedures). Importantly, the genes defined by our combined NET-seq/RNA-seq analysis had a strong correlation between the fold-decrease in their transcription and the fold-decrease in their mRNA abundance (Figure S2.2D).

Given that we defined ~10-fold fewer Hsf1 targets by NET-seq analysis than anticipated (Eastmond and Nelson, 2006; Hahn et al., 2004; Lee et al., 2002), we considered the possibility that a high level of technical or biological variability limited our statistical power to detect additional biologically significant transcriptional changes, thus underestimating the extent of overlap with Hsf1 targets defined by RNA-seq. However, there was no significant difference in the width of confidence intervals—which inversely relate to statistical power—between genes defined by our analysis and other genes (Figure S2.2E), arguing that scope of targets we defined was unconstrained by statistical sensitivity. Another possible source of error was to miss slower transcriptional effects of Hsf1 nuclear export. However, we defined only 3 significant changes in transcription after 30 or 60 minutes of rapamycin treatment, and none of these were corroborated by mRNA analysis. Rather, transcription of most genes was consistent and largely unperturbed by Hsf1 inactivation, both globally—R^2 = 0.98 for all adjacent time points (Figure S2.2A)—and at the level of individual loci (Figure S2.2F) across a wide range of expression levels (Figure S2.2G). Thus, detection of additional Hsf1 targets was not limited by the sensitivity or reproducibility of our analysis.

Figure 2.2: Hsf1 drives basal expression of a diverse set of protein folding factors. **(A)** Hsf1-AA cells were grown logarithmically at 30°C and harvested for analysis by native elongating transcript sequencing (NET-seq) or deep sequencing of mRNA (RNA-seq) immediately prior to and after 15', 30' and 60' of rapamycin treatment. Shown is a gene scatter plot of transcription versus mRNA changes induced by treatment with rapamycin for 15' and 60', respectively. The indicated Hsf1-dependent genes were defined by statistical tests described in Experimental Procedures. Note: Due to computational issues arising from the 94% sequence identity between *SSA1* and *SSA2*, data from these paralogs was averaged and reported as *SSA1/2* in parts (A) and (C), as described in the Experimental Procedures. **(B)** Venn diagram comparing Hsf1 target genes defined by ChIP-, NET- and RNA-seq, with the names of the 18 Hsf1-dependent genes (HDGs) detected by all 3 techniques indicated. **(C)** Gene scatter plot of change in HDG transcription resulting from 15' of rapamycin treatment versus Hsf1 occupancy at HDG promoters. **(D)** Bioinformatic analysis of the 18 HDGs defined by ChIP-, NET- and RNA-seq. Solid bars show the number of HDGs with the given annotation (GO term or promoter motif) and dashed bars show the remaining number of HDGs. The fill color indicates the significance level for the enrichment of the annotated HDGs versus other genes (p-values for GO terms are corrected for multiple testing using the Holm–Bonferroni method). See Supplementary Figure 2.2J for a similar bioinformatic analysis of Hsf1 targets defined by each individual genome-wide approache or by combining any two approaches.

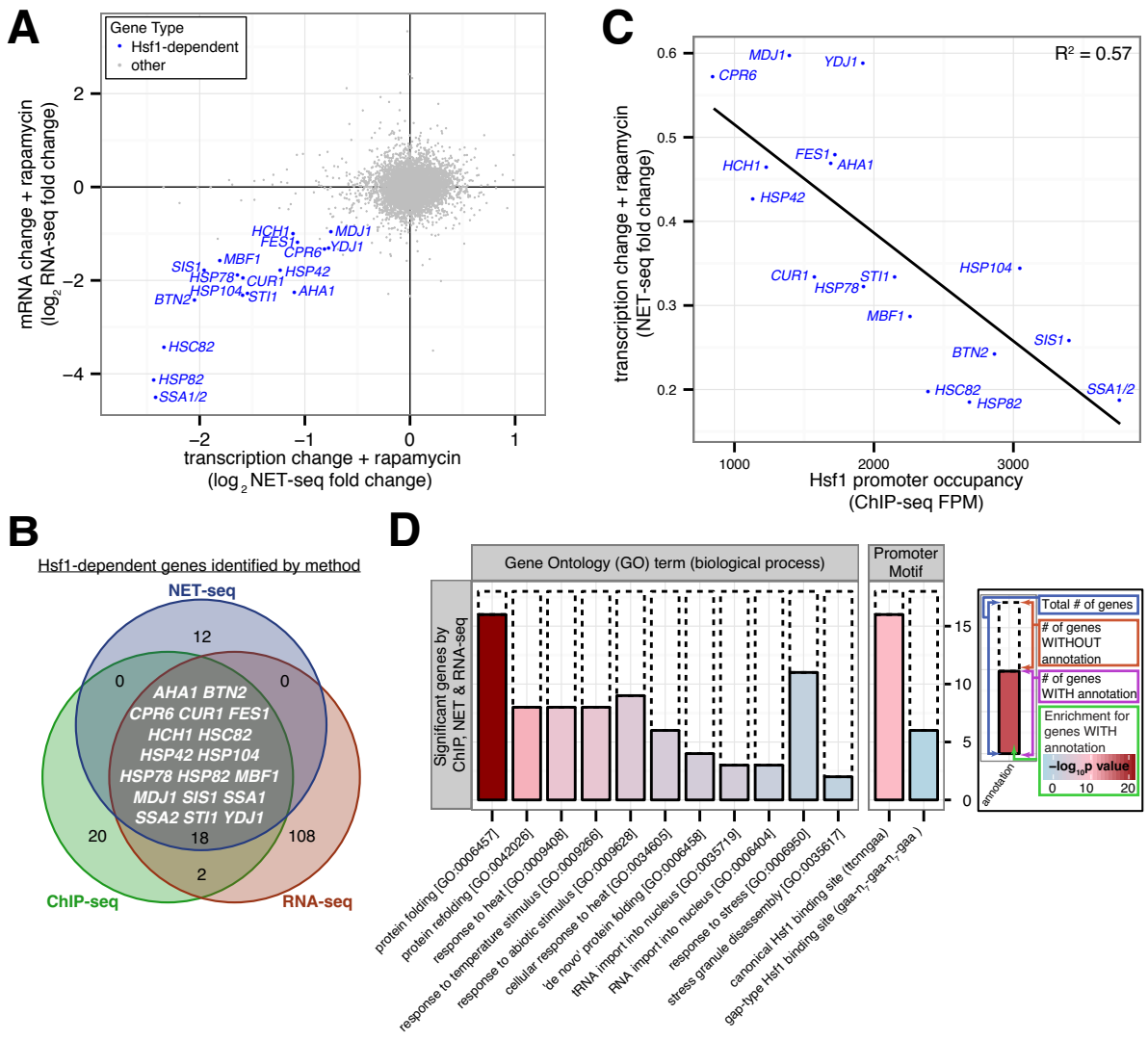

Figure 2.2: (Continued)

To assess whether the remaining Hsf1 targets defined by NET-seq but not by RNA-seq are *bona fide* Hsf1 gene targets with unusually long-lived mRNAs, we monitored Hsf1 DNA binding by chromatin immunoprecipitation followed by deep sequencing (ChIP-seq). To increase the signal-to-noise, we isolated chromatin using tandem affinity purification of dual epitope-tagged Hsf1-FLAG-V5 expressed as the only copy of Hsf1 in an otherwise wild type genetic background. Analysis using a stringent peak-calling algorithm (see Experimental Procedures) and bioinformatics identified 40 Hsf1 ChIP-seq gene targets with a strong promoter enrichment for Hsf1-binding sites (p-value < 10^{-9}). The ChIP-seq analysis identified none of the 12 NET-seq-only gene targets while it identified all 18 gene targets corroborated by NET-seq and RNA-seq (p-value < 10^{-42}) (Figure 2.2B and S2.2H). Importantly, the genes defined by combined NET-seq/ChIP-seq analysis showed a strong correlation between fold decrease in transcription and ChIP enrichment (Figure 2.2C and S2.2I), arguing that Hsf1 binding to their promoters drives their basal expression.

In summary, we combined three genome-wide approaches (NET-seq, RNA-seq, and ChIP-seq) to define 18 Hsf1-dependent genes (HDGs) (Figure 2.2B), which collectively encode two Hsp70 paralogs (*SSA1* and *SSA2*), both Hsp90 paralogs (*HSC82* and *HSP82*), nucleotide exchange factors and co-chaperones for Hsp70 and Hsp90 (*YDJ1*, *SIS1*, *FES1*, *AHA1*, *HCH1*, *STI1, CPR6*), nuclear and cytoplasmic aggregases (*BTN2, CUR1,* and *HSP42*), mitochondrial protein folding factors (*HSP78*, *MDJ1*), a disaggregase (*HSP104*), and a cell cycle transcriptional regulator (*MBF1*). Bioinformatic analysis of HDG promoters revealed a strong enrichment for consensus Hsf1 binding

sites (Sorger and Pelham, 1987) (p-value < 10^{-10}), and gene ontology analysis revealed a strong enrichment for protein folding function (*p*-value < 10^{-21}) (Figure 2.2D). We note that our analysis excludes genes that are regulated by Hsf1 under non-basal conditions, genes that Hsf1 controls redundantly with other transcription factors and genes that utilize Hsf1 as a pioneer factor (Fujimoto et al., 2012) (i.e., genes for which Hsf1 sets up favorable chromatin conditions for other factors to drive transcription). We conclude that Hsf1 drives a compact transcriptional program in basal conditions.

The majority of the yeast heat shock response is Hsf1-independent.

We considered the possibility that Hsf1-AA cells attempt to counteract proteotoxicity induced by prolonged rapamycin treatment by secondary changes in gene expression. Indeed, RNA-seq revealed that prolonged rapamycin treatment, which we defined as a comparison between 4 hours and 1 hour of treatment, caused a >4-fold induction of ~200 genes (Figure S2.3A), including >7-fold induction of 4 HDGs (*HSP42*, *HSP72*, *HSP104* and *HSP82*). Bioinformatic analysis suggested these changes were part of a multifaceted response, significantly enriched for factors associated with alternative metabolism and various stress responses, including heat shock (Figure S2.3B). To identify the regulators of this response, we computationally analyzed the promoters of induced genes to identify enriched sequence motifs (Carlson et al., 2007), which were cross-referenced with the known sequence specificities of yeast transcription factors (de Boer and Hughes, 2011). This analysis defined a highly enriched (p-value < 10^{-34}), ubiquitous motif that was found in 78% of induced genes, including the 4 strongly up-regulated HDGs (Figure S2.3C).

This motif corresponded to the consensus binding site for Msn2 and Msn4 (jointly Msn2/4), two redundant transcription factors activated by a variety of environmental stresses, including heat shock (Causton et al., 2001; Schmitt and McEntee, 1996). Msn2/4 activity is regulated by Protein Kinase A (PKA), which phosphorylates Msn2/4 under non-stress conditions preventing their nuclear entry (Görner et al., 1998). To test if Msn2/4 activation mimics gene activation induced by prolonged rapamycin treatment, we treated cells expressing analog-sensitive PKA (PKAas) with the cell-permeable ATP-analog 1-NM-PP1, an established chemical genetics approach for inducing Msn2/4 nuclear localization (Hao and O'Shea, 2012). RNA-seq analysis revealed that 1-NM-PP1 treatment of PKAas cells was well correlated with prolonged rapamycin treatment (R^2 = 0.70, Figure S2.3D). Specifically, Msn2/4 targets, as well as the up-regulated HDGs, comprised the vast majority of genes induced by both treatments. Comparative analysis of PKAas *msn2Δ msn4Δ* cells established that Msn2/4 targets (p-value < 10^{-103}) were significantly attenuated (Figure S2.3E and F). These data show that PKA inhibition mimics gene expression changes induced by prolonged rapamycin treatment.

Figure 2.3: Induction of most genes by heat shock is Hsf1-independent and Msn2/4-dependent.

(A) Hsf1-AA cells were grown logarithmically at 30°C or heat shocked (39°C for 30') prior to harvesting for analysis by RNA-seq. In a separate experiment, Hsf1-AA cells were treated with rapamycin for either 60' or 240' at 30°C prior to harvesting for analysis by RNA-seq. Shown is a gene scatter plot of mRNA changes induced by prolonged rapamycin treatment (240' vs. 60') (y-axis) versus changes induced by heat shock (x-axis). Msn2/4 targets were defined as genes with at least one Msn2/4 promoter binding site (AGGGG) that were in the top 10% of genes induced by Pka-inhibition (see Figure 2.3D). **(B)** Left: Locations of predicted bindings sites for Hsf1 (TTCnnGAA and TTC-n_7-TTC-n_7-TTC) and Msn2/4 (AGGGG) in HDG promoters. Right: Hsf1-AA cells were grown logarithmically at 30°C (control) or treated with rapamycin (30°C for 30') followed by heat shock (39°C for 30') prior to harvesting for RNA-seq analysis. Shown are HDG mRNA changes induced by sequential treatment relative to control. **(C)** Hsf1-AA cells were grown logarithmically at 30°C (control) or treated with either rapamycin (30' at 30°C) and then heat shock (39°C for 30') or carrier-only and then heat shock prior to harvesting for RNA-seq analysis. Shown is a gene scatter plot of mRNA changes induced by the two treatments relative to the control. **(D)** Hsf1-AA PKAas cells were grown logarithmically at 30°C (control) or treated with heat shock (39°C for 30') or the PKA inhibitor 1-NM-PP1 (30°C for 30') prior to harvesting for RNA-seq analysis. Shown is a gene scatter plot comparing mRNA changes induced by these two treatments relative to control. **(E)** Hsf1-AA PKAas cells were grown logarithmically at 30°C (control) or after treatment with either rapamycin (30' at 30°C) and then 1-NM-PP1 (30' at 30°C) or carrier-only and then 1-NM-PP1 prior to harvesting for RNA-seq analysis. Shown is a gene scatter plot comparing mRNA changes induced by these two treatments relative to control. **(F)** Left: HDG promoter locations of Hsf1 and Msn2/4 binding sites as in part (B). Right: Hsf1-AA PKAas cells were grown logarithmically at 30°C (control) or after treatment with rapamycin (30' at 30°C) and then 1-NM-PP1 (30' at 30°C) prior to harvesting for RNA-seq analysis. Shown are HDG mRNA changes induced by sequential treatment relative to control.

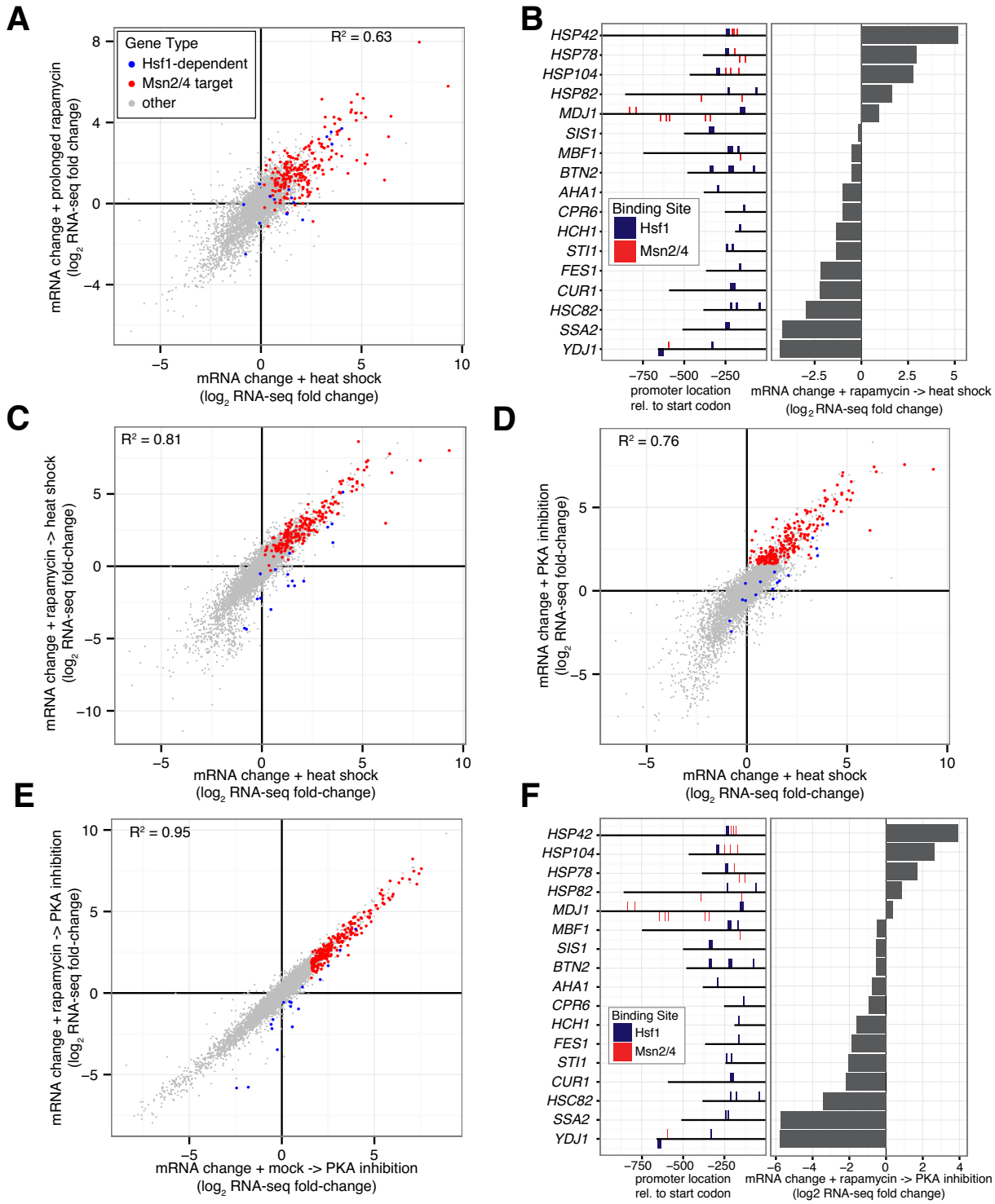

Figure 2.3: (Continued)

Hsf1 has an eponymous association with the heat shock response. However, when we measured the effect of heat shock on mRNA abundance, we observed a remarkable resemblance between the heat shock response and the response to prolonged rapamycin treatment (Figure 2.3A). While previous work has suggested that heat shock expands the scope of Hsf1 gene targets (Eastmond and Nelson, 2006; Hahn et al., 2004), the similarity between these two responses suggested that gene induction by heat was largely Hsf1-independent and Msn2/4-dependent. To test this, we used NET-seq and RNA-seq to measure the effect of a short rapamycin pre-treatment on the heat shock response of Hsf1-AA cells . Consistent with our previous observations, HDGs with multiple Msn2/4 binding sites were still induced by heat shock while the remaining HDGs were repressed (Figure 2.3B). Genome wide, the heat shock response remained generally intact in the absence of nuclear Hsf1 ($R^2 = 0.81$), including activation of Msn2/4 targets (Figure 2.3C). This was supported by our ChIP-seq analysis of Hsf1 promoter occupancy during heat shock, which revealed a list of target genes that significantly overlapped the list of basal targets (p-value $< 10^{-59}$) (Figure S2.2G). Unfortunately, our efforts to exploit Hsf1-AA to rigorously define the proximal transcriptional effects of Hsf1 inactivation on the heat shock response were hampered by their convolution with other indirect, secondary changes that we attribute to severe proteotoxicity (see Extended Discussion). Nonetheless, these data argue that in terms of gene target number, the role of Hsf1 is not significantly expanded by heat stress.

To further probe Hsf1's role in gene induction by heat but without actually using heat as a stimulus, we took advantage of the known observation that heat shock and PKA inhibition have similar effects on cell growth, protein synthesis and the activity of multiple transcription factors, including Msn2/4 (Causton et al., 2001; Smith et al., 1998; Thevelein, 1999). Indeed, 1-NM-PP1 treatment of PKAas Hsf1-AA cells induced a change in the transcriptome that resembled the heat-shock response ($R^2 = 0.76$) (Figure 2.3D), as well as prolonged rapamycin treatment (Figure S2.3D). Yet, unlike these responses, this one was not associated with apparent proteotoxicity, as measured by mCherry-ubc9^{ts} aggregation (Figure S2.3H). Strikingly, rapamycin pre-treatment of PKAas Hsf1-AA cells had a relatively minor effect on genome-wide expression changes induced by 1-NM-PP1 treatment ($R^2 = 0.95$) (Figure 2.3E) including the induction of Msn2/4 targets (Figure S2.3I). With the exception of HDGs with multiple Msn2/4 binding sites in their promoters, rapamycin still led to the expected decline in HDG expression (Figure 2.3F). These data support the notion that Msn2/4 drive expression of the majority of heat shock-induced genes independent of Hsf1.

Mammalian HSF1 drives a core transcriptional program of 9 genes during heat shock.

Mammalian cells have multiple heat shock factors (e.g., HSF1, 2, 4, 5, X and Y in the human genome) homologous to yeast Hsf1 (Akerfelt et al., 2010). None are normally essential for viability in the absence of stress, but loss of HSF1 uniquely renders cells heat sensitive and unable to acquire thermotolerance (McMillan et al., 1998; Zhang et al.,

2002). Comparison of heat-induced changes in mRNA abundance measured by DNA microarray analysis in wild-type mouse embryonic fibroblasts (MEFs) versus those derived from a *hsf1*$^{-/-}$ mouse has led to a long list of HSF1-dependent genes (Trinklein et al., 2004). To define what fraction of these changes represent the core HSF1 transcriptional program that is shared across many cell types and differentiation states, we used CRISPR/Cas9-mediated genome editing to generate *hsf1*$^{-/-}$ mouse embryonic stem cells (mESCs) and *hsf1*$^{-/-}$ MEFs (Figure S2.4A, B). Next, we measured mRNA abundance by RNA-seq in *hsf1*$^{-/-}$ mESCs and MEFs in reference to their wild type counterparts both in unstressed cells and following heat shock. In unstressed cells, the transcriptomes of the wild type and *hsf1*$^{-/-}$ cells were remarkably similar (Figure S2.4C). Only 2 genes were significantly upregulated and 2 genes were significantly downregulated in both cell types (both p-values = 0.33) (see Experimental Procedures), approximately the number of significant observations you would expect by random chance. There was no functional enrichment among these genes, and none encode chaperones. We conclude that HSF1 has little or no effect on basal transcription that is common to both mESCs and MEFs.

Figure 2.4: Mammalian HSF1 enables heat induction of a chaperone network similar to the yeast HDG network.
(A) Wild-type mouse embryonic stem cells (mESCs) and mouse embryonic fibroblasts (MEFs) were cultured at 37°C (control) or treated with heat shock (42°C for 60') prior to harvesting for RNA-seq analysis. Shown is a gene scatter plot of mRNA abundances in treated versus control samples for each cell type. Dark lines indicate statistical thresholds used to define genes with significant changes in expression (see Experimental Procedures) and genes with significant changes in both cell types are colored. Also indicated are gene names of HSF1-dependent genes (HDGs) defined by additional experiments and analyses (see Figures 2.4B and 2.4C and Experimental Procedures). **(B)** Wild-type (WT) and *hsf1*$^{-/-}$ mESCs and MEFs were heat shocked (42°C for 60') and then analyzed by RNA-seq. Shown is a gene scatter plot of mRNA abundances in heat shocked WT versus *hsf1*$^{-/-}$ cells for each cell type. For definition of dark lines and gene names see part (A). **(C)** Venn diagram comparing genes in mESC and MEFs that are significantly induced by heat shock in WT cells (purple) with genes whose expression is significantly reduced during heat shock in *hsf1*$^{-/-}$ vs. WT cells. HDGs are defined as genes in the 4-way intersection and their names indicated. **(D)** and **(E)** Mammalian and yeast HDG protein-protein interaction network (se Experimental Procedures). **(F)** Wild-type, *hsf1*$^{-/-}$, *hsf2*$^{-/-}$, and *hsf1*$^{-/-}$ *hsf2*$^{-/-}$ MEFs were cultured at 37°C prior to harvesting for RNA-seq analysis. Shown are mRNA abundances for HDGs in each cell line.

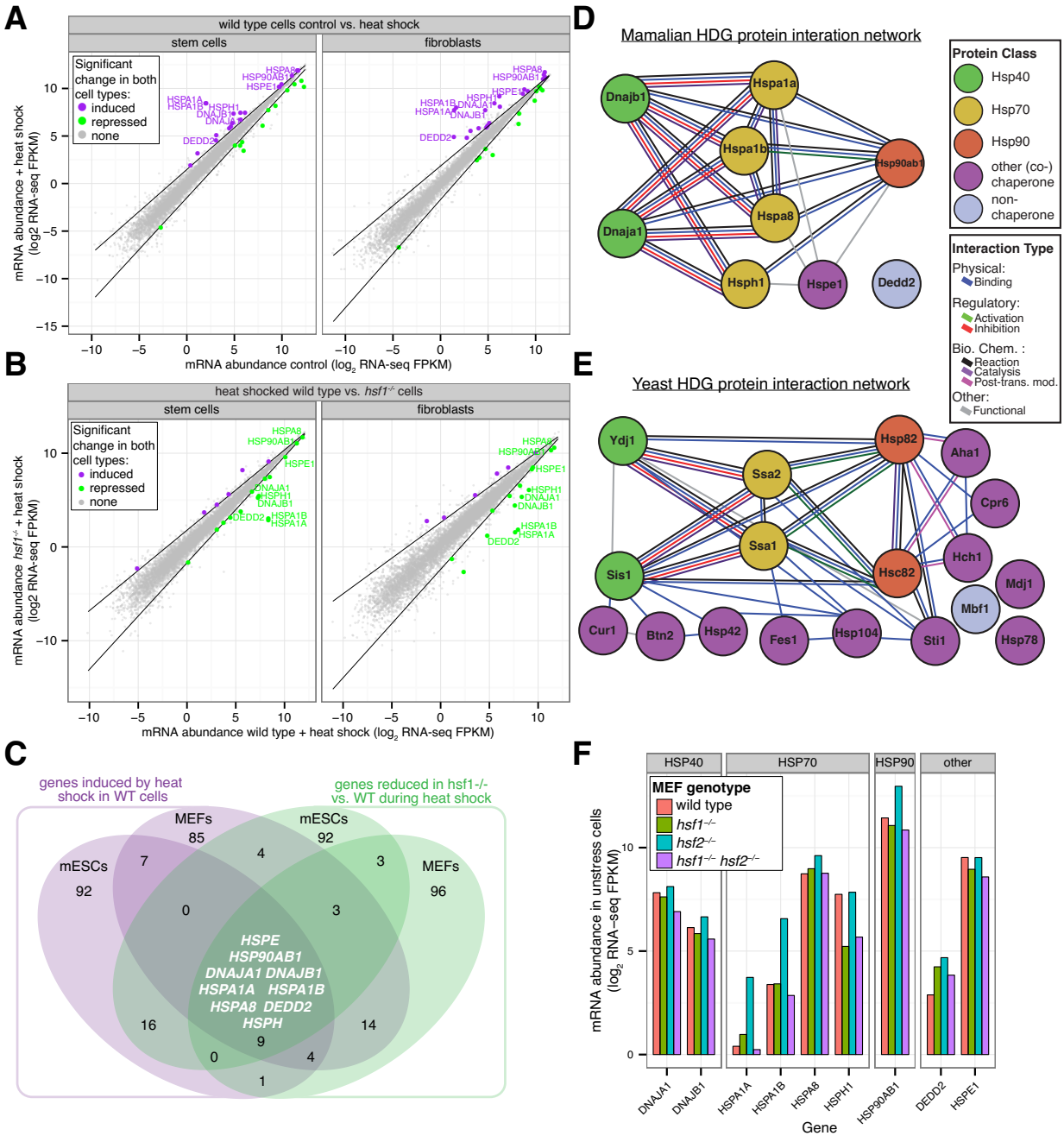

Figure 2.4: (Continued)

To define HSF1's core transcriptional program during heat shock, we first asked which genes are heat-induced in both wild type mESCs and MEFs and found 20 genes (p-value $< 10^{-18}$), many of which encode chaperones (Figure 2.4A). Next we asked which genes showed reduced expression in *hsf1*$^{-/-}$ cells compared to wild type cells following heat shock in both mESCs and MEFs and found 15 genes (p-value $< 10^{-11}$), again including many chaperone genes (Figure 2.4B). By intersecting these two gene lists, we found only nine genes that were induced by heat shock in both wild type mESCs and MEFs and repressed in both heat shocked *hsf1*$^{-/-}$ cell types (Figure 2.4C). We define these nine genes as the core mammalian HSF1-dependent genes (HDGs) and note that 8/9 form a densely linked interaction network with the cytosolic Hsp40, Hsp70 and Hsp90 chaperones at its center (Figure 2.4D). The structure of this network is remarkably similar to the one formed by yeast HDGs (Figure 2.4E).

Hsf1 is the sole heat shock factor in yeast that controls both basal and heat-induced expression of HDGs. By contrast, mammalian HSF1 is dispensable for high basal expression of HDGs. We wondered if HSF2, the only other HSF paralog with detectable expression in both the mESCs and the MEFs was responsible. Thus, we generated *hsf2*$^{-/-}$ MEFs and *hsf1*$^{-/-}$ *hsf2*$^{-/-}$ double mutant MEFs and measured mRNA abundance by RNA-seq in unstressed cells in comparison wild-type and *hsf1*$^{-/-}$ MEFs. In the absence of HSF2, mRNA levels for 3 HDGs—two Hsp70 homologs (HSPA1A and HSPA1B) and one Hsp90 homolog (HSP90AB1)—were significantly up-regulated (p-value $< 10^{-4}$) (Figure S2.4D), but we found that the basal expression of all HDGs in *hsf1*$^{-/-}$ *hsf2*$^{-/-}$ MEFs was

similar to wild-type (Figure 2.4F and S2.4E). Taken together, these data strongly argue that the HSF family does not control basal expression of chaperones in MEFs.

A synthetic transcriptional program bypasses Hsf1's essential function.

In mammalian cells, high HSF1-independent basal expression of chaperone genes may explain why HSF1 is not essential in the absence of stress. This prompted us to ask if the essential function of yeast Hsf1 can be obviated by constitutive expression of HDGs from strong, Hsf1-independent promoters driven by distinct transcription factors. To this end we constructed four plasmids carrying in total 15 HDG ORFs—to simplify construction, we excluded *SSA1*, *HSP82,* and *HCH1* because they are redundant with their paralogs (*SSA2*, *HSC82* and *AHA1*, respectively)—under the control of promoters from highly expressed housekeeping genes (Figures 2.5A and S2.5A). We termed these "synthetic HDGs" (synHDGs). Consistent with the idea that HDG expression provides negative Hsf1 feedback to maintain proteostasis, we found that Hsf1-AA cells expressing synHDGs had reduced Hsf1 basal activity (Figure S2.5B). Strikingly, even in the presence of rapamycin these cells continued to robustly proliferate (Figure 2.5B) and no longer formed visible mCherry-ubc9^{ts} aggregates (Figures 2.5C and S2.5C). To test if constitutive expression of chaperones can enable cells to live in the complete absence of Hsf1, we introduced synHDG expression plasmids into *hsf1Δ* cells carrying a Hsf1 expression plasmid. Following plasmid shuffling, we found that a *hsf1Δ* strain expressing synHDGs grew comparably to a strain from a control shuffle with a second Hsf1 expression plasmid

(Figure S51.D). Further, RNA-seq analysis did not reveal any coherent secondary changes to gene expression between these strains (Figure S2.5E).

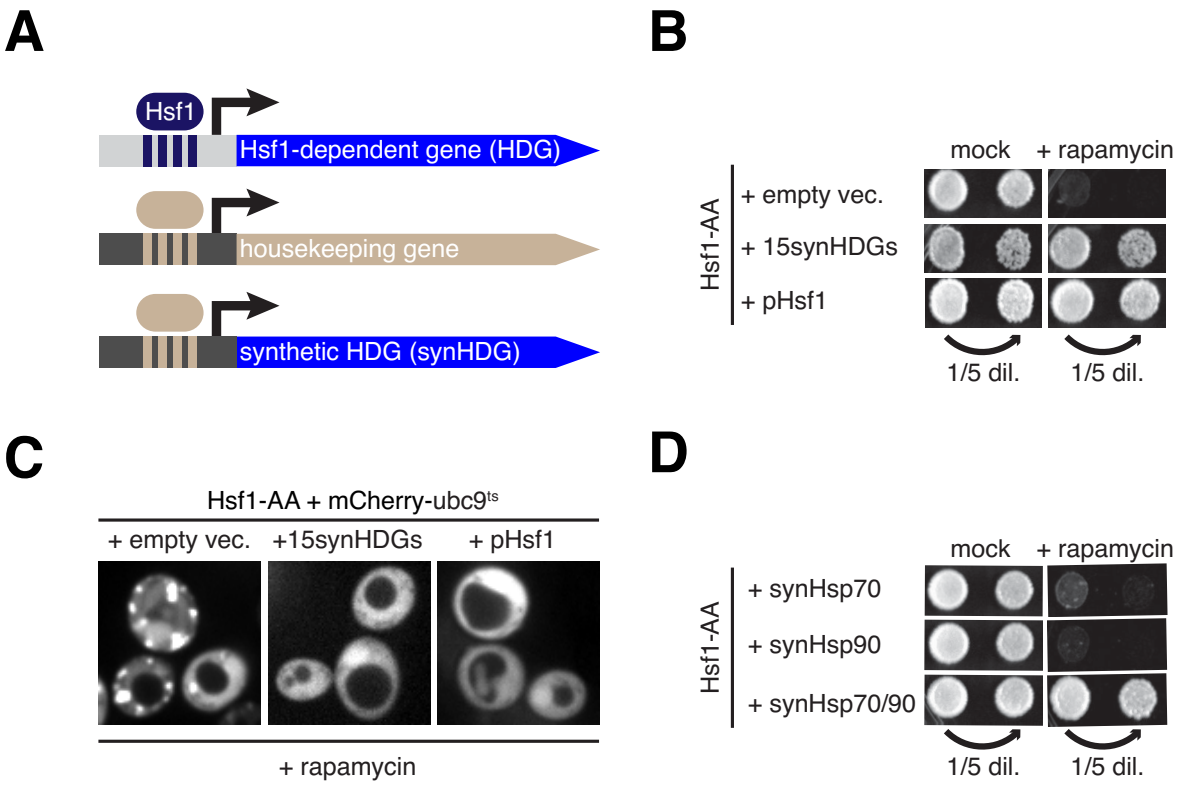

Figure 2.5: A synthetic transcriptional program reveals the essential function of Hsf1.
(A) Schematic of promoter swapping strategy for constitutive expression of Hsf1 targets from strong Hsf1-independent promoters. See Supplementary Figure 2.4A for details. **(B)** Hsf1-AA cells with indicated plasmids were spotted at two concentrations onto rapamycin or mock (carrier-only) plates. Shown are images of plates incubated for 5 days at 30°C. **(C)** Representative confocal micrographs of Hsf1-AA cells expressing plasmid-borne mCherry-ubc9^{ts} and indicated plasmids taken after treatment with rapamycin (360' at 30°C). **(D)** Hsf-AA cells with indicated transgenes were spotted at two concentrations onto rapamycin or mock (carrier-only) plates, which also contained β-estradiol to drive synHsp expression from β-estradiol-dependent promoters (see Experimental Procedures for details). Shown are images of plates incubated for 5 days at 30°C.

The essential function of Hsf1 is to drive high basal co-expression of Hsp70 and Hsp90.

To determine if all 15 synHDGs were necessary to bypass the essential function of Hsf1, we transformed Hsf1-AA cells with subsets of the four expression plasmids and found that only two of the four were necessary (Figure S2.5F): the plasmid containing *SSA2* (Hsp70) along with three other synHDGs, and the plasmid containing *HSC82* (Hsp90) and two other synHDGs. By deleting individual synHDGs on these two plasmids, we found that that only *SSA2* and *HSC82* were indispensable for Hsf1 bypass (Figure S2.5G). Impressively, co-expression of just *SSA2* and *HSC82*—but neither gene expressed alone—from a strong, Hsf1-independent promoter enabled Hsf1-AA cells to robustly grow without apparent mCherry-ubc9^{ts} aggregation in the presence of rapamycin (Figures 2.5D and S2.5H). These data demonstrate that the minimal essential function of Hsf1 is to drive high basal gene expression of Hsp70 and Hsp90. While it may not be surprising that cells require high levels of Hsp70 and Hsp90 to live, it is remarkable that Hsf1's required contribution to cell viability can be pared down to the expression of only two chaperone genes.

Hsf1 activity is adjusted to the state of protein folding in the cell (Anckar and Sistonen, 2011; Wu, 1995). By contrast, Hsf1-AA cells expressing synHDGs lack this transcriptional feedback and should be susceptible to proteotoxic stress in the presence of rapamycin. Consistent with this notion, we found that Hsf1-AA cells expressing the synHDGs showed marked growth impairment on rapamycin plates at the elevated temperature of 37ºC

compared to cells expressing untagged Hsf1 (Figure 2.5I). As an attempt to improve growth at 37ºC, we introduced additional copies of *synSSA2* and *synHSC82* but observed only a modest improvement (Figure 2.5I). These data argue that coordinated homeostatic control of HDG expression by Hsf1 is required for fitness at elevated temperature.

Discussion

Heat shock factors make up one of the most conserved families of sequence-specific transcription factors (Wu, 1995). In all eukaryotes that have been examined they have been implicated in the induction of heat shock protein (HSP) genes as a response to proteotoxic stress. However, mechanistic dissection of this deeply conserved core function has been challenging because members of this family have been deployed differentially through evolution to perform specific functions. In particular, yeast Hsf1 performs an essential function in all conditions, while mammalian HSF1 is dispensable for normal cell growth but becomes essential during oncogenic transformation (Dai et al., 2007). Here we used comparative genomics to understand how yeast Hsf1 and mammalian HSF1 have diverged from each other.

Lack of a suitable tool for acutely inactivating yeast Hsf1 has been a major obstacle to defining its function. Hsf1 inactivation by existing tools—partial loss-of-function Hsf1 mutations and *HSF1* promoter shut-off—is either chronic or conditionally slow, raising the possibility that secondary gene expression changes have complicated assignment of Hsf1 target genes in the literature. To get around these issues, we used “Anchor Away”

(AA) to induce rapid Hsf1 nuclear export following rapamycin addition (Hsf1 AA, for short) and studied the immediate and long-term transcriptional consequences at the physiological temperature. This temporal distinction was important because Hsf1 AA immediately affected transcription of a small number of genes only to later cause a genome-wide, general stress response (Figures 2.2A and 2.3A). At the cellular level, Hsf1 AA led to the accumulation of protein aggregates coincident with growth arrest and ultimately cell death. These observations are a hallmark of proteostasis collapse but they don't resolve whether Hsf1 AA induced eventual cell death due to toxic protein aggregates or whether protein aggregation was a futile cytoprotective response. We favor the mechanistic explanation that Hsf1 AA causes a global reduction in chaperone concentration leading to cytotoxicity due to protein misfolding. Future studies employing a recently developed proteomic approach for defining the composition cytoprotective protein aggregates induced by heat should help to resolve this issue (Wallace et al., 2015).

By combining information from three independent genome-wide approaches (NET-seq, RNA-seq, ChIP-seq), we were able to define an unexpectedly small number of HDGs. Remarkably, overlapping targets defined by 2/3 pairs of these approaches (NET-seq versus RNA-seq and NET-seq versus ChIP-seq) yielded the same set of HDGs (Figure 2.2B), while the intersection of targets defined by the remaining pair (ChIP-seq versus RNA-seq) included only two additional genes whose known functions are unrelated to protein folding (Figure S2.2J). Interestingly, for nearly half of the genes defined by NET-

seq analysis but no other approach (12/30 genes), the cross-correlation with RNA-seq was poor (R^2 = .007) (Figure S2.2D), and we could not detect significant Hsf1 promoter binding at these genes (Figure 2.2B). In stark contrast, for the HDGs defined by our multi-faceted approach, transcriptional changes induced by Hsf1 AA were well cross-correlated with both changes in mRNA abundance (R^2 = 0.71) (Figure S2.2D) and Hsf1 promoter occupancy (R^2 = 0.57) (Figure 2.2C). This argues that even the powerful combination of chemical genetics and genome-wide analysis is by itself insufficient to accurately predict transcription factor gene targets. However, we found that corroboration of putative target genes by an independent genomic approach yielded a great increase in specificity and reproducibility, without any apparent decrease in sensitivity, even when the number of targets defined by each approach differed significantly (Figure S2.2J). Our study should serve as a roadmap for revisiting other transcription factor target lists, as well as defining the gene targets of poorly characterized transcription factors.

We also found that prolonged Hsf1 AA triggered a global change in gene expression resembling the heat shock response. Controlled heat shock experiments and a chemical genetics approach that mimics heat as a stimulus revealed the heat shock response remains largely intact upon Hsf1 AA. Thus, despite its eponymous association with heat shock, the majority of the yeast heat shock response is the job of distinct general stress responsive transcription factors. Retrospectively, our study illustrates how earlier genomic approaches to dissect out Hsf1 gene targets from the complexities of the heat shock response have obscured the simplicity of Hsf1's role in maintaining proteostasis: Hsf1

tunes expression of a compact regulon according to the protein folding needs of the cell. Our work also provides a complementary perspective to an earlier yeast proteomic analysis of proteins induced by cytosolic expression of a misfolded mutant protein, which post-hoc analysis revealed are strongly enriched for HDGs (12/27 are HDGs; p-value < 10^{-21}) (Geiler-Samerotte et al., 2011). Although Hsf1's contribution to proteotoxic stress is limited, it is critical, as cells we engineered to bypass Hsf1's essential function with constitutive basal expression of synHDGs have diminished fitness at elevated temperature. This now provides a starting platform for introducing negative transcriptional feedback control of synHDGs to enable full functional replacement of Hsf1 with a synthetic proteostasis circuit.

Yeast Hsf1 is part of an essential transcriptional feedback loop that operates even at the physiological temperature. By contrast, we found that the mammalian HSF family is dispensable for cell growth in the absence of stress in two independent mouse cell types. The HSF1 core transcriptional program comprised nine genes and was only revealed following heat shock. Remarkably, 8/9 genes encoded chaperones that are organized into a strikingly similar functional network as the yeast HDGs. This provides a satisfying denouement for the previous seminal discovery that a constitutively active mutant of human HSF1 enables yeast cells to live without Hsf1 (Liu et al., 1997). We speculate that HSF1 is dispensable in unstressed mammalian cells because a distinct transcription factor or factors maintain high basal expression of HSPs. This raises the interesting possibility that multi-cellular organisms evolved a larger chaperone buffer under basal

conditions by uncoupling expression of HSPs from HSF1 while still maintaining HSP expression control by HSF1 under extreme conditions. Malignant growth is a case in point because in this context HSF1 inhibition results in cell proliferation arrest (Dai et al., 2007) and the accumulation of toxic protein aggregates (Tang et al., 2015). Surprisingly, HSF1 appears to drive a transcriptional program distinct from heat shock in cancer cells—both in tumor cells and the supporting stroma (Mendillo et al., 2012). Establishing the oncogenic contribution of HSF1 core gene targets defined by our work versus the cancer-specific gene targets is an important future goal. By demonstrating the superior contribution of Hsp70 and Hsp90 to Hsf1-mediated proteostasis in yeast, our work also provides the impetus for testing whether Hsp70 and Hsp90 inhibitors have synergistic anti-neoplastic effects on HSF1-dependent cancers.

Extended Discussion

Induction of heat shock proteins (HSPs) is the historic hallmark of the heat shock response, conserved from yeast to man (Richter et al., 2010). More recent studies in yeast, however, have revealed that heat shock induces vast gene expression changes by both transcriptional and post-transcriptional mechanisms (Pleiss et al., 2007; Rose et al., 2016). HSP heat induction is the complicated product of combinatorial transcriptional control by Hsf1 and Msn2/4 according to the current view (Boy-Marcotte et al., 1999b; Gasch et al., 2000; Treger et al., 1998). However, the overall scope of Hsf1's role in the heat shock response has not been established.

To measure Hsf1-dependent gene expression during heat shock, we used NET-seq and RNA-seq to monitor the effect of a brief rapamycin pre-treatment on the heat shock response of Hsf1-AA cells. This analysis revealed a much larger number of changes than we had observed by rapamycin treatment of cells in the absence of stress, which necessitated changes to our statistical analysis (see Experimental Procedures). We defined a set of 295 genes that had significantly reduced transcription and mRNA abundance in comparison to heat shock of mock pre-treated cells (Figure S2.3J). Gene ontology analysis revealed enrichment for various protein synthesis and metabolic functions (Figure S2.3K) while promoter analysis revealed enrichment (p-value $< 10^{-64}$) for binding sites of Sfp1, a canonical regulator of ribosome biogenesis (Fingerman et al., 2003; Jorgensen et al., 2004; Marion et al., 2004). In fact, 103/295 affected genes were

ribosomal protein genes (RPGs) (enrichment p-value < 10^{-116}) (Nakao et al., 2004), which heat shock normally represses and which were repressed even further as a gene set by rapamycin pre-treatment ($p < 10^{-64}$) (Figure S2.3L). An additional 144 affected genes had predicted Sfp1 binding sites in their promoters (Figure S2.3J,K) suggesting co-regulation with RPGs through heat inactivation of the transcriptional activator Sfp1 (Marion et al., 2004). One potential explanation for the genome-wide over-repression of Sfp1 gene targets is that rapamycin pre-treatment potentiates the strength of heat as a stimulus, similar to the way in which partial loss-of-function mutations in Hsf1 sensitize cells to heat stress (Imazu and Sakurai, 2005; Morano, 1999; Morano et al., 1999; Smith and Yaffe, 1991). As an independent test of this idea, we re-visited heat shock induced gene induction by Msn2/4 and found a significant over-induction of Msn2/4 gene targets relative to all other genes (p-value < 10^{-46}) (Figure S2.3L). We conclude by speculating that even a short rapamycin pre-treatment of Hsf1-AA cells reduces chaperone expression enough to potentiate regulation of Sfp1 and Msn2/4 gene targets by heat-induced proteotoxicity.

Having found no compelling evidence that Hsf1 directly regulates 247/295 genes defined by our gene expression analysis we looked more closely at the remaining 48. Among these, we found a subset of basal HDGs (6/18), all but one of which lacked Msn2/4 binding sites in their promoters. We note that the 18 basal HDGs, as an entire set, had a significant ~5-fold decrease in median mRNA abundance (p-value < 10^{-6}) relative to all other genes (Figure S2.3L). Along the same lines, heat shock induction of *SSA3* and *SSA4,* which encode Hsp70 paralogs that lack significant basal expression at 30ºC, was

strongly reduced by rapamycin pre-treatment (Figure S2.3J). Lastly, we found no common themes by either promoter motif or gene ontology analysis among the remaining 40 affected genes (Figure S2.3K). We note that the size of this seemingly random gene set is consistent with the false discovery rate (FDR) for our statistical analysis (at our theoretical 1% FDR, we would expect ~46 false discoveries by chance from the total population of 4590 detected genes).

To independently test if Hsf1-dependent genes defined by the NET-seq/RNA-seq analysis of heat shock are *bona fide* Hsf1 gene targets, we measured Hsf1 DNA binding during heat shock by chromatin immunoprecipitation followed by deep sequencing (ChIP-seq). As before, we isolated chromatin using tandem affinity purification of dual epitope-tagged Hsf1-FLAG-V5 expressed as the only copy of Hsf1 in an otherwise wild type genetic background. Analysis using a stringent peak-calling algorithm (see Experimental Procedures) defined 32 Hsf1 gene targets, including all 18 HDGs (p-value < 10^{-36}) and, more broadly, 27/40 genes we previously defined by ChIP-seq analysis of basal targets (p-value < 10^{-59}) (Figure S2.3G). By contrast, only 8 of these gene targets were among the 296 genes defined by our heast shock gene expression analysis: 5 of the original 18 basal HDGs, *SSA4, SSE1* (a member of the Hsp110 branch of the Hsp70 family), and *HSP10* (a mitochondrial matrix co-chaperonin). We note that for certain non-HDGs in this overlapping set (*e.g., SSE1*) under basal conditions we detected significant Hsf1 promoter binding and Hsf1 AA was associated with small—but not statistically

significant—decreases in their expression (Figure S2.2I), thus raising the possibility that they make a small but real fitness contribution as HDGs even in the absence of stress.

In summary, our combined NET-seq/RNA-seq/ChIP-seq analysis provides little evidence for significant expansion of Hsf1's gene targets beyond HDGs during heat shock. Rather, it argues that Hsf1's primary role during heat shock is to overexpress key chaperones that are already under its basal control.

Experimental Procedures

Yeast strains and plasmids.

Yeast strains and plasmids used in this work are described in Table S2.1 and Table S2.2, respectively.

Stable genome modifications. All strains are in the W303 genetic background. PCR-mediated gene deletion and gene tagging was carried out as described (Longtine et al., 1998). Cassettes for β-estradiol-dependent expression of *HSC82* and *SSA2* were targeted to the *HIS3* locus by homologous recombination as described (Sikorski and Hieter, 1989).

FRB tagging. Constructs for FRB and FRB-GFP tagging with either the *HIS3* or *KANMX* marker genes were obtained from EUROSCARF and described elsewhere (Haruki et al., 2008).

Hsf1 reporter. *Pr_{TEF2}-mKATE–URA3–4×HSE-Pr_{CYC1}-GFP* was PCR amplified from genomic DNA obtained from previously described strains containing the Hsf1 reporter (Brandman et al., 2012) and integrated into the *ura3-1* locus. *URA3* was eliminated from the reporter cassette in VDY2595 by transforming cells with a PCR amplicon of the *ura3-1* locus of wild-type W303 and counterselecting for *ura3*$^-$ transformants on 5-FOA.

pHsf1 construction. PCR amplicon comprising the Hsf1 promoter, open reading frame and 3' UTR obtained from wild-type yeast genomic DNA (Novagen) was ligated into BamHI-linearized pRS413 (Sikorski and Hieter, 1989) using Gibson assembly (Gibson et al., 2009) to generate pVD476. A second construct with an alternate marker gene was generated by subcloning the NotI/XmaI fragment of pVD476 into the corresponding sites on pRS412 (Brachmann et al., 1998) to generate pVD565.

mCherry-Ubc9 constructs. pESC vectors for expressing mCherry-Ubc9 wild type (pVD380) and -ubc9^{ts} (Ubc9 Y68L) (pVD381 and pVD632) were obtained from Stratagene and described elsewhere (Kaganovich et al., 2008).

pRS412 *ade2Δ::HPHMX.* To create the *HPHMX*-marked pRS41x-series plasmid pVD579, the backbone of pRS412 was digested to remove the BstAPI fragment (*ADE2* promoter and first 721bp of the ORF) and ligated to an HPHMX cassette amplicon from pAG32 (Goldstein and McCusker, 1999) by Gibson assembly (Gibson et al., 2009).

Construction of synHDG expression plasmids (pA-D). To engineer high levels of constitutive expression of Hsf1-dependent genes (HDGs) without Hsf1, we PCR amplified *ADH1, CYC1, PKG1, TDH3,* and *TEF1* promoters and HDG ORFs (with endogenous 3' UTRs) from genomic DNA (Novagen). Promoter sequences were first fused to the start codon of the HDG ORF by overlap-extension PCR (OE-PCR). Gibson assembly (Gibson et al., 2009) was then used to ligate promoter-ORF-UTR fusions into linearized *CEN/ARS* plasmids. The resulting plasmids were validated by sequencing. pA and pB vectors carrying single synHDG gene deletions were made by PCR-mediated gene deletion in yeast followed by plasmid recovery using a miniprep column (Qiagen) and sequence validation. Primer sequences used to construct pA-D are available upon request.

Construction of synHsp70/90 cassettes. To engineer β-estradiol-dependent expression of *HSC82* and *SSA2,* we PCR amplified ZEV promoter (consisting of 6×Z4 zinc-finger array binding sites (McIsaac et al., 2013)—Z_4BS—upstream of a minimal *CYC1*-promoter), *HSC82* and *SSA2* ORFs (with endogenous 3' UTRs), and an expression cassette for ZEV (a chimeric transcription factor comprising Z4 zinc finger array - estrogen receptor - VP16 activation domain that is activated by the hormone β-estradiol (McIsaac et al.,

2013)). ZEV promoter was fused to the start codon of the *HSC82* and *SSA2* ORFs by OE-PCR. Gibson assembly was then used to ligate ZEV promoter-ORF fusions (or a control empty ZEV promoter with no downstream ORF) and ZEV expression cassette into linearized pRS416 to generate pVD783-786. NotI/XhoI fragments from the resulting plasmids containing the control promoter, synHsp70, synHsp90, or both were subcloned into pNH605 to generate pVD794-797. SfiI digestion of the resulting plasmids produced Pr_{ScLEU2}–*CgLEU2*–ZEV–*6×Z₄BS-*Pr_{CYC1}-ORF(s)–3'-UTR_{ScLEU2} linear fragments that were each integrated separately at the *leu2* genomic locus by yeast transformation.

Yeast media and growth conditions.

Cells were grown at 30ºC with shaking unless noted otherwise. Plasmid selection was maintained at all times by growing cells in standard synthetic media lacking the appropriate amino acid(s)/nucleotide base(s). All synthetic media contained dextrose (2%) as the carbon source, except for those used to induce expression of $Ubc9^{wt}$ and $ubc9^{ts}$, which contained 2% raffinose + 2% galactose. All synthetic media were supplemented with 100mg/L adenine to suppress the growth defect and autofluorescence caused by the *ade2-1* mutation in the W303 genetic background, except for those used to select for *ADE2*-marked plasmids. All synthetic media contained ammonium sulfate as the nitrogen base, except for those used to select for *HPHMX*-marked plasmids, which contained 1g/L monosodium glutamate to enable selection with 200 mg/L Hygromycin B (Invitrogen).

Mammalian cell lines, tissue culture, genetic manipulation and validation.

Wild-type murine embryonic fibroblasts (MEFs) and embryonic stem cells (mESCs) were obtained from Jackson Laboratories (Immortalized MEFs: CBA316; mESCs: 129X1/SvJ strain).

Growth of mouse embryonic fibroblasts.

MEFs were cultured at 37ºC in DMEM with 10% FBS, antibiotics 100 µM nonessential amino acids (Invitrogen, 11140-050), 2 mM L-glutamine (Invitrogen, 25030-081) and 100 U/ml penicillin/100 µg/ml streptomycin (Invitrogen, 15140-122).

Growth and maintenance of pluripotent mouse embryonic stem cells.

mESCs were cultured on a feeder layer of mitomycin C-treated MEFs with 0.2% gelatinized (Sigma, G1890) tissue culture plates in ESC media containing DMEM-KO (Invitrogen, 10829-018) supplemented with 15% fetal bovine serum, 1000 U/ml LIF (ESGRO, ESG1106), 100 µM nonessential amino acids (Invitrogen, 11140-050), 2 mM L-glutamine (Invitrogen, 25030-081), 100 U/ml penicillin, 100 µg/ml streptomycin (Invitrogen, 15140-122), and 8 nL/ml of 2-mercaptoethanol (Sigma, M7522).

Generation of *hsf1*$^{-/-}$ cell lines using CRISPR/Cas9. A single guide RNA (sgRNAs) targeting exon 1 of murine *HSF1* was designed using the Broad Institute Web interface (Doench et al., 2014). A single plasmid based on the pcDNA3-hCas9 plasmid (Mali et al., 2013) that includes both Cas9 expressed from the CMV promoter and the sgRNA

expressed from the U6 promoter was transiently transfected into immortalized MEFs and mESC. Following NEO selection for plasmid uptake, single cells were obtained by limiting dilution and allowed to grow into colonies. Colonies were picked by microdissection and allowed to proliferate in 6 well plates. Isolated lines were screened by PCR and sequencing for the presence of a lesion in exon 1.

Western blotting:

Whole cell lysates were prepared by treating cells with mammalian protein extraction reagent (M-PER, Life technologies) according to manufacturer's instructions. Lysate proteins were resolved by SDS-PAGE (4-15% gradient tris/glycine/SDS gel (BioRad) for 1 hour at 30 mA) and electroblotted onto PVDF membrane (Millipore) for 1 hour at 225 mA. Blots were blocked with Li-Cor blocking buffer (Li-Cor) and probed with anti-HSF1 (Cell Signaling #4356) and anti-ACT (Sigma A2066) primary antibodies. Blots were washed 3× with TBST and probed with anti-rabbit-800 IR conjugated secondary antibody (Li-Cor). Blots were scanned on the Li-Cor IR imaging system.

Immuno-flourescence.

Cells were seeded on 8-well chamber slides (Lab-Tek) for 18 hr prior to processing for immunofluorescence. Following cell fixation with 4% paraformaldehyde in PBS pH 7.4 for 10 minutes, slides were rinsed with phosphate-buffered saline (PBS) and blocked for 1 hr at room temperature with 0.5% bovine serum albumin (BSA) in PBS. After overnight incubation at 4°C with an anti-HSF1 rabbit antibody diluted 1:1000 (Cell Signaling #4356),

slides were washed three times (5 min each time) with PBS and then incubated for 1 hr at room temperature in a secondary anti-rabbit antibody labeled with Alexa Dye 488 diluted 1:1000 (Molecular Probes). Lastly, slides were washed three additional times with PBS before mounting them with antifade reagent containing DAPI (Life Technologies P-36931) and imaged using a Zeiss epifluorescence microscope with a 40x objective.

Yeast cell fluorescence microscopy.

ubc9^{ts} aggregation assay. VDY2130 cells transformed with pVD380 or pVD381 were inoculated into SG/R-LEU media and grown overnight to $OD_{600} \approx 0.1$. Cells were then treated with 10 μM rapamycin for the indicated times and then fixed in ice-cold 4% formaldehyde in PBS pH 7.4 for 10 minutes. Fixed cells were imaged with an oil-immersion 63×objective (63x, NA 1.4, oil Ph3, Plan - Apochromat) on an AxioObserver Z1 inverted microscope (Zeiss) equipped with a CoolSNAP-HQ CCD camera (Photometrics) and LED excitation (Colibri). Blinded images were background subtracted and at least 100 cells scored manually after local contrast optimization for mCherry foci using ImageJ. Note that local contrast optimization was necessary due to plasmid copy number variation, a known feature of 2μ plasmids, which resulted in some cells with very high expression of mCherry-Ubc9 fusions that dominated global contrast optimization.

VDY2578 transformed with pVD632 and 15synHDGs (pVD576, pVD577, pVD578 and pVD580) or pHsf1 (pRS412, pRS415, pVD476 and pVD579) or empty vectors (pRS412,

pRS413, pRS415 and pVD579) were assayed as above, except after growth in SG/R-ADE-HIS-LEU-URA containing 200 µg/ml hygromycin-B (Invitrogen).

VDY2130 transformed with pVD632 and cassettes from pVD794, 795, 796 or 797 were assayed as above, except after growth in SG/R-URA and pre-treatment with 10 μM β-estradiol.

Confocal live-cell microscopy. 96 well glass bottom plates were coated with 100 μg/ml concanavalin A in water for 1 hour, washed three times with water and dried at room temperature. 80 μl of low-density cells were added to a coated well. Cells were allowed to settle and attach for 15 minutes, and unattached cells were removed and replaced with 80 μl SD media. Imaging was performed at the W.M Keck Microscopy Facility at the Whitehead Institute using a Nikon Ti microscope equipped with a 100×, 1.49 NA objective lens, an Andor Revolution spinning disc confocal setup and an Andor EMCCD camera.

To monitor the effect of rapamycin on Hsf1-FRB-GFP localization in VDY1877, cells were logarithmically grown in SD media to maintain OD_{600} below 0.1 for 8 hours and attached to the glass bottom of a 96 well plate as described. Hsf1 nuclear depletion was performed with 1 μM rapamycin added directly to the 80 μl of media in the wells of the 96 well plate, and cells were imaged over time as described using the spinning disc microscope setup. Contrast was adjusted globally and images were cropped for presentation in Photoshop.

To monitor protein aggregation in live cells, identical strains were grown under the same conditions as the fixed protein aggregation assay and maintained at OD_{600} less than 0.1 for 8 at least hours before starting the treatments. Cells were attached to the glass bottom of a 96 well plate as described. For heat shock experiments, cells were incubated in the plate at 37ºC for 15 minutes before imaging. Hsf1 nuclear export was induced with 1 μM rapamycin as described for the times indicated prior to imaging using the spinning disc microscope setup. Note that local contrast optimization was again necessary due to mCherry-Ubc9 plasmid copy number variation as described above. Contrast adjustment and cropping were performed in Photoshop.

Analysis of Hsf1 reporter activity by flow cytometry.

Hsf1-AA heat shock experiments. VDY1852 cells transformed with pRS412 or pVD565 were inoculated into SD-ADE media and grown overnight to $OD_{600} \approx 0.1$. Following transfer to a 96-well plate and pretreatment with 10 μM rapamycin or carrier-only (90% EtOH, 10% Tween-20) at 30ºC for 10 minutes, cells were split into two plates: one that was heat-shocked at 39ºC for 30 minutes using a C1000 Touch thermal cycler (Bio Rad), the other control plate was immediately analyzed. Single-cell GFP and mKate fluorescence was measured for ~10,000 cells using a LSRII (BD) flow cytometer. Single cell fluorescence values were normalized by dividing GFP by mKate fluorescence from the same cell, and then these values were rescaled by dividing by the median GFP/mKate value for VDY1852 + pRS412 cells after mock pretreatment without heat

shock. Custom R scripts that were used to analyze the fluorescence data are available upon request.

Effect of synHDG expression on Hsf1 reporter. VDY2367 transformed with 15synHDGs (pVD576, pVD577, pVD578 and pVD580) or empty vectors (pRS412, pRS413, pRS415 and pVD579) were grown in SD-ADE-HIS-LEU media containing 200 μg/ml hygromycin-B (Invitrogen) overnight at 30ºC to a final density of OD_{600} ≈ 0.1 before being analyzed as the control plate above.

Colony growth assays. Cells transformed with synHDG plasmids and matching control vectors were inoculated into SD plasmid selection media with 10μM β-estradiol, if appropriate. After overnight growth to OD_{600} ≈ 0.2, equal numbers of cells were harvested and serially diluted into fresh media in 96-well plates before being spotted with a multi-channel pipette or a 36-well pinning tool onto corresponding SD selection plates with 10μM rapamycin or carrier control (90% EtOH, 10% Tween-20). Plates were parafilmed and incubated at 30ºC for 3-5 days before imaging with an Alpha Imager (Alpha Innotech).

Native elongating transcript sequencing (NET-seq).

For the NET-seq analysis of basal transcription, VDY2254 cells were grown overnight in 5 × 1L YPD (1% yeast extract, 2% peptone, 2% dextrose) at 30ºC with shaking until they reached OD_{600} ≈ 0.3. One culture was harvested by filtration onto a 90-mm diameter

0.45μm filter (Whatman) and cells scraped with a cooled spatula and transferred to liquid N_2. Other cultures were treated with rapamycin (1μM) for 15, 30 and 60 minutes prior to harvesting as described above. For the NET-seq analysis of heat shock transcription, VDY2254 cells were grown overnight in 2L YPD to mid-log at 30ºC until they reached $OD_{600} \approx 0.66$. The culture was then split equally and one half treated with rapamycin (1μM) and the other half left untreated. After further incubation with shaking for 10 minutes at 30ºC, each half was mixed with 1L of 50ºC YPD and moved to to 39ºC shaking water bath for 30 minutes prior to harvesting as described above.

Each sample was lysed frozen in a ball mill (Retsch). Rpb3 immunoprecipitatation from lysates and sequencing library creation from immunopurified RNA was carried out as described (Churchman and Weissman, 2011) with one notable difference: circularized cDNA samples were barcoded during PCR amplification to enable multiplexing in an Illumina Hi-Seq 2500 (Bauer Core Facility). Reads were assigned by the barcode to the appropriate sample. Sequenced nascent transcript fragments were groomed and aligned to the *S. cerevisiae* ORF coding reference genome using Bowtie before being assembled and quantified using Cufflinks. Fold changes were computed using Cuffdiff.

Yeast RNA-seq.

Cells were grown in YPD overnight at 30ºC with shaking until they reached $OD_{600} \approx 0.5$. Cultures were split into 5 ml aliquots before indicated treatments. 1.5 ml of treated cells were harvested by spinning for 30 seconds at 15,000 rpm speed in an Eppendorf 5430 benchtop centrifuge and snap frozen before storage at -80˚C. The small culture volume

and quick spin obviated the need for filtration. Frozen cell pellets were thawed on ice, resuspended in 1 ml water, transferred to fresh 1.5 ml tubes and harvested by spinning as above. Washed cell pellets were resuspended in 200 μl AE (50 mM NaOAc, pH 5.2, 10 mM EDTA) and vortexed. 20 μl of 10% SDS was added, followed by 250 μl acid phenol, and samples were incubated at 65˚C with shaking for 10 minutes. After an additional 5 minutes on ice, samples were spun at 15,000 rpm for 5 minutes at 4ºC. Supernatants were transferred to pre-spun heavy phase lock tubes (5 Prime) and 250 μl chloroform was added. Tubes were spun at full speed for 5 minutes at 15,000 rpm and aqueous layers (above the wax) were transferred to fresh 1.5 ml tubes. 30 μl of 3M NaOAc, pH 5.2 was added followed by 750 μl ice cold 100% ethanol. RNA was precipitated at -80˚C for 30 minutes and samples were spun at 15,000 rpm for 30 minutes at 4˚C. Pellets were washed with 1 ml 70% ethanol, spun at 15,000 rpm for 10 minutes at 4ºC for. The supernatant was removed and pellets were allowed to dry on ice for 10 minutes. Lastly, RNA pellets were resuspended in 30 μl DEPC water and the RNA concentrations of the resulting solutions measured by Nano Drop.

Total RNA samples were submitted to the Whitehead Institute Genome Technology Core (WIGTC) where polyA + RNA was purified, fragmented and sequencing libraries barcoded to enable multiplexing in an Illumina Hi-Seq 2500. Reads were assigned by the barcode to the appropriate sample.

Data were processed using a local version of the Galaxy suite of next-generation sequencing tools. Sequenced mRNA fragments were groomed and aligned to the *S. cerevisiae* ORF coding reference genome (Feb. 2011) using Tophat before being assembled and quantified using Cufflinks. Fold changes were computed using Cuffdiff.

Defining Hsf1-dependent genes in yeast.

Significance analysis of transcription under basal conditions. Hsf1-dependent genes were defined by combining statistical analyses of NET-seq and RNA-seq data. First, we used the CuffDiff (Trapnell et al., 2012) time series analysis algorithm to jointly analyze the NET-seq time course (15, 30, and 60 minutes of rapamycin treatment). We identified genes with significantly different transcription after 15 minutes that persisted for the remainder of the time course (no additional significant changes at the 30 or 60 minute time points). This analysis identified 30 genes that met these criteria using the most stringent p-value cutoff of $p < 10^{-4}$. We then tested whether these genes had significant changes in mRNA levels measured by RNA-seq that were caused by 60' of rapamycin treatment. We used genes without significant NET-seq changes to construct a null distribution of fold-changes. Using the 1st and 99th percentile of the null fold-change distribution as cutoffs, we identified 18 of the initial 30 gene as also having significant differences in mRNA levels.

Analysis of *SSA1* and *SSA2* sequencing data. The 94% sequence identity between the open reading frames for *SSA1* and *SSA2* makes computational deconvolution of

sequencing reads between the two paralogs unreliable. Thus, we averaged the FPKM values for the two genes into one *SSA1/2* value for the NET-seq and ChIP-seq analysis in Figure 2.2a,b. As the two genes are computational indistinguishable by mRNA-seq, we focus the remainder of our expression analysis on *SSA2*, which has ~5-fold greater expression than *SSA1*, with the caveat that a fraction of *SSA2* reads are likely from *SSA1*.

Statistical analysis of Hsf1-dependent gene expression during heat shock. In contrast to the small number of gene expression changes induced by short-term rapamycin treatment of Hsf1-AA cells at 30ºC, rapamycin pre-treatment induced correlated changes in transcription and mRNA abundance of hundreds of genes during subsequent heat shock. As the cuff-diff algorithms for computing p-values and false discovery rates become less reliable when there are large-scale expression changes (Trapnell et al., 2012), we decided to use a non-parametric, rank-based statistical significance analysis for changes to both transcription and mRNA abundance. We defined Hsf1-dependent gene expression during heat shock as those genes that fell below the 10^{th} percentile for both the NET-seq and RNA-seq datasets comparing rapamycin pre-treated versus mock pre-treated heat shock samples. As these two datasets were collected during independent experiments, we were comfortable assuming that the random factors that drive false discovery are independent and therefore the false discovery rate should be limited to 1% overall. We considered alternative significance thresholds for our rank-based analysis, but bioinformatic analysis of significant genes suggested that the 10%

threshold optimized our sensitivity to detect small, coherent changes without a high rate of false discovery, as judged by the relative enrichment for GO terms and promoter motifs between the different significance thresholds.

Defining Msn2/4 target genes.

Msn2/4 targets were defined as those genes in the top 10% of expression changes induced by 1-NM-PP1 treatmetn of PKAas cells that also contained at least one Msn2/4 binding site (AGGGG) in their promoter (defined as the intergenic region between the start codon of the gene of interest and the start or stop codon of the closest 5' open reading frame) using SCOPE (Carlson et al., 2007).

Defining ribosomal protein genes and Sfp1 targets.

Yeast genes that encode ribosomal proteins are easily identified based on their RPL-, RPS- and RPP- gene name prefixes to denote components of the large and small ribosomal subunits, along with other ribosomal proteins (Nakao et al., 2004). Their expression is transcriptionally controlled by Sfp1, which has a known promoter binding site (AAA[A/T]TTTT) (Fingerman et al., 2003; Jorgensen et al., 2004). Among the 295 genes with significant changes in heat shock expression due to Hsf1 AA, we found 103 RPL/RPS/RPP genes, plus 144 additional genes that had at least one Sfp1 binding site in their promoter (defined as the intergenic region between the start codon of the gene of interest and the start or stop codon of the closest 5' open reading frame) using SCOPE (Carlson et al., 2007).

Mammalian cell RNA-seq.

MEFs and mESCs were cultured to 75% confluence in 10 cm dishes as described above. Heat shock was performed by transferring dishes to a 42ºC incubator for 1 hour. Total RNA was extracted using RNeasy kits (Qiagen) according to the manufacturer's directions. Sequencing libraries were prepared and sequenced by the WIGTC as described above. Data was processed using Galaxy, aligned to the annotated Mm10 genome and quantified as described above.

Defining HSF1-dependent changes in gene expression during heat shock in mammalian cells.

In general, we found that changes in mammalian gene expression were smaller in both magnitude and the number of genes affected compared to yeast. While in each gene expression analysis most genes were highly correlated, the variance was not constant across genes—high expression genes tended to be less variable than low expression genes. To identify significant changes in gene expression, we needed a statistical inference strategy that accounts for the variance-expression relationship and adjusts the significance threshold accordingly. While there are parametric statistical inference methods that can account for non-constant variance, they require specification of a variance model and are very sensitive to its misspecification. Therefore, we choose to use a simple non-parametric approach based on quantile regression of gene expression levels between two samples to define significant changes. Intuitively, our strategy is

similar to calling the top 1% of fold changes as significant, but the quantile regression allows us to take into account that the top 1% of fold changes for high expression genes will be smaller than for low expression genes. For example, by regressing the 99th percentile of heat shock gene expression on control expression, we obtain a linear function that defines for each control expression level a corresponding value that 99% of heat shock expression measurements should fall below. A similar regression for the 1st percentile of fold changes allowed us to define a lower significance threshold. Together these two regressions define an interval with 98% coverage both globally and locally. That is, using regression of heat shock expression on control as an example, heat shock expression for 98% of all genes will fall between their respective fitted values from the 1st and 99th percentile regressions, and further for any subset of genes with similar control expression approximately 98% of their heat shock expression values will fall between the regression fits. We defined genes above and below the bounds defined by these two regressions as significantly induced and repressed, respectively.

One caveat of this approach is that the number of changes that we call as significant for any experiment is set by design at 1% of the total number of genes. Even during heat shock, our exploratory analysis suggested that expression of less than 1% of genes was affected and therefore many significant changes defined by our analysis of a single experiment will be false positives due to random variation. However, because we were ultimately interested in genes that have significant changes in *both* cell types, our false discovery rate due to random variation—which should be independent between cell

types—is limited to .01%. Thus, the fact that we defined 129 heat shock induced genes in mESCs is not interpretable (since 129 is ~1% of the 13,356 genes detected), however that we defined 20 heat shock induced genes in both mESCs and MEFs is highly significant (p-value < 10^{-17}), since the number of false discoveries should follow a binomial(n= 13,356, p= .0001) distribution and therefore we expect to call only 1.3 significant genes in both cell types by random chance. One additional caveat of our analysis is that because the 1st and 99th percentile regressions are not parallel, they will cross and beyond this intersection the fit for the 1st percentile will be greater than that of the 99th. After this point, our interpretation of these as upper and lower bounds no longer holds and therefore their utility for our statistical inference breaks down. Our conservative approach to avoid this was to compare the qualtile regression fits for the 1st and 99th percentiles to the median regression (50th percentile) fit, and exclude from our inference genes where the fit from the 1st percentile regression is greater than, or the 99th percentile fit is less than, the median regression fit. This approach, though conservative, affected a very small fraction of genes (~0.1%). For example, we excluded only 8/13,356 genes from our inference for heat shock analysis of mESCs.

We defined genes as HSF1-dependent if their expression was significantly induced by heat shock vs. control in wild type cells, and significantly reduced during heat shock in *hsf1*$^{-/-}$ vs. wild type cells, for both mESCs and MEFs. This analysis defined 9 HSF1-dependent genes. Since our statistical inference used expression from heat shocked wild type cells in both statistical tests for each cell type, we cannot comfortably assume that

our inference was based on 4 independent tests—which would imply an over all false discovery rate of $.01^4$, or 10^{-8}). However, even under the very conservative assumption that our inference is equivalent to just two independent statistical tests (one for each cell type), the probability of observing 9 (or more) significant genes is $\sim 10^{-5}$. We note that our choice of a 1% rate of false discovery for individual tests was based on bioinformatic analysis of gene sets defined using alternative significance thresholds, which showed that the 1% level optimized sensitivity and specificity.

Chromatin immunoprecipitation and sequencing.

50 ml of cells were grown to OD_{600}=0.5. Cells were fixed with addition of 1% formaldehyde for 20 minutes at room temperature followed by quenching with 125 mM glycine for 10 minutes. Cells were pelleted, washed with ice-cold PBS. Pellets were frozen in liquid N_2 and stored at -80˚C. Cells were lysed frozen in a coffee grinder with dry ice. After the dry ice was evaporated, lysate was resuspended in 2 ml ChIP buffer (50 mM Hepes pH 7.5, 140 mM NaCl, 1 mM EDTA, 1% triton x-100, 0.1% DOC) and sonicated 10 times using a probe sonicator (18W, 30 seconds on, one minute off) during which time they were kept on ice. 1 ml was transferred to a 1.5 ml tube and spun to remove cell debris. Input was set aside, and a serial IP was performed. First, 25 μl of anti-FLAG magnetic beads (50% slurry, Sigma) were added the mixture was incubated for 2 hours at 4ºC on a rotator. Beads were separated with a magnet and the supernatant was removed. Beads were washed 5 times with 1 ml ChIP buffer (5 minute incubations at 4ºC

between each wash) and bound material eluted with 1 ml of 1 mg/ml 3xFLAG peptide (Sigma) in ChIP buffer by incubating at room temperature for 10 minutes. Beads were separated with a magnet and eluate was transferred to a fresh tube. Next, 25 μl of anti-V5 magnetic beads (50% slurry, MBL International) were added and the mixture was incubated for 2 hours at 4ºC on a rotator. Beads were separated with a magnet and the supernatant was removed. Beads were washed 3 times with l ChIP buffer, followed by a high salt wash (ChIP buffer + 500 mM NaCl) and a final wash in TE (all washes were with 1 ml with 5 minute incubations at 4ºC between each wash). Bound material was eluted with 250 μl TE + 1% SDS by incubating at 65ºC for 15 minutes. Beads were separated with a magnet and eluate was transferred to a fresh tube and incubated overnight at 65ºC to reverse crosslinks. Protein was degraded by adding 250 μl 40 μg/ml proteinase K in TE (supplemented with GlycoBlue to visualize subsequent pellets) and incubating at 37ºC for 2 hours. DNA fragments were separated from protein by adding 500 μl phenol/chloroform/isoamyl alcohol (25:24:1), and the aqueous layer was added to a fresh tube. 55 μl of 4M LiCl was added along with 1 ml of 100% EtOH, and DNA was precipitated at -80˚C overnight. DNA was pelleted by spinning at 15,000 rpm in an Eppendorf 5424 benchtop centrifuge for 30 minutes at 4˚C and resuspended in 50 μl TE. Sequencing libraries were prepared by the WIGTC, and sequenced on the Illumina Hi-Seq 2500. Reads were aligned to the yeast genome with Bowtie and Wiggle files were generated. Peaks were called with MACS v1.4.2 using a stringent p-value cutoff ($p < 10^{-30}$).

Promoter motif and gene ontology analysis.

Enrichment for DNA motifs was calculated using the SCOPE web interface (Carlson et al., 2007), and enrichment for gene ontology terms was calculated using YEAST Mine (Balakrishnan et al., 2012). Enrichment p-values for GO terms were corrected for multiple hypothesis testing using the Holm–Bonferroni correction implemented in YEAST Mine. Gene set enrichment analysis for over-representation of one gene within another set was determined using the hypergeometric distribution.

Protein-protein interaction network analysis.

Protein interaction networks were generated using the STRING database (Jensen, 2009). Yeast interactions were generated with a required confidence score of .90 and "Active Prediction Methods" based on experiments, co- occurrence and databases. Mouse interaction networks were generated with a required confidence score of 0.70 and "Active Prediction Methods" based on neighborhood, gene fusion, co-occurrence, experiments, databases and text mining. We explicitly did not allow co-expression data to be used in the network construction because HDGs were defined based on expression analysis and we wanted the protein-protein interaction network data to be derived from independent data sets. Also, we used a lower confidence threshold and additional data sources for construction of the mouse network because there was far less high-confidence experimental interaction data than for yeast resulting in an artificially sparse mouse network *ceteris paribus.*

References

Akerfelt, M., Morimoto, R.I., and Sistonen, L. (2010). Heat shock factors: integrators of cell stress, development and lifespan. Nat Rev Mol Cell Biol *11*, 545–555.

Anckar, J., and Sistonen, L. (2011). Regulation of HSF1 function in the heat stress response: implications in aging and disease. Annu Rev Biochem *80*, 1089–1115.

Balakrishnan, R., Park, J., Karra, K., Hitz, B.C., Binkley, G., Hong, E.L., Sullivan, J., Micklem, G., and Michael Cherry, J. (2012). YeastMine--an integrated data warehouse for Saccharomyces cerevisiae data as a multipurpose tool-kit. Database *2012*, bar062–bar062.

Balch, W., Morimoto, R., and Dillin, A. (2008). Adapting Proteostasis for Disease Intervention. Science.

Boy-Marcotte, E., Lagniel, G., Perrot, M., Bussereau, F., Boudsocq, A., Jacquet, M., and Labarre, J. (1999a). The heat shock response in yeast: differential regulations and contributions of the Msn2p/Msn4p and Hsf1p regulons. Molecular Microbiology *33*, 274–283.

Boy-Marcotte, E., Lagniel, G., Perrot, M., Bussereau, F., Boudsocq, A., Jacquet, M., and Labarre, J. (1999b). The heat shock response in yeast: differential regulations and contributions of the Msn2p/Msn4p and Hsf1p regulons. Molecular Microbiology *33*, 274–283.

Brachmann, C.B., Davies, A., Cost, G.J., Caputo, E., Li, J., Hieter, P., and Boeke, J.D. (1998). Designer deletion strains derived from Saccharomyces cerevisiae S288C: a useful set of strains and plasmids for PCR-mediated gene disruption and other applications. Yeast *14*, 115–132.

Brandman, O., Stewart-Ornstein, J., Wong, D., Larson, A., Williams, C.C., Li, G.-W., Zhou, S., King, D., Shen, P.S., Weibezahn, J., et al. (2012). A ribosome-bound quality control complex triggers degradation of nascent peptides and signals translation stress. Cell *151*, 1042–1054.

Carlson, J.M., Chakravarty, A., DeZiel, C.E., and Gross, R.H. (2007). SCOPE: a web server for practical de novo motif discovery. Nucleic Acids Research *35*, W259–W264.

Causton, H.C., Ren, B., Koh, S.S., Harbison, C.T., Kanin, E., Jennings, E.G., Lee, T.I., True, H.L., Lander, E.S., and Young, R.A. (2001). Remodeling of yeast genome expression in response to environmental changes. Mol Biol Cell *12*, 323–337.

Churchman, L.S., and Weissman, J.S. (2011). Nascent transcript sequencing visualizes transcription at nucleotide resolution. Nature *469*, 368–373.

Clos, J., Westwood, J.T., Becker, P.B., Wilson, S., Lambert, K., and Wu, C. (1990). Molecular cloning and expression of a hexameric Drosophila heat shock factor subject to negative regulation. Cell *63*, 1085–1097.

Dai, C., Whitesell, L., Rogers, A.B., and Lindquist, S. (2007). Heat Shock Factor 1 Is a Powerful Multifaceted Modifier of Carcinogenesis. Cell *130*, 1005–1018.

de Boer, C.G., and Hughes, T.R. (2011). YeTFaSCo: a database of evaluated yeast transcription factor sequence specificities. Nucleic Acids Res *40*, gkr993–D179.

Doench, J.G., Hartenian, E., Graham, D.B., Tothova, Z., Hegde, M., Smith, I., Sullender, M., Ebert, B.L., Xavier, R.J., and Root, D.E. (2014). Rational design of highly active sgRNAs for CRISPR-Cas9–mediated gene inactivation. Nat Biotechnol *32*, 1262–1267.

Eastmond, D.L., and Nelson, H.C.M. (2006). Genome-wide analysis reveals new roles for

the activation domains of the Saccharomyces cerevisiae heat shock transcription factor (Hsf1) during the transient heat shock response. J Biol Chem *281*, 32909–32921.

Erkine, A.M., Adams, C.C., Diken, T., and Gross, D.S. (1996). Heat shock factor gains access to the yeast HSC82 promoter independently of other sequence-specific factors and antagonizes nucleosomal repression of basal and induced transcription. Mol Cell Biol *16*, 7004–7017.

Fingerman, I., Nagaraj, V., Norris, D., and Vershon, A.K. (2003). Sfp1 plays a key role in yeast ribosome biogenesis. Eukaryotic Cell *2*, 1061–1068.

Fujimoto, M., Takaki, E., Takii, R., Tan, K., Prakasam, R., HAYASHIDA, N., Iemura, S.-I., Natsume, T., and Nakai, A. (2012). RPA Assists HSF1 Access to Nucleosomal DNA by Recruiting Histone Chaperone FACT. Mol Cell *48*, 182–194.

Gasch, A.P., Spellman, P.T., Kao, C.M., Carmel-Harel, O., Eisen, M.B., Storz, G., Botstein, D., and Brown, P.O. (2000). Genomic expression programs in the response of yeast cells to environmental changes. Mol Biol Cell *11*, 4241–4257.

Geiler-Samerotte, K.A., Dion, M.F., Budnik, B.A., Wang, S.M., Hartl, D.L., and Drummond, D.A. (2011). Misfolded proteins impose a dosage-dependent fitness cost and trigger a cytosolic unfolded protein response in yeast. Proc Natl Acad Sci USA *108*, 680–685.

Gibson, D.G., Young, L., Chuang, R.-Y., Venter, J.C., Hutchison, C.A., and Smith, H.O. (2009). Enzymatic assembly of DNA molecules up to several hundred kilobases. Nat Meth *6*, 343–345.

Glover, J.R., and Lindquist, S. (1998). Hsp104, Hsp70, and Hsp40: a novel chaperone system that rescues previously aggregated proteins. Cell *94*, 73–82.

Goldstein, A.L., and McCusker, J.H. (1999). Three new dominant drug resistance

cassettes for gene disruption inSaccharomyces cerevisiae. Yeast *15*, 1541–1553.

Görner, W., Durchschlag, E., Martinez-Pastor, M.T., Estruch, F., Ammerer, G., Hamilton, B., Ruis, H., and Schüller, C. (1998). Nuclear localization of the C2H2 zinc finger protein Msn2p is regulated by stress and protein kinase A activity. Genes & Development *12*, 586–597.

Gross, D.S., Adams, C.C., Lee, S., and Stentz, B. (1993). A critical role for heat shock transcription factor in establishing a nucleosome-free region over the TATA-initiation site of the yeast HSP82 heat shock gene. Embo J *12*, 3931.

Hahn, J.-S., Hu, Z., Thiele, D.J., and Iyer, V.R. (2004). Genome-wide analysis of the biology of stress responses through heat shock transcription factor. Mol Cell Biol *24*, 5249–5256.

Hao, N., and O'Shea, E.K. (2012). Signal-dependent dynamics of transcription factor translocation controls gene expression. Nat. Struct. Mol. Biol. *19*, 31–39.

Hartl, F.U., Bracher, A., and Hayer-Hartl, M. (2011). Molecular chaperones in protein folding and proteostasis. Nature *475*, 324–332.

Haruki, H., Nishikawa, J., and Laemmli, U.K. (2008). The Anchor-Away Technique: Rapid, Conditional Establishment of Yeast Mutant Phenotypes. Mol Cell *31*, 925–932.

Imazu, H., and Sakurai, H. (2005). Saccharomyces cerevisiae heat shock transcription factor regulates cell wall remodeling in response to heat shock. Eukaryotic Cell *4*, 1050–1056.

Jakobsen, B.K., and Pelham, H.R. (1988). Constitutive binding of yeast heat shock factor to DNA in vivo. Mol Cell Biol *8*, 5040–5042.

Jakobsen, B.K., and Pelham, H.R. (1991). A conserved heptapeptide restrains the activity of the yeast heat shock transcription factor. Embo J *10*, 369–375.

Jensen, L.J. (2009). STRING 8---a global view on proteins and their functional interactions in 630 organisms. Nucleic Acids Res *37*, D412–D416.

Jorgensen, P., Rupes, I., Sharom, J.R., Schneper, L., Broach, J.R., and Tyers, M. (2004). A dynamic transcriptional network communicates growth potential to ribosome synthesis and critical cell size. Genes & Development *18*, 2491–2505.

Kaganovich, D., Kopito, R., and Frydman, J. (2008). Misfolded proteins partition between two distinct quality control compartments. Nature *454*, 1088–1095.

Lee, T.I., Rinaldi, N.J., Robert, F., Odom, D.T., and Bar-Joseph, Z. (2002). Transcriptional regulatory networks in Saccharomyces cerevisiae. Science.

Liu, X.D., Liu, P.C.C., Santoro, N., and Thiele, D.J. (1997). Conservation of a stress response: human heat shock transcription factors functionally substitute for yeast HSF. Embo J *16*, 6466–6477.

Longtine, M.S., McKenzie, A., Demarini, D.J., Shah, N.G., Wach, A., Brachat, A., Philippsen, P., and Pringle, J.R. (1998). Additional modules for versatile and economical PCR-based gene deletion and modification in Saccharomyces cerevisiae. Yeast *14*, 953–961.

Mali, P., Yang, L., Esvelt, K.M., Aach, J., Guell, M., DiCarlo, J.E., Norville, J.E., and Church, G.M. (2013). RNA-Guided Human Genome Engineering via Cas9. Science *339*, 823–826.

Marion, R.M., Regev, A., Segal, E., Barash, Y., Koller, D., Friedman, N., and O'Shea, E.K. (2004). Sfp1 is a stress- and nutrient-sensitive regulator of ribosomal protein gene expression. Proc Natl Acad Sci USA *101*, 14315–14322.

McIsaac, R.S., Oakes, B.L., Wang, X., Dummit, K.A., Botstein, D., and Noyes, M.B. (2013). Synthetic gene expression perturbation systems with rapid, tunable, single-gene specificity in yeast. Nucleic Acids Research *41*, e57.

McMillan, D.R., Xiao, X., Shao, L., Graves, K., and Benjamin, I.J. (1998). Targeted disruption of heat shock transcription factor 1 abolishes thermotolerance and protection against heat-inducible apoptosis. J Biol Chem *273*, 7523–7528.

Mendillo, M.L., Santagata, S., Koeva, M., Bell, G.W., Hu, R., Tamimi, R.M., Fraenkel, E., Ince, T.A., Whitesell, L., and Lindquist, S. (2012). HSF1 drives a transcriptional program distinct from heat shock to support highly malignant human cancers. Cell *150*, 549–562.

Morano, K.A. (1999). The Sch9 protein kinase regulates Hsp90 chaperone complex signal transduction activity in vivo. Embo J *18*, 5953–5962.

Morano, K.A., Santoro, N., Koch, K.A., and Thiele, D.J. (1999). A trans-activation domain in yeast heat shock transcription factor is essential for cell cycle progression during stress. Mol Cell Biol *19*, 402–411.

Nakao, A., Yoshihama, M., and Kenmochi, N. (2004). RPG: the Ribosomal Protein Gene database. Nucleic Acids Research *32*, D168–D170.

Nicholls, S., Leach, M.D., Priest, C.L., and Brown, A.J.P. (2009). Role of the heat shock transcription factor, Hsf1, in a major fungal pathogen that is obligately associated with warm-blooded animals. Molecular Microbiology *74*, 844–861.

Pleiss, J.A., Whitworth, G.B., Bergkessel, M., and Guthrie, C. (2007). Rapid, transcript-specific changes in splicing in response to environmental stress. Mol Cell *27*, 928–937.

Rabindran, S.K., Giorgi, G., Clos, J., and Wu, C. (1991). Molecular cloning and expression of a human heat shock factor, HSF1. Proc Natl Acad Sci USA *88*, 6906–6910.

Richter, K., Haslbeck, M., and Buchner, J. (2010). The Heat Shock Response: Life on the Verge of Death. Mol Cell *40*, 253–266.

Rose, R.E., Pazos, M.A., Curcio, M.J., and Fabris, D. (2016). Global profiling of RNA post-transcriptional modifications as an effective tool for investigating the epitranscriptomics of stress response. Mol Cell Proteomics.

Sakurai, H., and Ota, A. (2011). Regulation of chaperone gene expression by heat shock transcription factor in Saccharomyces cerevisiae: Importance in normal cell growth, stress resistance, and longevity. FEBS Letters.

Sarge, K.D., Murphy, S.P., and Morimoto, R.I. (1993). Activation of heat shock gene transcription by heat shock factor 1 involves oligomerization, acquisition of DNA-binding activity, and nuclear localization and can occur in the absence of stress. Mol Cell Biol *13*, 1392–1407.

Scharf, K.D., Rose, S., Zott, W., Schöffl, F., Nover, L., and Schöff, F. (1990). Three tomato genes code for heat stress transcription factors with a region of remarkable homology to the DNA-binding domain of the yeast HSF. Embo J *9*, 4495–4501.

Schmitt, A.P., and McEntee, K. (1996). Msn2p, a zinc finger DNA-binding protein, is the transcriptional activator of the multistress response in Saccharomyces cerevisiae. Proc Natl Acad Sci USA *93*, 5777–5782.

Sikorski, R.S., and Hieter, P. (1989). A system of shuttle vectors and yeast host strains designed for efficient manipulation of DNA in Saccharomyces cerevisiae. Genetics *122*,

19–27.

Smith, A., Ward, M.P., and Garrett, S. (1998). Yeast PKA represses Msn2p/Msn4p-dependent gene expression to regulate growth, stress response and glycogen accumulation. Embo J *17*, 3556–3564.

Smith, B.J., and Yaffe, M.P. (1991). A Mutation in the Yeast Heat-Shock Factor Gene Causes Temperature-Sensitive Defects in Both Mitochondrial Protein Import and the Cell-Cycle. Mol Cell Biol *11*, 2647–2655.

Sorger, P.K., and Pelham, H.R. (1987). Purification and characterization of a heat-shock element binding protein from yeast. Embo J *6*, 3035–3041.

Sorger, P.K., and Pelham, H.R. (1988). Yeast heat shock factor is an essential DNA-binding protein that exhibits temperature-dependent phosphorylation. Cell *54*, 855–864.

Tang, Z., Dai, S., He, Y., Doty, R.A., Shultz, L.D., Sampson, S.B., and Dai, C. (2015). MEK Guards Proteome Stability and Inhibits Tumor-Suppressive Amyloidogenesis via HSF1. Cell *160*, 729–744.

Thevelein, J. (1999). Novel sensing mechanisms and targets for the cAMP–protein kinase A pathway in the yeast Saccharomyces cerevisiae - Thevelein - 2002 - Molecular Microbiology - Wiley Online Library. Molecular Microbiology.

Torres, F.A.G., and Bonner, J.J. (1995). Genetic Identification of the Site of Dna Contact in the Yeast Heat-Shock Transcription Factor. Mol Cell Biol *15*, 5063–5070.

Trapnell, C., Roberts, A., Goff, L., Pertea, G., Kim, D., Kelley, D.R., Pimentel, H., Salzberg, S.L., Rinn, J.L., and Pachter, L. (2012). Differential gene and transcript expression analysis of RNA-seq experiments with TopHat and Cufflinks. Nat Protoc *7*, 562–578.

Treger, J.M., Schmitt, A.P., Simon, J.R., and McEntee, K. (1998). Transcriptional factor mutations reveal regulatory complexities of heat shock and newly identified stress genes in Saccharomyces cerevisiae. J Biol Chem *273*, 26875–26879.

Trinklein, N.D., Murray, J.I., Hartman, S.J., Botstein, D., and Myers, R.M. (2004). The role of heat shock transcription factor 1 in the genome-wide regulation of the mammalian heat shock response. Mol Biol Cell *15*, 1254–1261.

Wallace, E.W.J., Kear-Scott, J.L., Pilipenko, E.V., Schwartz, M.H., Laskowski, P.R., Rojek, A.E., Katanski, C.D., Riback, J.A., Dion, M.F., Franks, A.M., et al. (2015). Reversible, Specific, Active Aggregates of Endogenous Proteins Assemble upon Heat Stress. Cell *162*, 1286–1298.

Wu, C. (1995). Heat Shock Transcription Factors: Structure and Regulation. Annu. Rev. Cell Dev. Biol. *11*, 441–469.

Zarzov, P., Boucherie, H., and Mann, C. (1997). A yeast heat shock transcription factor (Hsf1) mutant is defective in both Hsc82/Hsp82 synthesis and spindle pole body duplication. J. Cell. Sci.

Zhang, Y., Huang, L., Zhang, J., Moskophidis, D., and Mivechi, N.F. (2002). Targeted disruption of hsf1 leads to lack of thermotolerance and defines tissue-specific regulation for stress-inducible Hsp molecular chaperones. J. Cell. Biochem. *86*, 376–393.

ACKNOLEDGEMENTS

We thank S. Churchman and B. Tye for reagents and assistance with NET-seq

experiments and data analysis; J. Krakowiak for technical assistance with RNA preps; A.

S. Hansen for *TPKas* strains and 1-NM-PP1; W. Reilly for generating HDG knockout

plasmids; J. Offermann for reagents; P. Arvidson for administrative support; P. Stoddard, Q. Justman, B. Zid and R. Subramaniam for useful discussions; P. Rogers for flow cytometry and general support; Members of the Denic and Lindquist labs for comments and suggestions; C. Chan for help with figures; S. Churchman, A. Murray, J. Taunton, L. Whitesell, B. Stern, J. Stewart-Ornstein, B. Tye, C. Chan and C. Shoemaker for helpful comments on the manuscript. This work was supported by the National Institute on Aging R21 (R21 AG050134-01 to V.D.) and Kirschstein NRSA diversity fellowship (F31 AG044967-03 to E.S.), a NIH Early Independence Award (DP5 OD017941-01 to D.P.), and a Cancer Research Fellowship from the Alexander and Margaret Stewart Trust (D.P.).

AUTHOR CONTRIBUTIONS

V.D., D.P. and E.S. conceived of the project and designed the experiments. E.S. performed the cloning and yeast strain construction; E.S. developed the quantitative microscopy, flow cytometry and genetics assays and performed these experiments with the Hsf1-AA strain, with help from D.P. for live-cell confocal microscopy; V.D. performed the NET-seq experiments; X.Z. performed the ChIP-seq experiments; E.S and D.P. prepared yeast samples, which D.P. purified RNA from, for RNA-seq; J.P., D.J. and P.G. developed the CRISPR/Cas9 genome editing protocol; J.P. and D.J. generated the hsf1 knockout cell lines; J.P. prepared mammalian cell samples for RNA-seq. E.S., D.P. and

V.D. analyzed the data with help from E.A.; E.S., D.P. and V.D. made the figures and wrote the paper. All authors edited the manuscript.

Chapter 3: Stress pathway cross-talk mediates attenuation of Hsf1 activity during stress and replicative aging in yeast.

Introduction

Protein folding information is contained in each protein's amino acid sequence (Anfinsen, 1973). In the crowded intracellular milieu, however, protein folding intermediates are aggregation prone and depend on complex chaperoning mechanisms to rapidly and efficiently assume their native conformations (Dobson, 2003). Stochastic failure of proteins to adopt their native structure can result in the formation of protein aggregates, which can impair cellular functions by inducing co-aggregation of newly synthesized proteins and pre-existing proteins with exposed unstructured regions (Olzscha et al., 2011). Moreover, cell function is maintained in the face of transient environmental conditions (*e.g.*, high temperatures) that cause global protein unfolding and aggregation by transcriptional homeostasis pathways that up-regulate expression of protein quality control components (Tyedmers et al., 2010).

Aging is associated with an increase in disease incidence and the appearance of protein aggregates in the affected tissues (Lindner and Demarez, 2009). This connection is clearly illustrated by the high incidence of Alzheimer's and Huntington's disease in the elderly and the accompanying presence of protein aggregates in the degenerating neuronal tissues (Chiti and Dobson, 2006). The establishment of model organisms for studying the biology of aging has lead to the realization that protein aggregates are also

age-associated in the nematode worm *C. elegans* (Ben-Zvi et al., 2009), the budding yeast *S. cerevisiae* (Aguilaniu et al., 2003), and many others.

Why are old cells unable to prevent protein aggregation? We still don't know the precise answer to this question but several studies have implicated the age-associated collapse of protein homeostasis pathways. Specifically the heat shock response is a conserved transcriptional mechanism for increasing the protein folding capacity of the cell in response to protein unfolding (Richter et al., 2010). A key component of this pathway is the transcription factor Hsf, which in response to protein unfolding recruits the general transcriptional machinery to genes with heat shock elements (HSEs) in their promoter regions (Pirkkala et al., 2001). Many of the resulting heat shock proteins (HSPs) are chaperones that help maintain protein homeostasis when the protein folding capacity of the cell has been challenged. Many aging studies have found that Hsf activation by thermal stress is compromised in old cells. For example, Hsf activity in worms decreases with age in a tissue specific manner: muscle cells are unresponsive to heat stress, while neurons maintain normal Hsf inducibility (Kern et al., 2010a). Additional worm studies have found that certain genetic mutations extend lifespan in an Hsf-dependent manner (Hsu et al., 2003). Moreover, in budding yeast, loss of Hsp104, a protein disaggregase chaperone and transcriptional target of the heat shock response, shortens lifespan, while Hsp104 over-expression restores longevity in the short-lived *Δsir2* mutant (Erjavec et al., 2007). These studies argue that maintenance of protein folding homeostasis by Hsf promotes longevity.

Hsf is regulated by a complex set of both excitatory and inhibitory post-translational modifications, as well as associations with certain HSPs (Akerfelt et al., 2010; Anckar and Sistonen, 2011; Buchberger et al., 2010). Efforts to understand how aging inhibits Hsf's ability to sense folding stress have been hampered by technical limitations. Specifically, because Hsf is expressed at a very low level (de Godoy et al., 2008), it is challenging to isolate enough cells of a defined age to carry out biochemical analysis of purified Hsf. Moreover, the effects of aging on Hsf in the worm aging model are tissue specific making it difficult to obtain a homogenous cell preparation for analysis. These considerations illustrate the impetus for a complementary genetic and biochemical system that doesn't suffer from cell scarcity or homogeneity issues for studying at a mechanistic level the effects of aging on Hsf.

We have established such a system in budding yeast for monitoring the effects of replicative cell aging on heat shock factor 1 (Hsf1) activity. Budding yeast cell division is asymmetric, with a large mother cell giving rise to a smaller daughter cell (Hartwell and Unger, 1977). The replicative lifespan of the mother cell is finite and defined as the total number of daughter cells it produces before undergoing cell senescence and lysis (Henderson and Gottschling, 2008). Notably, the replicative lifespan of daughter cells is reset after each cell division (except for daughters from very old mothers). This implies that cell senescence factors *asymmetrically accumulate* in the mother cells over replicative age. By this criterion, protein aggregates have been implicated as a potential

cause of replicative senescence (Kennedy and McCormick, 2011). Here we show that Hsf1 activation by thermal stress is suppressed with replicative age in budding yeast. Further, we have identified multiple loss-of-function mutations in the general stress response, a distinct protein folding homeostasis pathway, that rescue Hsf1 inducibility in old cells. We found that replicative aging induces the general stress response in the absence of any extrinsic stress, and engineered activation of this response in unstressed young cells by chemical genetics is sufficient to inhibit Hsf1 activation by thermal stress. While previous work has suggested that Hsf1 and Msn2/4—the transcriptional regulators of the general stress response—are concurrently activated by heat shock, here we show that temperature increase causes rapid activation of Hsf1, which is then attenuated by subsequent heat-induced activation of the general stress response. Finally, we explored the mechanism of Hsf1 inactivation by the general stress response and found evidence that Hsf1 transcriptional activation is compromised independent from changes in Hsf1 DNA binding or post-translational modifications. Thus, by asking why replicative aging attenuates Hsf1 activation by thermal stress, we revealed a novel mode of Hsf1 regulation during the yeast heat shock response.

Hsf1 activation by heat shock is attenuated during yeast replicative aging.

Yeast replicative aging is an asymmetric process that is asymmetrically inherited by the mother cell, the larger cell from which smaller daughter cells bud off. In other words, the lifespan of daughter cells is reset during cell division (except for the last few divisions) while the mother cell divides a fixed number of times before it undergoes cell senescence

and lysis. Previous studies have shown that protein aggregates asymmetrically accumulate in the mother cell (Aguilaniu et al., 2003), suggesting an age-associated decline in protein homeostasis mechanisms. In young cells, expression of a misfolded, aggregation-prone mutant protein causes up-regulation of a gene-set that is strongly enriched for Hsf1-dependent genes (Geiler-Samerotte et al., 2011). We therefore wondered if replicative aging is associated with an asymmetric decline in Hsf1 function in mother cells. The technical challenge of asymmetry is illustrated when one considers that after 20 generations of exponential growth, a culture that started with a single daughter cell, which becomes a mother cell during the first cell division, will now have ~1,000,000 cells, only one of which will be a 20-generation old mother and about half-of which will be daughters budded in the previous generation.

To avoid these limitations, we have used a genetic system called the Mother Enrichment Program (MEP) in which mother cells, following addition of a drug, maintain their normal RLS, but daughter cells are rendered non-proliferative following birth (Lindstrom and Gottschling, 2009). To monitor Hsf1 activity in old cells, we first introduced a fluorescent transcriptional reporter for the heat shock response into the MEP strain background (Brandman et al., 2012). Hsf1 binds to short tandem repeats of DNA sequence known as the heat shock element (HSE) (Sorger and Pelham, 1987). A synthetic promoter comprising four copies of the HSE next to a basal promoter is sufficient to induce expression of GFP following heat shock, as measured by flow cytometry (Figure 3.1A). To normalize for any non-specific changes in gene expression (*e.g.*, due to global

changes in protein translation), we also introduced mCherry (a red fluorescent protein) under the constitutive TEF2 promoter (Figure 3.1A). Next, to distinguish mother cells from daughters, we labeled actively dividing cells with an impermeable fluorescent cell wall dye that is not inherited by future daughter cells and inoculated a culture at very low density. Following a single cell division, which converts the labeled daughters into mothers, we added a drug that initiates mother enrichment and monitored heat shock-induced changes in the Hsf1 reporter as a function of replicative age. Notably, we also use a fluorescent cell viability dye to exclude any dead mothers that accumulate over time. As expected, we observed that a shift from 30° to 39°C elicits a robust Hsf1 response in young mother cells (Figure 3.1B). In contrast, this response was attenuated progressively during replicative aging such that it became almost uninducible after 48 hours of growth in the presence of drug (corresponding to ~25 mother cell divisions) (Figure 3.1B). These data argue that suppression of Hsf1 activation by heat is an aging phenotype that is conserved in budding yeast.

Activation of the Msn2/4-dependent general stress response is necessary for age-associated inactivation of Hsf1.

To gain mechanistic insights into the effects of aging on Hsf1 in yeast, we crossed the yeast gene deletion library into the MEP with the fluorescent Hsf1 reporter genetic background. Next, we carried out a genetic screen for suppressors of the age-associated Hsf1 phenotype. We identified several mutations that cause activation of protein kinase A (Pka), which exists as three isoforms encoded by the *TPK1/2/3* genes (Figure 3.1C). Pka

activity is normally repressed by complex formation with the regulatory protein (Bcy1) (Zaremberg and Moreno, 1996). Pka activation is brought about by binding of intracellular 3'-5'-cyclic adenosine monophosphate (cAMP) to Bcy1 to induce its dissociation from Pka. cAMP level is itself tightly regulated by competing biosynthetic and degradation pathways. In the former, the adenylate cyclase is an essential enzyme that converts ATP to cAMP in response to activation by Ras, an essential GTPase that is under negative control by Ira2 (Colombo et al., 2004). In the latter, cAMP is degraded by two phosphodiesteases (Pde1 and Pde2) (Park et al., 2005). In our genetic screen, we found that Hsf1 inducibility was restored by several mutations that elevate cAMP levels to activate Pka (*Δpde1*, *Δpde2*, *Δira2*) (Figure 3.1C).

Pka regulates multiple downstream effectors, including the redundant transcription factors Msn2 and Msn4 that become activated by heat stress, as well as a variety of other perturbations, a phenomenon known as the general stress response (Smith et al., 1998). Msn2/4 bind to short tandem repeats of DNA sequence known as the stress response element (STRE) found in the promoters of a subset of genes also targeted by Hsf1 (Schmitt and McEntee, 1996). When Pka is active, it phosphorylates Msn2/4 to prevent their nuclear localization and transcriptional activity (Jacquet et al., 2003). To test if Msn2/4 enable age-dependent Hsf1 suppression, we analyzed Hsf1 activity in the *Δmsn2 Δmsn4* double mutant, and found that Hsf1 activation by heat stress is restored in aged cells (Figure 3.1C).

Figure 3.1: Constitutive activity of the Msn2/4-mediated general stress response is necessary for age-associated attenuation of Hsf1.
(A) A fluorescent reporter for Hsf1 activity. Synthetic promoter consisting of a 4x repeat of the Hsf1 binding element (4xHSE) driving a GFP. A constitutively expressed mCherry allows normalization for non-specific changes in expression. Examples of fluorescence as measured by flow cytometry with and without heat shock. Fluorescence normalized for cell size by dividing by side scatter. **(B)** Hsf1 becomes uninducible with age. MEP strains expressing the Hsf1 fluorescent reporter were aged for the indicated times, then heat shocked at 39°C (or 30°C control) for 60'. Median Hsf1 activity corresponds to the median, size-normalized fluorescence at the indicated age/temperature as measured by flow cytometry. **(C)** Suppressor mutants identified in a flow cytometry-based genetic screen for gene deletions that maintain Hsf1 inducibility in old cells. Cells of the indicated genotype were heat shocked at 39°C for 60' after 0 and 48 hours of aging with the MEP. Median Hsf1 induction corresponds to the ratio of the median size-normalized fluorescence from the 4xHSE-GFP reporter at 39°C/30°C measured by flow cytometry, shown for young cells (open bars) and old cells (closed bars) in four suppressor mutants and wild type. **(D)** Potential models for Hsf1 inactivation consistent with the observed genetic data. **(E)** Activity of the Msn2/4-dependent general stress response across RLS. Cells engineered to express a fluorescent Msn2/4 reporter consisting of an 8x repeat of the Msn2/4 binding element (STRE) driving GFP. At the indicated ages, aliquots were heat shocked as in (B). Median Msn2/4 activity corresponds to the median size-normalized GFP fluorescence as measured by flow cytometry.

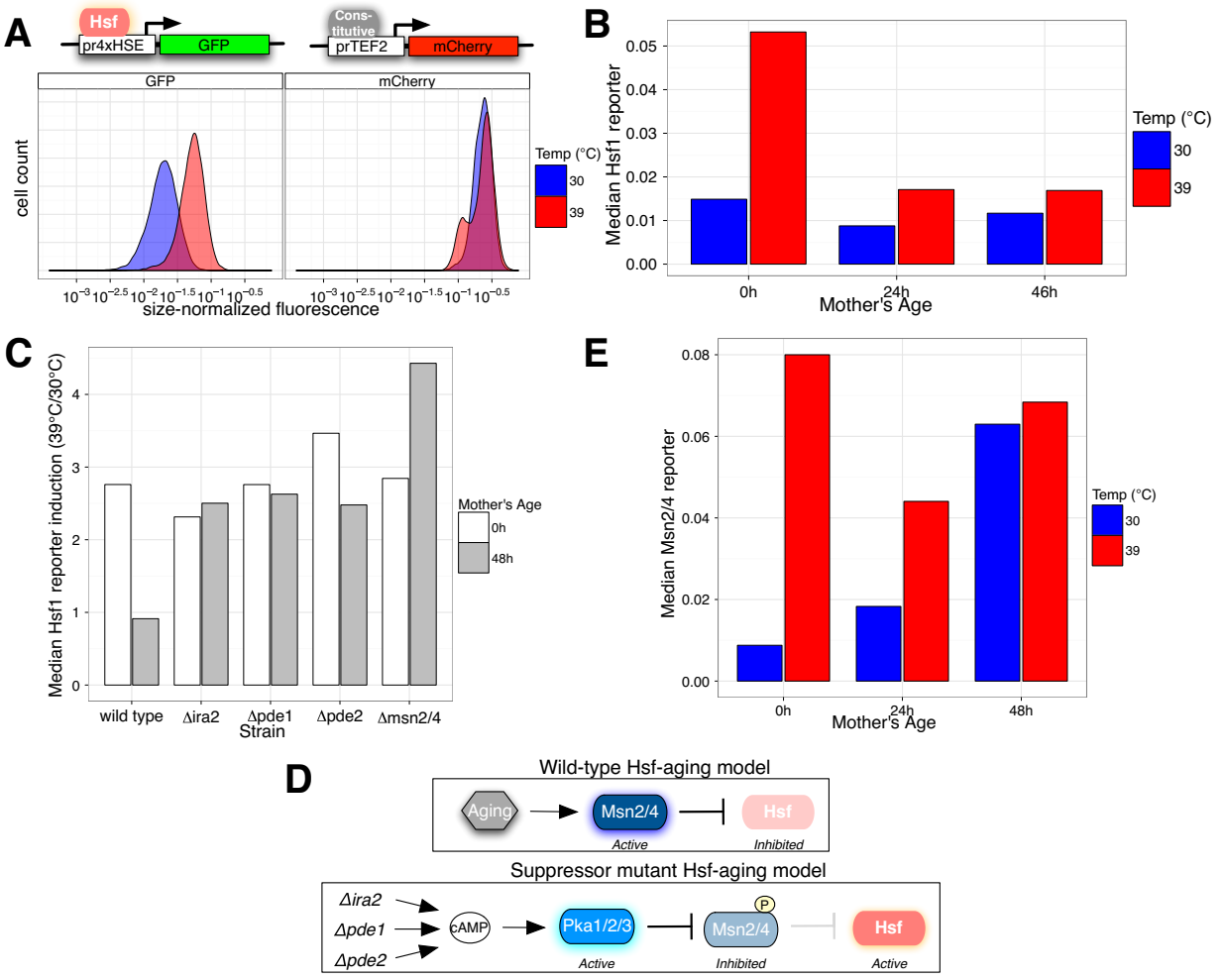

Figure 3.1: (Continued)

Based on these observations, we hypothesized that replicative aging in budding yeast inhibits Hsf1 activity by activating the general stress response (Figure 3.1D). To test this, we used a fluorescent transcriptional reporter with multiple copies of the general stress response element that is recognized by Msn2/4 (Brandman et al., 2012). Indeed, we found that Msn2/4 activity increases progressively with age in synch with the suppression of Hsf1 (Figure 3.1E). In further support of this observation, a recent study also showed that Msn2/4 transcriptional activity increases with replicative age (Xie et al., 2012).

Activation of Msn2/4 is sufficient to inactivate Hsf1 in young cells.

To test if activation of the general stress response is sufficient to inhibit Hsf1, we introduced our transcriptional fluorescent reporters into a strain genetically engineered for Pka inhibition by the ATP-analog 1-NM-PP1 (this genetic background will be referred to as *PKAas*, for analog sensitive, and 1-NM-PP1 will be referred to as the Pka inhibitor) (Bishop et al., 2000; Hao and O'Shea, 2012). As expected, the Pka inhibitor caused induction of the general stress response in *PKAas* but not wild-type cells (Figure 3.2A). Strikingly, we found that inhibition of Pka suppressed Hsf1 induction by heat shock (Figure 3.2B). We note that complete inactivation of Hsf1 required three hours of Pka inhibition prior to heat shock, with significant, but incomplete inhibition observed after 1 hour (not shown). We hypothesize that the temporal offset between Pka inhibition and inhibition of Hsf1 is due to the need for the expression of Msn2/4 gene transcripts.

Figure 3.2: Engineered activation of the general stress response inhibits Hsf1 induction by thermal and AZC stress.
(A) Chemical genetic Pka-inhibition activates Msn2/4. *PKA* and *PKAas* cells were incubated with the Pka inhibitor (or mock treated with carrier-only) for 180' at 30°C prior to heat shock at 39°C (or 30°C control) for 60'. Msn2/4 activity was monitored using the Msn2/4 fluorescent reporter (prSTRE-GFP) measured by flow cytometry for ~10,000 single cells in each condition. Data was normalized to the median for mock pretreated 30°C samples. **(B)** Pka inhibition suppresses Hsf1 activation by heat shock. Shown are single-cell fluorescence distributions for cells with the indicated genotypes expressing the Hsf1 reporter (prHSE-GFP) and treated as in (A). Plotted are $\log_2$ reporter fold-changes for ~10,000 single cells versus the median fluorescence for the control sample as in (A). **(C)** Comparison of the changes in Hsf1 basal activity in unstressed cells with chronic (*Δmsn2/4*) and acute (Msn2/4 anchor away) Msn2/4 loss-of-function. Top: Hsf1 reporter fluorescence versus cell size distribution for unstressed *PKAas* and *PKAas Δmsn2/4* cells using data from (B) for mock pretreated 30°C samples (*i.e.*, same samples as the blue-filled densities in the top row, middle and right columns of B). Bottom: Hsf1 reporter fluorescence versus cell size distributions for unstressed *PKAas* Msn2/4 Anchor Away (Msn2/4-AA) cells incubated with rapamycin to prevent Msn2/4 nuclear localization (or carrier-only mock treatment) for 240' at 30°C using data from (D) (*i.e.*, same samples as the blue-filled densities in the top row of D). Fluorescence and size data was normalized independently in each panel to the median value for the *MSN2/4* (top panel) and mock treated (bottom panel) controls. **(D)** Preventing Msn2/4 nuclear localization following Pka inhibition in Msn2/4 Anchor Away (Msn2/4-AA) cells rescues Hsf1 heat activation. *PKAas Msn2/4-AA* cells expressing the Hsf1 reporter were incubated with rapamycin, or mock treated with carrier-only, for 60' at 30°C before being treated as in (B). Data normalized to the median for the mock pretreated 30°C sample. **(E)** Titrated expression of a constitutive Msn2 allele (Msn2*) from a β-estradiol regulated promoter leads to dose-dependent activation of the GSR. Cells were pretreated for 3 hours with the indicated concentration of β-estradiol at 30°C, then heat shocked at 39°C for 60' (or 30°C degree control treatment). GSR activity was measured by flow cytometry using the Msn2/4 reporter (prSTRE-GFP) and normalized to the median fluorescence for the no β-estradiol 30°C sample. **(F)** Activation of the GSR is sufficient to inhibit Hsf1 heat activation. Cells expressing the Hsf1 reporter (prHSE-GFP) were treated as in (E). **(G)** Engineered GSR is sufficient to inhibit Hsf1 activation by the toxic proline analog l-azetidine-2-carboxylic acid (AZC). Expression of Msn2* from a β-estradiol regulated promoter was induced for three hours by incubating cells with 1μM β-estradiol (or mock pretreatment with carrier-only) for 180' at 30°C before treatment with the indicated concentration of AZC for 90' at 30°C. Hsf1 reporter (prHSE-GFP) fluorescence was measured by flow cytometry and data was normalized to the median value for the mock-pretreated no-AZC sample.

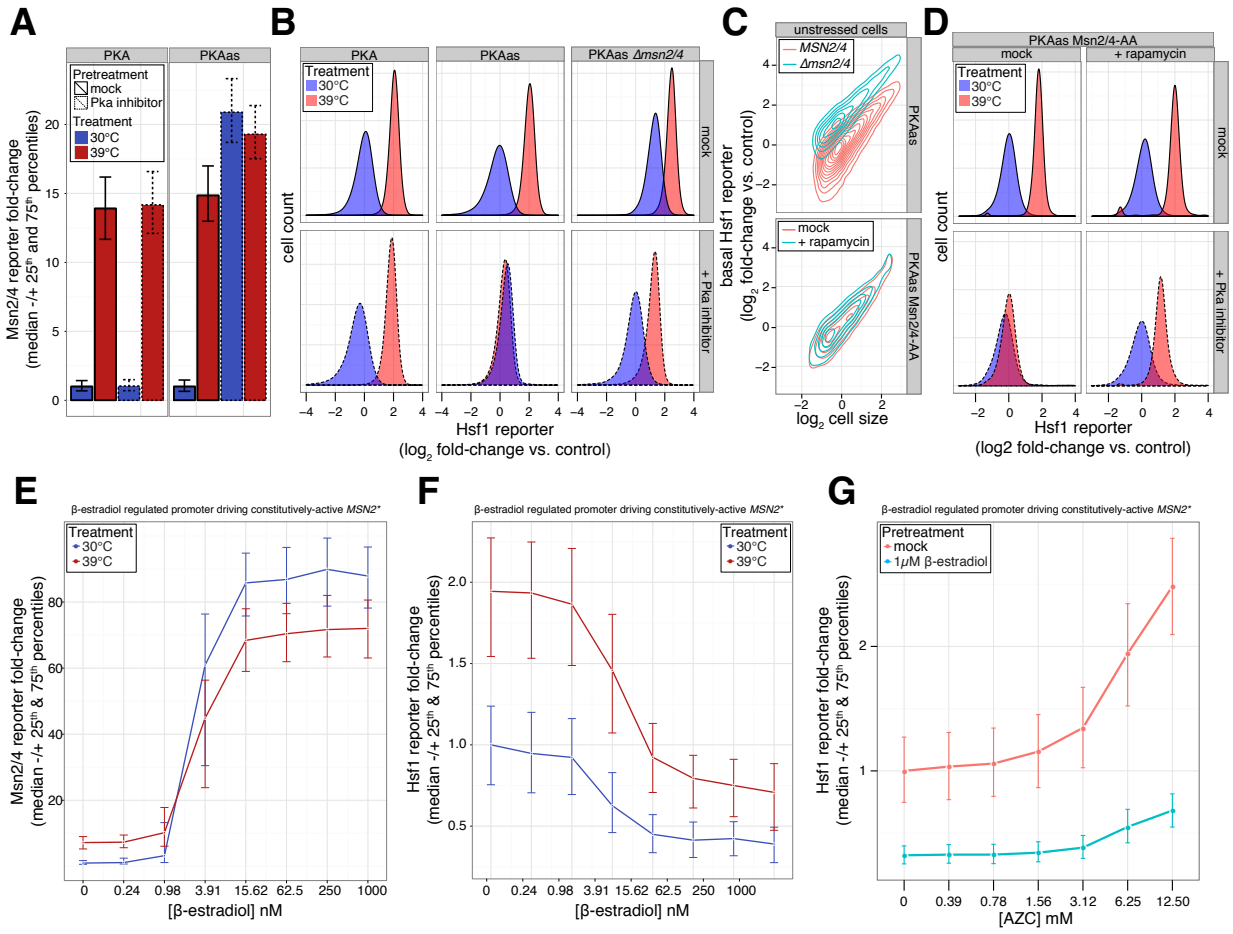

Figure 3.2: (Continued)

Supporting the notion that Msn2/4 are required for inactivation of Hsf1 by Pka inhibition, we found that Hsf1 remained heat inducible following Pka inhibition in *PKAas Δmsn2/4* cells (Figure 3.2B). However, we noted that the extent of increase in Hsf1 activity following heat stress is lower in the *PKAas Δmsn2/4* strain (with or without Pka inhibition) due to an increase in basal (*i.e.*, pre-heat shock) Hsf1 activity relative to the *MSN2/4* parent strain (Figure 3.2C). We wondered if derepression of Hsf1 basal activity in *Δmsn2/4* cells was a consequence of broader Hsf1 disregulation due to chronic Msn2/4 loss-of-function. In this case, rescue of heat induction of Hsf1 in *PKAas Δmsn2/4* cells could be due ectopic effects of the *MSN2/4* deletion on general Hsf1 regulation, rather than from loss of Msn2/4 target gene induction following Pka inhibition. To test if acute Msn2/4 inactivation just prior to Pka inhibition is sufficient to rescue heat inducibility of Hsf1, we used the "anchor away" (AA) approach to prevent Msn2/4 nuclear localization. Briefly, we created a yeast strain (*PKAas Msn2/4-AA*) that is resistant to Tor1 inhibition by rapamycin (*TOR1-1*, *Δfpr1*) and co-expresses Msn2-FRB (FKBP rapamycin-binding domain) and Msn4-FRB fusions and a ribosomal protein L13a-FKBP12 fusion (Rpl13A-FKBP12). In this strain, rapamycin should induce FRB-FKBP12 heterodimerization, thus tethering nuclear Msn2 and Msn4 to nascent ribosome subunits prior to their nuclear export to the cytoplasm, or cytoplasmic Msn2 and Msn4 to mature ribosomes preventing any subsequent nuclear entry. Using the fluorescent Hsf1 reporter, we confirmed that pretreatment of *PKAas Msn2/4-AA* cells with the Pka inhibitor for 3 hours was sufficient to render Hsf1 uninducible by heat shock (Figure 3.2D), as we expected based on our previous experiments. However, when we pretreated these cells with rapamycin for 60

minutes, sequestering Msn2/4 in the cytoplasm, prior to identical treatments we found that Hsf1 inducibility was largely rescued (Figure 3.2D) without the increase in basal Hsf1 activity we observed in *Δmsn2/4* cells (Figure 3.2C). These observations suggest that Msn2/4 nuclear localization is necessary for suppression of Hsf1 by Pka inhibition, independent of their effects on Hsf1 basal activity.

While our results demonstrate that Msn2/4 are necessary for inactivation of Hsf1 by Pka inhibition, they do not rule out the possibility that other factors are also required. To test whether activation of the general stress response alone is sufficient to inactivate Hsf1 without the other changes induced by Pka inhibition, we engineered ectopic expression of a constitutively active allele of *MSN2,* referred to as *MSN2**, under control of a β-estradiol dependent promoter (McIsaac et al., 2013). In this mutant, all of the regulatory Pka phosphorylation sites that typically repress Msn2 nuclear localization have been mutated, thus when expressed Msn2* is constitutively nuclear and drives expression of general stress response genes (Hao et al., 2013). Treating cells with β-estradiol to induce expression of *MSN2** caused dose-dependent induction of our Msn2/4 reporter (Figure 3.2E), and was associated with a similar dose-dependent inhibition of Hsf1 under basal and heat shock conditions (Figure 3.2F). In addition to heat shock, which activates Msn2/4 and Hsf1, we found that ectopic activation of the general stress response was sufficient to suppress activation of Hsf1 by the toxic proline analog AZC (Figure 3.2G), which has been previously shown to activate Hsf1, but not Msn2/4 (Trotter et al., 2002).

These results demonstrate that engineered activation of Msn2/4 is sufficient to inhibit up-regulation of Hsf1-dependent transcription during stress caused by heat and AZC.

Activation of the general stress response antagonizes Hsf1 activity during heat shock.

Heat stress causes large-scale gene expression changes known as the heat shock response (Richter et al., 2010). Our previous work demonstrated that Msn2/4 mediates the majority of heat-induced transcription independent of Hsf1, which drives overexpression of a small but critical set of folding chaperones in response to thermal stress (see Chapter 2). Given that heat shock causes robust and apparently coincident activation of both Hsf1 and Msn2/4 (Gasch et al., 2000), we wondered if our observation that engineered activation GSR is sufficient to inhibit Hsf1 only holds under synthetic, non-physiological conditions. To enable simultaneous measurement of Hsf1 and Msn2/4 activity changes during heat shock, we constructed a two-color fluorescent reporter with synthetic promoters containing Hsf1 and Msn2/4 binding sites driving *GFP* and *RFP*, respectively. To monitor the kinetics of Hsf1 and Msn2/4 activation, we heat shocked cells expressing the reporter and then transferred aliquots of the culture to chilled media containing cycloheximide at various time points after temperature increase. Incubating cells after heat shock with cycloheximide allows fluorescent reporter proteins that were synthesized during heat shock to mature, while preventing any additional protein translation. Further, since the fluorescent proteins we used have very long half-lives, the increase in fluorescence between adjacent time points should reflects the change in

expression of proteins encoded by Hsf1 and Msn2/4 target genes during this period. This analysis revealed that activation of Hsf1 and Msn2/4 by heat shock are temporally distinct (Figure 3.3A). Synthesis of the Hsf1 Gfp reporter was strongly induced immediately after temperature increase, with maximal induction after ~10 minutes, but induction was short-lived and rapidly attenuated (Figure 3.3B). By contrast, robust expression of the Msn2/4 reporter was comparatively slow, with sustained induction occurring after 30 minutes of heat stress (Figure 3.3B). Thus, we conclude that attenuation of Hsf1 activity during heat stress coincides with activation of the GSR.

Figure 3.3: Attenuation of Hsf1 activity following heat shock is hastened by induction of the GSR.
(A) Time course analysis of Hsf1 reporter (prHSE-GFP) and Msn2/4 reporter (prSTRE-RFP) activity kinetics after temperature increase from 30°C to 39°C. Cell expressing both reporter constructs were incubated at 39°C and aliquots of the culture were taken at indicated time points and transferred to chilled media with 50ug/mL cycloheximide to stop additional reporter protein synthesis. Cells were incubated for at least 60' in cycloheximide prior to analysis flow cytometery analysis to allow fluorophore maturation. Fold-changes were calculated relative to the median reporter fluorescence at 30°C ten minutes before temperature increase. Note: This data is repeated in (C), as this sample was actually the mock pretreatment control for the experiment in (C) and (D). **(B)** Rate of change for Hsf1 and Msn2/4 reporter fluorescence data from (A) as a function of time. Rates were computed by dividing the fluorescence fold-change between adjacent time points by the length of time between them in minutes. Note: This data is repeated in (D), as this sample was actually the mock pretreatment control for the experiment in (C) and (D). **(C)** Engineering faster GSR activation by inducing Msn2* expression limits the total Hsf1 activity induced by temperature increase. Cells expressing the Hsf1 and Msn2/4 reporters were pretreated with 20nM β-estradiol at 30°C for the indicated times in the legend (or mock treated with carrier-only for 75') before temperature increase to 39°C, followed by a reporter time course as in (A). The text in the lower panel indicates the apparent increase in GSR activation kinetics for each sample based the time at which the Msn2/4 reporter fold-change approximately matched the change for the mock pretreated sample after 60' at 39°C. Note: The data from (A) and (B) is the same as the mock pretreatment control in (C) and (D). **(D)** Faster GSR activation kinetics hasten the rate of attenuation of Hsf1 activity following heat shock. Rate of change for Hsf1 and Msn2/4 reporter fluorescence data from (C) as a function of time as described in (B). **(E)** Preventing GSR activation during heat shock is associated with increased Hsf1 activity. *PKAas* and *PKAas Δmsn2/4* cells were either untreated or incubated with the Pka inhibitor for 30' at 25°C prior to temperature increase. Wild type cells expressing *RAS2(G19V)* from a β-estradiol regulated promoter were grown continuously in 20nM β-estradiol to allow *RAS2(G19V)* expression to reach steady state before temperature increase. Hsf1 reporter activity was monitored by time course analysis after transferring cells to 39°C as in (A) and values were normalized to the mean of the untreated *PKAas* sample just prior to temperature increase. **(F)** Preventing GSR activation by heat shock extends Hsf1 activation following heat shock. Rate of change for Hsf1 reporter fluorescence data from (E) as a function of time as described in (B). **(G)** The effect of Msn2/4 on Hsf1 activity induced by AZC treatment and during stress recovery. Wild type (*MSN2/4*) and *Δmsn2/4* cells expressing the Hsf1 reporter were incubated with 5mM AZC at 30°C and activity was followed for 180' by a reporter time course as in (A). After 180', cells were washed and resuspended in fresh media with or without AZC and followed by a second time course for 5 hours. Samples from the pre-washout and post-washout time courses were analyzed separately by flow cytometry. Data was normalized to the median fluorescence of the *MSN2/4* sample immediately after adding AZC. **(H)** Msn2/4 does not

Figure 3.3: (Continued)

alter Hsf1 activity kinetics during AZC stress or recovery from it. Rate of change for Hsf1 reporter fluorescence data from (G) as a function of time as described in (B).

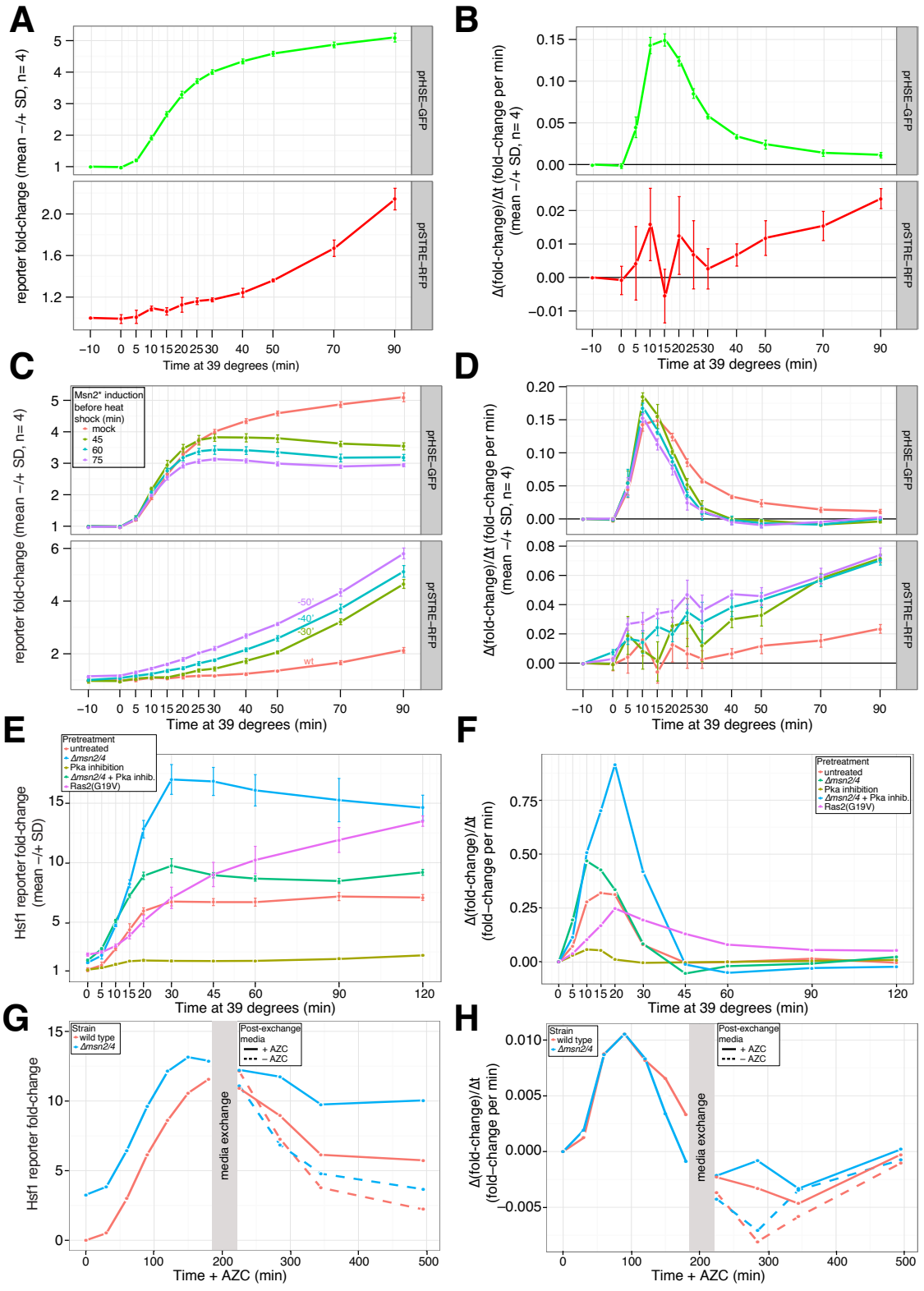

Figure 3.3: (Continued)

Rather than demonstrating that Hsf1 and Msn2/4 are contemporaneously activated by heat shock, our kinetic reporter analysis lead us to hypothesize that rapid heat-activation of Hsf1 is subsequently attenuated by delayed expression of Msn2/4 targets. Under this hypothesis, we would expect that more rapid activation of the GSR by heat stress would lead to more rapid attenuation of Hsf1. To engineer more rapid GSR activation, we induced expression of Msn2* by incubating unstressed cells with β-estradiol prior to temperature increase and reporter time course analysis. Post-hoc analysis of the Msn2/4 reporter showed that adding β-estradiol 75, 60 or 45 minutes before heat shock was associated with 50, 40 and 30 minutes faster reporter activation based on comparison to the Msn2/4 reporter change for the mock pretreated control after 60 minutes of heat shock (Figure 3.3C). Consistent with our hypothesis, more rapid induction of the GSR was associated with a decrease in total Hsf1 reporter induction over the time course (Figure 3.3C). Strikingly, the rate of initial activation for the Hsf1 reporter was unaffected by GSR kinetics, but the rate of subsequent attenuation monotonically increased with faster GSR activation (Figure 3.3D). In further support of our hypothesis, we found that heat shock caused stronger and more sustained activation of Hsf1 in *Δmsn2/4* cells, even when Pka was inactivated before heat shock (Figure 3.3E). Finally, we tested the effect of ectopically preventing Pka inactivation during heat shock by engineering *RAS2(G19V)* expression prior to temperature increase, since *RAS2(G19V)* expression is a well-established strategy for maintaining Pka activity during stress (Pincus et al., 2014). Fully consistent with our previous results, maintaining Pka activity during heat shock caused a significant increase in Hsf1 reporter expression, reaching a similar level after 2 hours of

stress to the *Δmsn2/4* strain (Figure 3.3E). However, we noted that *RAS2(G19V)* expression had a unique effect on Hsf1 kinetics, as the peak induction rate was dampened and the initial activation phase was prolonged, while the attenuation phase was extended far longer than any of the other conditions we tested (Figure 3.3F). In summary, these experiments clearly support the hypothesis that Hsf1 activity during heat shock is antagonized by subsequent activation of the GSR.

A corollary of our hypothesis that activation of Msn2/4 antagonizes Hsf1 during heat shock is that Hsf1 activity should be Msn2/4-independent under stress conditions that activate Hsf1 but not Msn2/4. To test this, we monitored Hsf1 reporter activity in wild type and *Δmsn2/4* cells treated with AZC, as it is well established that AZC activates Hsf1 but not Msn2/4 (Trotter et al., 2002). Other than the expected difference in basal expression, treatment with AZC for 3 hours induced similar changes in Hsf1 reporter expression (Figure 3.3G) and with similar kinetics (Figure 3.3H) for wild type and *Δmsn2/*4 cells. After 3 hours of treatment, we performed a media exchange in which half the cells were transferred to media lacking AZC and the other half was transferred to fresh AZC-containing media. For cell transferred to media without AZC, the rate at which Hsf1 activity reset to basal levels was independent of Msn2/4 (Figure 3.3H). Similarly, the difference in steady state Hsf1 activity after a total of 8 hours of AZC treatment mirrored the differences in basal activity in unstressed wild type versus *Δmsn2/4* cells. Thus, while engineered GSR is sufficient to inhibit Hsf1 activation by AZC (Figure 3.2G), the lack of

physiological GSR stimulation by AZC renders Hsf1 dynamics refractory to Msn2/4 under this stress.

Global analysis shows the GSR antagonizes activation of Hsf1 target genes during heat shock.

We next sought to test whether the inhibition of Hsf1 by the GSR that we observed for fluorescent reporter proteins expressed from synthetic promoters reflected *bona fide* effects on expression of endogenous Hsf1 target genes. Our previous work revealed that the basal transcriptional program for Hsf1 is comprised of just 18 genes, predominately encoding chaperones and other proteostasis factors (see Chapter 2). Additionally, we found that during heat shock Hsf1 increases the magnitude of its transcriptional program without expanding its breadth. Rather, we showed that Msn2/4 independently drive the vast majority of heat-induced gene expression, with just four common targets shared by Hsf1 and Msn2/4. We first tested the effect of Pka inhibition prior to temperature increase on the heat shock response using mRNA deep sequencing (RNA-seq). Genome wide the heat shock response remained largely intact after Pka inhibition ($R^2 = 0.71$) (Figure 3.4A), with a significant, but expected, increase in expression of Msn2/4 targets ($p < 10^{-56}$) (Figure 3.4B). As a whole, Hsf1-dependent gene expression was not significantly decreased ($p = .30$). However, when we focused on the set of Hsf1 targets that are not co-regulated by Msn2/4, we found Pka inhibition was associated with reduced heat shock expression of 13/14 genes (Figure 3.4A), and expression of this gene set as a whole was significantly reduced compared to all other genes ($p < 10^{-2}$) (Figure 3.4B). Next, we

monitored changes in heat shock gene expression that result from maintaining Pka activity during stress by inducing Ras2(G19V) expression prior to temperature increase. In contrast to the minimal effect of Pka inhibition on the heat shock response, we found that Ras2(G19V) expression caused a much larger perturbation to heat induced expression changes ($R^2 = 0.46$) (Figure 3.4C), and as expected Msn2/4 targets were acutely sensitive ($p < 10^{-67}$) (Figure 3.4D). However, consistent with our Hsf1 reporter experiments (Figure 3E), expression of Ras2(G19V) caused a significant increase in expression of all Hsf1 targets ($p < 10^{-7}$) (Figure 3.4D), including those co-regulated with Msn2/4. Finally, we directly tested the effect of *MSN2/4* deletion on the heat shock response. Fully consistent with our previous experiments, most heat-induced expression was ablated in *Δmsn2/4* cells (Figure 3.4E), and a significant decrease in Msn2/4 target expression ($p < 10^{-72}$) was associated with a significant increase in Hsf1-dependent gene expression ($p < 10^{-5}$) (Figure 3.4F). In summary, our expression analysis for endogenous Hsf1 and Msn2/4 targets corroborates the antagonism we observed between these two factors using synthetic reporter constructs. They also demonstrate that in the absence of Msn2/4, Hsf1 is sufficient to drive heat induction of their common gene targets.

Figure 3.4: Expression of Msn2/4 target genes antagonizes up-regulation of Hsf1 target genes during heat shock.
(A) *PKAas* cells growing logarithmically at 30°C (control), and after treatment first with either Pka inhibitor or carrier (180' at 30°C) followed by heat shock (30' at 39°C), were analyzed by RNA-seq. Shown is a gene scatter plot comparing mRNA changes induced by these two treatments relative to control. Colors denote gene sets previously defined in Chapter 2: Hsf1 targets that are not co-regulated by Msn2/4 are blue, Hsf1 targets that are co-regulated by Msn2/4 are purple, Msn2/4 targets are red, and all other genes are gray. **(B)** CDF of mRNA abundance fold-changes induced by heat shock after pretreatment with the Pka inhibitor versus mock pretreatment as in (A). Colors denote gene sets previously defined in Chapter 2: Hsf1 targets that are not co-regulated by Msn2/4 are blue, all Hsf1 targets including those that are co-regulated by Msn2/4 are purple, Msn2/4 targets are red, and all other genes are gray. For each gene set, the y-axis corresponds to the proportion of genes in that set with fold-change ratios less than or equal to the corresponding value on the x-axis. P-values are for the Wilcoxon rank-sum test for equal distributions of fold-changes for the indicated gene set versus the distribution of changes for the other gene sets combined. **(C)** Preventing heat inactivation of Pka by expressing Ras2(G19V) suppresses activation of Msn2/4 targets following heat shock, while increasing expression of Hsf1 target genes. Cells expressing *RAS2(G19V)* from a β-estradiol regulated promoter growing logarithmically at 30°C (control), and after treatment first with either 100nM β-estradiol or carrier (120' at 30°C) followed by heat shock (30' at 39°C), were analyzed by RNA-seq. Shown is a gene scatter plot comparing mRNA changes induced by these two treatments relative to control. Note: The expression system for inducing *RAS2(G19V)* uses an artificial transcription factor with the Gal4 DNA binding domain, thus β-estradiol causes up-regulation of Gal4 targets, which are indicated in green. Other colors denote the same gene sets as in (A). **(D)** CDF of mRNA abundance fold-changes induced by heat shock after pretreatment inducing *RAS2(G19V)* expression versus mock pretreatment as in (C). For each gene set, the y-axis corresponds to the proportion of genes in that set with fold-change ratios less than or equal to the corresponding value on the x-axis. P-values are for the Wilcoxon rank-sum test for equal distributions of fold-changes for the indicated gene set versus the distribution of changes for the other gene sets combined. **(E)** *MSN2/4* deletion enhances up-regulation of Hsf1 target genes following heat shock. Wild type (*MSN2 MSN4*) and *Δmsn2 Δmsn4* cells growing logarithmically at 30°C (control), and after heat shock (30' at 39°C), were analyzed by RNA-seq. Shown is a gene scatter plot comparing mRNA changes induced by these two treatments relative to the wild type control. **(F)** CDF of mRNA abundance fold-changes induced by heat shock in *Δmsn2 Δmsn4* versus wild type cells as in (E). For each gene set, the y-axis corresponds to the proportion of genes in that set with fold-change ratios less than or equal to the corresponding value on the x-axis. P-values are for the Wilcoxon rank-sum test for equal distributions of fold-changes for the indicated gene set versus the distribution of changes for the other gene sets combined.

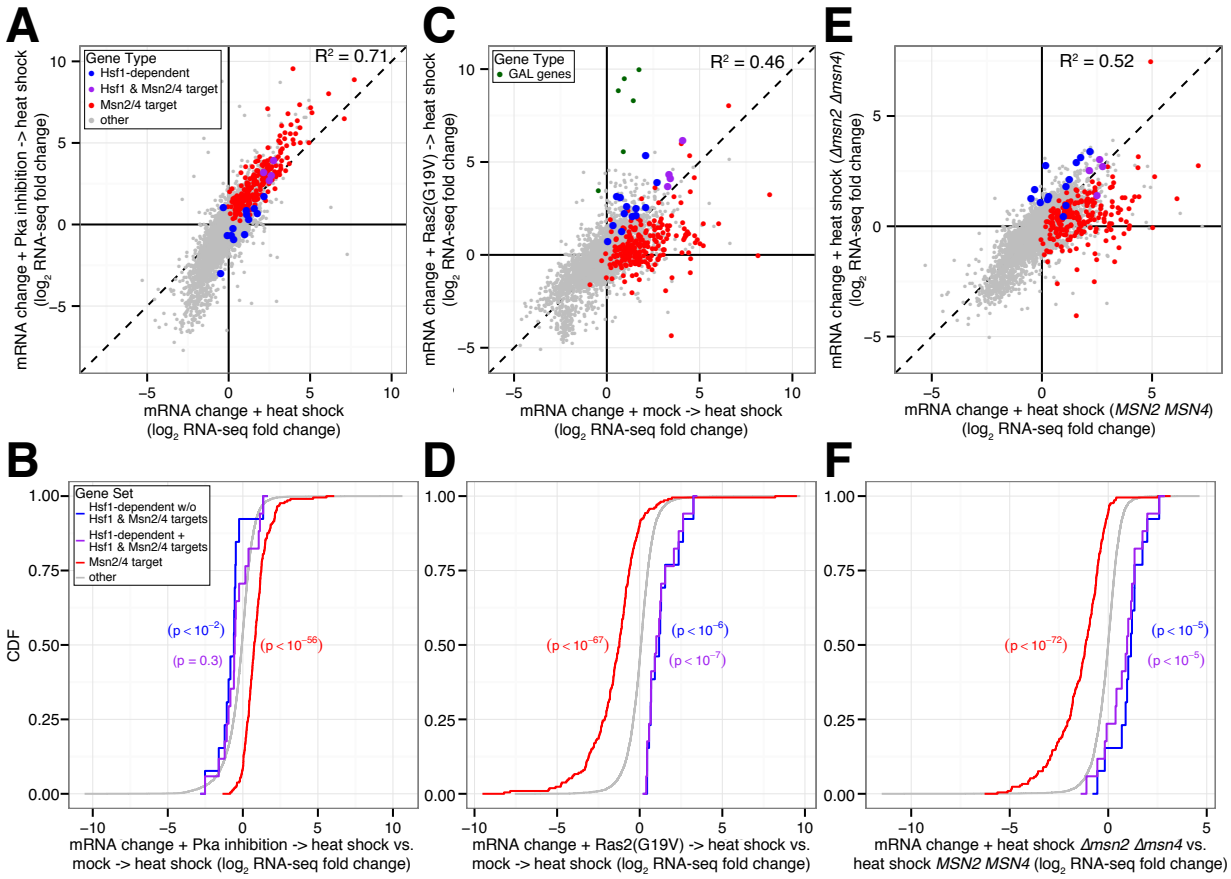

Figure 3.4: (Continued)

Hsf1 inactivation is associated with hyperphosphorylation.

Post-translational modification of Hsf1 has previously been suggested to play a role in regulation of Hsf1 activity (Anckar and Sistonen, 2011). This motivated us to monitor broad changes in Hsf1 modification state under various stress conditions by SDS-PAGE and immunoblotting. First, we performed a comparative time course analysis of heat-induced changes in Hsf1 activity and electrophoretic mobility in cells expressing epitope-tagged Hsf1-FLAG-V5 as the sole copy of Hsf1. These experiments revealed that after a brief period of acute Hsf1 activation following temperature increase, attenuation of Hsf1 activity was associated with a large change in mobility consistent with multiple Hsf1 modifications (Figure 3.5A). By contrast, AZC stress induces persistent Hsf1 activation (Figure 3.3G) and was not associated with a change in Hsf1 electrophoretic mobility (Figure 3.5B), in agreement with previous experiments in mammalian cells showing that mammalian HSF1 is not phosphorylated after treatment with AZC (Sarge et al., 1993). Additional analysis of Hsf1 after oxidative stress caused by menadione treatment (Figure 3.5C), and after glucose or amino acid depletion (Figure 3.5D) revealed similar mobility changes were associated with low levels of Hsf1 activity. As a variety of stresses have been associated with decreased Pka activity and we previously demonstrated that engineered Pka inactivation was sufficient to inhibit Hsf1, we directly tested the effect of our stress panel on Pka activity (Figure 3.5E). This analysis revealed a clear correlation: stresses that decrease Pka activity are associated with low levels of Hsf1 activity and Hsf1 modifications. Further, we found that chemical inhibition of Pka in *PKAas* cells expressing Hsf1-FLAG-V5 was sufficient to induced Msn2/4-dependent changes in Hsf1

electrophoretic mobility in the absence of any external stress (Figure 3.5F). We also found that *MSN2/4* deletion prevented the large change in Hsf1 mobility that we previously observed following heat and oxidative stress by SDS-PAGE (Figure 3.5G,H), arguing that Msn2/4 are required for many Hsf1 modifications. Finally, proteomic analysis of Hsf1-FLAG-V5 affinity purified from cells subjected to our stress panel revealed that Hsf1 is hyperphosphorylated under conditions associated low Hsf1activity (Figure 3.5I), suggesting hyperphosphorylation as a potential mechanism of Hsf1 inactivation under these conditions.

Figure 3.5: Diminished Hsf1 activity is associated with Msn2/4-dependent hyper-phosphorylation under conditions with low Pka activity.
(A) Top: Anti-FLAG western blot of cells expressing Hsf1-FLAG-V5 as the only copy of Hsf1 shifted from 25ºC to 39ºC for the indicated times. Bottom: Cells expressing the HSE-YFP reporter were shifted from 25ºC to 39ºC for the indicated times and protein synthesis was terminated with cycloheximide. YFP levels were measured by flow cytometry, median values were normalized to the median basal signal, and the difference between consecutive time points is plotted. Error bars represent the standard deviation of 3 biological replicates. **(B)** Top: Anti-FLAG western blot of cells expressing Hsf1-FLAG-V5 treated with the indicated doses of AZC for 2 hours. Bottom: Cells expressing the HSE-YFP reporter were treated with the indicated doses of AZC for 4 hours, YFP levels were measured by flow ctyometry and median values normalized to untreated cells are plotted. Error bars represent the standard deviation of 3 biological replicates.
(C) Top: Anti-FLAG western blot of cells expressing Hsf1-FLAG-V5 treated with the indicated doses of menadione for 2 hours. Bottom: Cells expressing the HSE-YFP reporter were treated with the indicated does of menadione for 4 hours, YFP levels were measured by flow ctyometry and median values normalized to untreated cells are plotted. Error bars represent the standard deviation of 3 biological replicates.
(D) Top: Anti-FLAG western blot of cells expressing Hsf1-FLAG-V5. Cells were filtered, washed 3x in PBS, resuspended in media lacking either leucine or glucose and incubated for 30 minutes at 30ºC. Bottom: Cells expressing the HSE-YFP reporter were treated as above for 2 hours, YFP levels were measured by flow ctyometry and median values normalized to untreated cells are plotted. Error bars represent the standard deviation of 3 biological replicates. **(E)** Pka activity was measured in lysates prepared from cells treated as indicated using a commercial *in vitro* fluorescence assay calibrated to dilutions of a Pka standard. **(F - H)** Western blots as above; 1-NM-PP1 was added for 30 minutes; menadione for 2 hrs, heat shock as above. The arrowhead indicates the middle of the most-shifted Hsf1-FLAG-V5 band for samples from identically treated wild type cells on the same blot that are not shown. **(I)** Summary of IP/MS/MS of Hsf1-FLAG-V5 identifying phosphorylation sites in indicated conditions. Yellow represents S225.

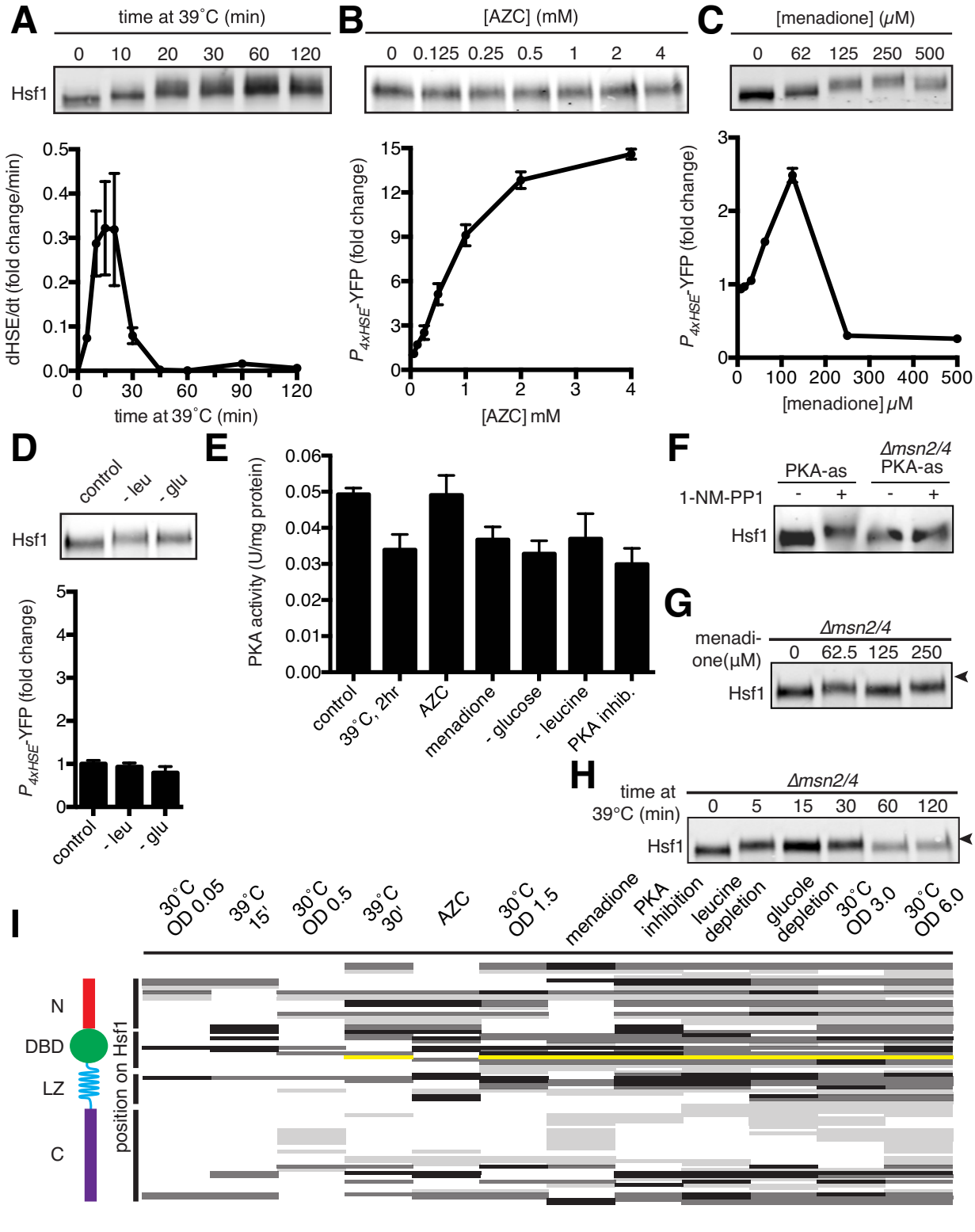

Figure 3.5: (Continued)

Hsf1 inactivation by the GSR in independent of hyperphosphorylation.

Based on modifications identified by our proteomic analysis, we used site-directed mutagenesis to determine the role of both individual and groups of phosphorylation sites on Hsf1 inactivation by replacing phosphorylated residues with non-phosphorylatable substitutions (*e.g.*, S-to-A). We generated and analyze a library of single Hsf1 phosphosite mutants, but none had an effect on Hsf1 function (not shown) other than mutation of S225 to alanine, which was unable to complement the *HSF1* deletion (Figure 3.6A), consistent with a previous mutagenic analysis of Hsf1 that suggested mutation of S225 to any amino acid other than threonine ablates Hsf1 function (Hubl et al., 1994). After similar results were obtained when multiple mutations were combined (not shown), we decided to work backwards from an Hsf1 mutant lacking all 153 S/T residues. Unsurprisingly cells expressing this *HSF1(153A)* mutant—with nearly 20% of its primary sequence mutated—in place of wild type *HSF1* were not viable (Figure 3.6B), however this was expected as it contained the lethal S225A mutation. Strikingly, restoring S225 in *HSF1(153A)* to obtain *HSF1(152A)* restored growth (Figure 3.6B) demonstrating S225 is the *only* essential S/T residue in Hsf1. Even more strikingly, strains expressing *HSF1(152A)* as the only copy of Hsf1 were capable of growth at elevated temperatures (Figure 3.6C) suggesting that phosphorylation is dispensable for Hsf1 function. As our proteomic analysis identified phosphorylation of S225 under a number of conditions associated with Hsf1 inactivation (Figure 3.5I), we attempted to detect phosphorylation of S225 by in the *HSF1(152A)* mutant using ^{32}P incorporation. However, immunoprecipitation and autoradiography analysis after heat shock showed a lack of

detectable phosphorylation of *HSF1(152A)*, similar to the *HSF1(153A)* mutant that lacks any S/T residues, and in contrast to the multiply phosphorylated wild type (Figure 3.6D). We therefore introduced the *HSF1(152A)* mutant into the *PKAas* background to test if bypassing Hsf1 hyperphosphorylation could restore Hsf1 function in the presence of the GSR. As expected, heat shock induced the fluorescent Hsf1 reporter in cells expressing wild type *HSF1* and the *HSF1(152A)* allele (Figure 3.6E). Disappointingly, we found that Pka inhibition still suppressed heat activation of the Hsf1 reporter by *HSF1(152A)* similar to—if not more than—the wild type (Figure 3.6E). Thus, while hyperphosphorylation is associated with low Hsf1 activity, these results strongly argue that hyperphosphorylation is not required for inhibition of Hsf1 by the GSR.

Figure 3.6: Inactivation of Hsf1 by the GSR is phosphorylation-independent and does not alter Hsf1 DNA binding.
(A) Plasmid-shuffle assay testing the viability of *HSF1* phosphorylation site mutants. The indicated *HSF1* mutants were integrated into the TRP1-locus under control of the native HSF1-promoter in strains with the endogenous, genomic copy of *HSF1* deleted (*Δhsf1*) and replaced with a wild type copy on a counter-selectable plasmid (*pRS316 HSF1*). Selection against the *URA3*-marked plasmid-borne copy of *HSF1* via 5-fluoroorotic acid (5-FOA) leaves the *HSF1* allele in the TRP1-locus as the only copy. Mutation of S225 to alanine is inviable. (**B)** Similar to (A), mutation of all S/T residues simultaneously in *HSF1(153A)* is inviable. However, restoring S225 in *HSF1(153A)*, referred to as *HSF1(152A)*, rescues growth and demonstrates S225 is the only S/T residue required for viability. Plates incubated at room temperature for 3 days before being photographed. **(C)** *HSF1(152A)* supports growth at elevated temperatures. Spotting assay comparing growth of strains expressing either *HSF1* wild type or *HSF1(152A)* at the indicated temperatures after 2 days. **(D)** *HSF1(152A)* and *(153A)* mutants, unlike *HSF1* wild type, are not phosphorylated during heat shock. Phosphorylation was monitored by ^{32}P incorporation (autoradiography show in top panel) into Hsf1 that was immunoprecipitated (anti-Hsf1 blot shown bottom panel) from strains transiently expressing the indicated mutants for 2 hours before transferring to ^{32}P-containing media followed by a 30 minute heat shock at 39°C. **(E)** Fluorescent Hsf1 reporter assay testing heat-induced Hsf1 activation after engineered Msn2/4 activation. Comparison of *PKAas* strains expressing *HSF1* wild type or the non-phosphorylatable *152A* mutant. Cells were incubated at 30 degrees for 3 hours with the Pka inhibitor to induce Msn2/4 (or carrier control) before 39°C heat shock (or 30°C control) for 60'. Reporter activity was measured by flow cytometry and fluorescence was normalized to the median of the wild type control sample (0uM Pka inhibitor and 30°C mock heat shock). Data reported as median fluorescence with error bars showing the 25th and 75th percentiles of the population of ~10,000 cells measured from each sample. **(F)** Pka inhibition does not cause a dramatic change in the genome-wide patter of Hsf1 DNA binding. *PKAas* cells expressing *HSF1-FLAG* as the sole copy of Hsf1 were pretreated with the Pka inhibitor (or mock treated with carrier-only) for 180' at 30°C before a 60' heat shock at 39°C (or 30°C control). Chromatin associated with Hsf1-FLAG was affinity purified and then analyzed by deep sequencing. Shown is the relative binding of Hsf1 under the indicated conditions across all genomic loci, with chromosome boundaries indicated below. **(G)** Hsf1 binding to the promoters of the 18 Hsf1 dependent genes we defined in Chapter 2 using the same Hsf1-FLAG ChIP-seq data as in (F). Blue arrows demarcate the location of the open reading frame and purple boxes indicate the location of predicted Hsf1 binding sites (TTCnnGAA and TTC-n_7-TTC-n_7-TTC). **(H)** Schematic of the reporter locus with overlapping Hsf1 and Gal4 binding sites indicated in red and blue, respectively. In this locus, the binding sites are followed by a crippled *CYC1* minimal promoter, the *GFP* open reading frame and the *ACT1* terminator. **(I)** Schematic of the control reporter locus derived from the promoter in (H), with the Hsf1 binding sites mutated (mutated positions in the Hsf1 binding sites are indicated in pink) without altering the Gal4 binding motif (blue). In this locus, the binding sites are followed by a crippled

Figure 3.6: (Continued)

CYC1 minimal promoter, the *RFP* open reading frame and the *ADH1* terminator. **(J)** Schematic of the Hsf1 DNA binding fluorescent reporter assay. The assay consists of three components: the two reporters described in (H) and (I), and a chimeric artificial transcription factor containing the Gal4 DNA binding domain, the human estrogen receptor and the Msn2 activation domain (referred to as GEM). In the absence of β-estradiol, Hsf1 will bind to the GFP promoter but not the RFP promoter, and constitutively expressed GEM will be sequestered in the cytoplasm (left). Treating cells with β-estradiol causes a dose-dependent accumulation of GEM in the nucleus. (Top right) Binding of inactive Hsf1 will occlude the Gal4 binding sites in the GFP promoter making it less accessible to GEM and resulting in a different dose-response relationship for Gfp and Rfp expression as a function of β-estradiol concentration. (Bottom right) In the absence of Hsf1 binding, both the GFP and RFP promoters will be equally accessible, and the dose-response relationship between β-estradiol concentration and expression of Gfp versus Rfp should be similar. **(K)** *Hsf1-AA PKAas* cells were pretreated with the Pka inhibitor (or mock carrier-only control) for 180' at 30°C followed by treatment with the indicated concentration of β-estradiol for 90' at 30°C, after treatment cycloheximide was added before flow cytometer analysis to prevent any additional reporter synthesis. As a no Hsf1 binding control, rapamycin was added to a second mock pretreated sample concomitant with β-estradiol. Plots show the median fluorescence from ~10,000 single cells analyzed in each condition, with values normalized to the median of the mock-pretreatment no-β-estradiol control. Comparison of the Pka inhibitor treated samples to the two controls suggests that Pka inhibition does not impair Hsf1 DNA binding as the dose-response profile for Pka inhibition samples does not resemble that of the Hsf1 AA samples.

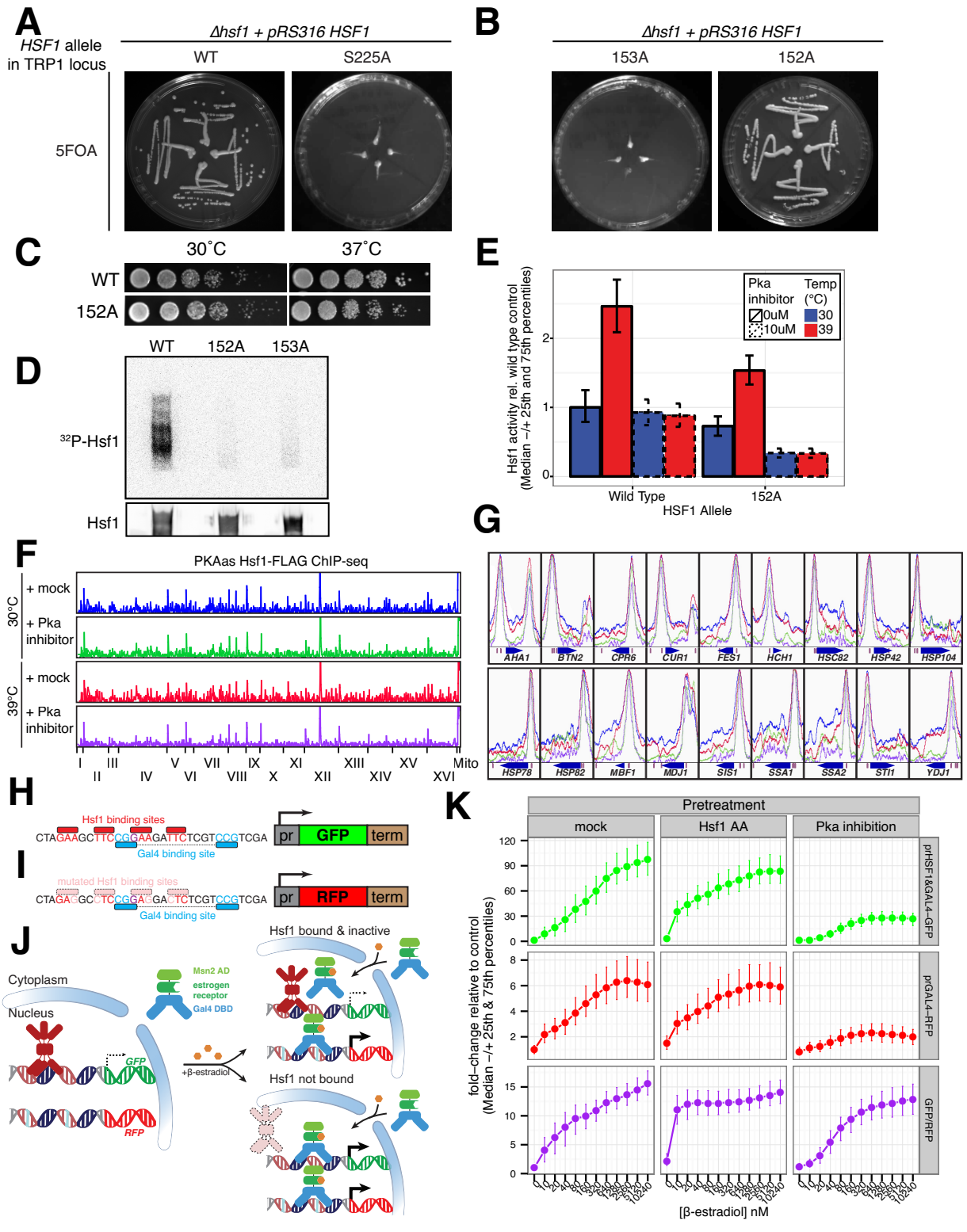

Figure 3.6: (Continued)

Pka inhibition does not alter Hsf1 DNA binding.

Structural analysis of the Hsf1 DNA binding domain has shown that S225 directly contacts and hydrogen bonds with DNA (Harrison et al., 1994), thus disruption of the hydroxyl group by phosphorylation or mutation to any residue other than threonine should disrupt Hsf1 DNA binding (Hubl et al., 1994). While our ^{32}P incorporation assay did not detect any apparent phosphorylation of S225 after heat shock in the *HSF1(152A)* mutant, we sought to further explore attenuated Hsf1 DNA binding as a potential mechanism for inactivation because of the strong association between conditions where Hsf1 activity is low or repressed and S225 phosphorylation according to our phosphorproteomics analysis (Figure 3.5I). First, we tested the effect of Pka inhibition on genome-wide Hsf1 DNA binding under both control and heat shock conditions using chromatin immunoprecipitation followed by deep sequencing (ChIP-seq). Sequencing analysis of chromatin affinity purified from *PKAas* cells expressing epitope-tagged Hsf1-FLAG as the sole copy of Hsf1 did not detect any dramatic change in the global Hsf1 binding pattern after Pka inhibition (Figure 3.6F). Similarly, when we focused our analysis on the 18 Hsf1-dependent genes we previously defined, we found that Pka inhibition did not alter binding of Hsf1 to heat shock elements in the up-stream promoters of any of these genes (Figure 3.6G). Thus, we conclude that inactivation of Hsf1 by Pka inhibition is not due to a dramatic change in the genomic loci bound by Hsf1.

While our Hsf1 ChIP-seq analysis supports that Pka inhibition is not associated with a change in Hsf1 DNA binding specificity (*i.e.*, the relative amount of Hsf1 binding to target

gene promoters versus other genomic loci was unchanged), ChIP-seq is relative insensitive to uniform changes in binding and therefore we could not determine from this data whether Pka inhibition causes a decrease in absolute Hsf1 binding to individual loci. We therefore developed a quantitative assay to monitor changes in Hsf1 binding to a reporter locus in live cells under these conditions. Our assay is based on a classic observation that for an engineered promoter with overlapping Hsf1 and Gal4 binding sites, under conditions where Hsf1 is bound but inactive and Gal4 is active (*e.g.*, cells growing at low temperature using galactose as a carbon source) Hsf1 binding occludes the Gal4 binding site and attenuates activation of a down-stream reporter gene relative to its expression under these conditions from a Gal4-only promoter (Jakobsen and Pelham, 1988). For our assay, we generated two reporter loci: the first was engineered with overlapping Hsf1 and Gal4 binding sites before a minimal promoter driving *GFP* (Figure 3.6H), and the second construct was similar except the Hsf1 binding sites were mutated without disrupting the Gal4 binding motif and this second promoter drives expression of *RFP* (Figure 3.6I). Tight binding of inactive Hsf1 to the *GFP* promoter should decrease the accessibility of the of the Gal4 binding site versus the *RFP* promoter which has non-functional Hsf1 binding sites, thus changes in the amount of Hsf1 binding can be indirectly detected by changes in expression of Gfp versus Rfp driven via the Gal4 binding site (Figure 3.6J). Rather than activating expression of our reporter genes with Gal4 by growing cells on galactose, we used a chimeric artificial transcription factor consisting of the Gal4 DNA binding domain fused to the human estrogen receptor and the Msn2 transcriptional activation domain (referred to as GEM) (Pincus et al., 2014). Expression of

Gal4 targets by GEM is regulated by the hormone β-estradiol independent of nutrient conditions. In the absence of β-estradiol GEM is constitutively expressed but sequestered in the cytoplasm, however β-estradiol causes a dose-dependent relocalization of GEM from the cytoplasm to the nucleus where it drives expression of genes with Gal4 binding sites in their promoter. In cells expressing our reporter constructs and GEM, changes in Hsf1 DNA binding should alter the ratio of Gfp-to-Rfp expression as a function of β-estradiol concentration. For example, in the complete absence of Hsf1 binding, both promoters should be equally accessible to GEM and therefor the relative expression of Gfp and Rfp should be similar across a range of β-estradiol concentrations (Figure 3.6J). However if Hsf1 is inactive but competent for DNA binding, competition between Hsf1 and GEM for binding to the *GFP* promoter, but not the *RFP* promoter*,* should cause a relative attenuation of Gfp versus Rfp expression that will be exacerbated by tighter Hsf1 binding, especially at low β-estradiol concentrations (Figure 3.6J).

To test the effect of Pka inhibition on Hsf1 DNA binding using our reporter assay, we pretreated *PKAas* cells with the Pka inhibitor for 3 hours, followed by a 90-minute β-estradiol titration and then flow cytometry analysis. We also concurrently analyzed mock-pretreated cells as a control for unperturbed Hsf1 binding, as well as Hsf1-AA cells treated with rapamycin—which causes Hsf1 to be exported from the nucleus into the cytoplasm—as a no Hsf1 binding control. Consistent with our expectation, the dose response relationship between the Gfp/Rfp ratio and β-estradiol concentration differed dramatically between mock and Hsf1 AA samples. While the maximal Gfp/Rfp ratio was

similar, the absence of Hsf1 binding after Hsf1 AA was associated with a nearly constant Gfp/Rfp ratio over a 1000-fold range of β-estradiol, which contrasted with the dose-dependent increase in the ratio when Hsf1 binding was unperturbed (Figure 3.6K). We found that Pka inhibition caused an overall decrease in both Gfp and Rfp expression—consistent with previous observations that Pka inhibition causes an overall decrease in protein synthesis (Smith, 1998). However the range of Gfp/Rfp ratios was similar to the control samples, which suggested that the change in protein synthesis affected expression of both reporters equally (Figure 3.6K). Comparison of changes to the Gfp/Rfp ratio as a function of β-estradiol concentration for cells pretreated with the Pka inhibitor versus the two controls clearly showed that the dose-response profile was similar to mock pretreatment (Figure 3.6K). These results further argue that Pka inhibition does not cause a decrease in Hsf1 DNA binding.

Reactivation of Hsf1 targets in the presence of the GSR by an engineered Hsf1 chimera.

In addition to excluding diminished Hsf1 DNA binding as a mechanism for Hsf1 inactivation by the GSR, our DNA binding assay also showed that GEM could stimulated transcription at our engineered GFP reporter locus under conditions where Hsf1 cannot. Since GEM drives transcription using the Msn2 activation domain, we wondered if we could reactivate expression of Hsf1 targets in the presence of the GSR by replacing the endogenous Hsf1 activation domains with the Msn2 activation domain. Previous work has shown that expression of chimera containing the Hsf1 DNA binding domain fused to a

viral transcriptional activator results in constitutive expression of Hsf1 targets (Bonner et al., 1992). Thus, we replaced the Gal4 DNA binding domain in our GEM construct with the Hsf1 DNA binding domain to generate a β-estradiol-regulated Hsf1 chimera we referred to as HEM. To test if HEM could drive expression of Hsf1 targets, we first constitutively expressed it in addition to the wild type copy of Hsf1 in a strain with the Hsf1 fluorescent reporter. We found that β-estradiol treatment of cells expressing HEM, but not a control chimera lacking the Hsf1 DNA binding domain, stimulated dose-dependent expression of the Hsf1 reporter under basal conditions, and when cells were treated with AZC causing concomitant activation of HEM and endogenous Hsf1 (Figure 3.7A). To test if endogenous Hsf1 was required for HEM to up-regulate reporter expression, we introduced the chimera in the Hsf1-AA background and pretreated cells with rapamycin for 3 hours before adding β-estradiol. Inducing export of endogenous Hsf1 from the nucleus by anchor away did not compromise activation of the reporter after β-estradiol treatment in cells expressing HEM even in the presence of AZC (Figure 3.7A). Finally, we tested whether our Hsf1 chimera could activate the Hsf1 reporter in the presence of the GSR. After pretreating *PKAas* cells expressing HEM with the Pka inhibitor for 3 hours, we observed that a 90-minute β-estradiol treatment induced the Hsf1 reporter to a similar level as mock-pretreated cells (Figure 3.7A). Thus, replacing the endogenous Hsf1 activation domains with the Msn2 activation domain enables activation of Hsf1 targets independent of Pka inhibition. Also, they further suggest that the Hsf1 DNA binding domain in the HEM chimera remains functional after Pka inhibition, supporting a model in which the GSR attenuates Hsf1 transcriptional activation rather than DNA binding.

Genetic bypass of Hsf1 inactivation by the GSR.

Previous studies of Hsf1 have identified a number of Hsf1 mutants that are constitutively active under basal conditions. While we already established for the HEM chimera that repression of Hsf1 by the GSR could be bypassed by replacing its activation domains, we wondered if these constitutively active mutants could bypass inhibition by the GSR without the dramatic reengineering of the chimera (Figure 3.7B). Surprisingly, in our hands, F256S Hsf1 was not constitutively active but, strikingly, it remained responsive to heat after engineered GSR activation. In contrast, the N-terminal truncation mutant *HSF1(147-833)* was constitutively active, as expected, but remained sensitive to Msn2/4-mediated inhibition. These results provide genetic evidence for a defined mechanism of Hsf1 inhibition by engineered GSR activation that can be bypassed by mutation of a single residue.

Figure 3.7: Inactivation of Hsf1 by the GSR can be bypassed using an engineered Hsf1 chimera and the *HSF1(F256S)* mutant.
(A) *Hsf1-AA PKAas* cells expressing the indicated chimeras were pretreated with the Pka inhibitor, rapamycin or mock (carrier-only) control for 180' at 30°C. Following pretreatment, cells were incubated with the indicated concentration of β-estradiol concomitant with addition of 1mM AZC or carrier-only (unstressed) for 90' at 30°C and then analyzed by flow cytometry. Plots show the median Hsf1 reporter fluorescence from ~10,000 cells analyzed in each condition normalized to the median value from cells expressing the ER-Msn2AD chimera after mock-pretreatment, and no β-estradiol, no AZC treatment. **(B)** The indicated Hsf1 alleles were introduced in place of the endodgenous copy of Hsf1. Cells were grown at 25°C with either 20nM β -estradiol to induce Msn2* expression and activate the GSR (or 0nM control) for 180'. After pretreatment, cells were shifted to 39°C, or maintained at 25°C for 60'. Hsf1 reporter activity was monitored in three biological replicates per allele and activity was normalized to the mean of the wild type Hsf1 allele at 25°C without β-estradiol. Error bars are mean -/+ SD. **(C)** Time course analysis of the Hsf1 reporter in cells expressing wild type *HSF1* and *HSF1(F256S)* after transferring cells from 30°C to 39°C, as described in the Figure 3 legend. **(D)** Rate of change for Hsf1 reporter fluorescence data from (C) as a function of time after temperature increase, as described in the Figure 3.3 legend.

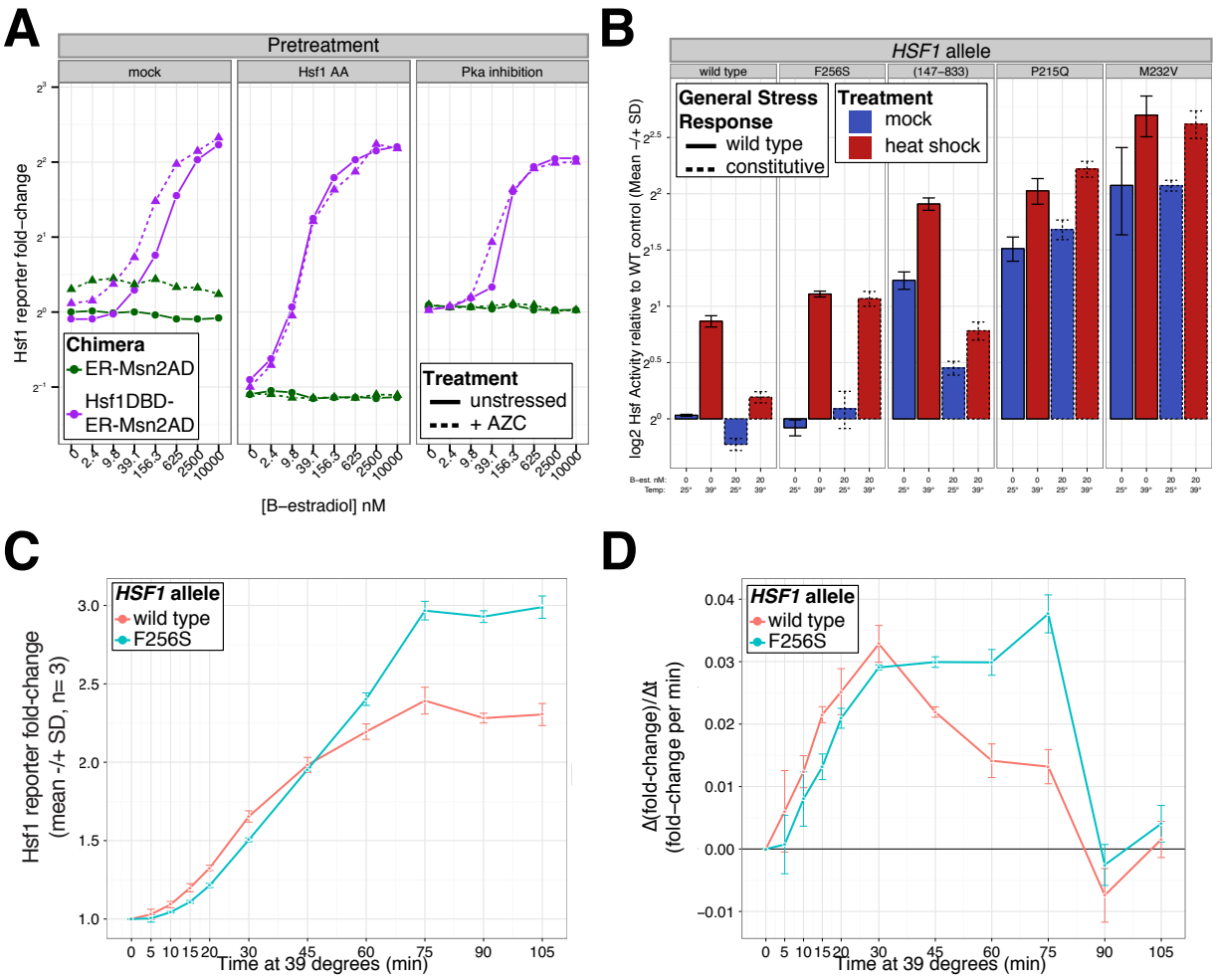

Figure 3.7: (Continued)

We noted that without engineered GSR activation, heat shock caused a modest increase in Hsf1 reporter induction by the F256S mutant compared to wild type Hsf1 (Figure 3.7B). As our previous experiments suggested that the GSR also attenuates Hsf1 activity during heat shock, we sought to test if the kinetics of Hsf1 F256S activity during heat shock differed from wild type. Time course analysis of the Hsf1 F256S confirmed that heat shock induced greater increase in reporter expression than the wild type (Figure 3.7C). We found that acute activation of the reporter immediately after temperature increase was similar for wild type and F256S cells (Figure 3.7D). However, the F256S mutant maintained its peak activity for ~45 minutes before attenuating, in contrast to the wild type whose activity progressively attenuated immediately after reaching its peak (Figure 3.7D). These results support the notion that a common mechanism mediates repression of Hsf1 by chronic and acute activation of the GSR, as a single mutation can genetically bypass them both.

Discussion

A common phenotype associated with cell senescence is the accumulation of intracellular protein aggregates (Balch et al., 2008). In contrast, young cells robustly fold proteins even following conditions of folding stress. This is enabled by a variety of protein homeostasis pathways that adjust the cellular folding capacity according to need. For example, thermal stress activates the heat shock transcription factor (Hsf) to up-regulate heat shock proteins (HSPs), including protein folding chaperones, which counteract protein unfolding at elevated temperatures. In contrast, thermal stress fails to robustly activate Hsf in aged

worms and mammalian cells (Heydari et al., 2000; Kern et al., 2010b). Together with numerous findings that genetic enhancement of Hsf function enables lifespan extension (Baird et al., 2014; Hsu et al., 2003), these observations hint at the existence of a direct mechanistic link between longevity and protein folding homeostasis.

Here we showed that yeast heat shock factor (Hsf1) is rendered uninducible by heat stress during replicative aging and investigated the underlying mechanism. Using a suite of classic and chemical genetic tools, we revealed that age-associated inactivation of Hsf1 is due to activation of the general stress response (GSR), a distinct stress pathway, in old cells. Further, we showed that engineering GSR activation in young cells was sufficient to inhibit Hsf1 inducibility, which could be genetically bypassed by a single Hsf1 mutation or with an engineered Hsf1 chimera. However, a number of key questions are still outstanding and should be addressed in the future. First and foremost, it needs to be determined whether restoring Hsf1 function in old cells is sufficient to extend lifespan. In addition to the tools that we developed in this study to bypass inhibition of Hsf1 by the GSR, our previous work showed that the essential function of Hsf1 in yeast can be complemented by engineering Hsf1-independent expression of a small set of its target genes (see Chapter 2). If these tools for reactivating Hsf1 function in old cells enable lifespan extension in yeast, similar tools will need to be developed to test whether this strategy can be applied to extend lifespan in other organisms. A more modest question is whether reactivation of Hsf1 can suppress the accumulation of protein aggregates during replicative aging. One potential scenario is that restoring Hsf1 in old cells causes ablation

of age-induced aggregates, but has no effect on lifespan. This would argue that protein aggregates are akin to human wrinkles—a superficial consequence of aging and not one of its causes. Such a clear demonstration that cell aging is not a result of protein aggregation would motivate a refocusing on other potential senescence factors, such as age-induced nucleolar (Guarente, 1997) or mitochondrial (Veatch et al., 2009) damage.

Our work also revealed that antagonism of Hsf1 by the GSR is not confined to old cells. Rather, the complete inhibition of Hsf1 in old cells appears to be an extreme consequence of a regulatory mechanism that attenuates Hsf1 function during stresses that also activate the GSR in young cells. However, the physiological consequences of inhibition of Hsf1 by GSR remain to be elucidated. Our genome wide analysis in this and previous work have shown that the GSR comprises the vast majority of the heat shock response, while Hsf1 drives overexpression of less than 20 genes during heat shock. Thus, it is tempting to assume that the GSR simply obviates the need for expression Hsf1 targets. However, our attempts to support this model by complementing Hsf1 loss-of-function with the GSR have not been successful (data not shown), although it is possible that this negative result is due to technical rather than biological issues. Comparing the relative fitness and stress sensitivity of the wild type and *HSF1(F256S)* mutant, which is resistant to inhibition by the GSR, under a range of environmental and genetic perturbations should yield insight into the physiological consequences of Hsf1 inactivation by the GSR.

Finally, while we were unable to pinpoint the exact mechanism of Hsf1 inactivation by the GSR, our work provides some insight into Hsf1 regulation. Phosphorylation of Hsf1 has long been suggested as a key mechanism for regulating Hsf1 activity (Wu, 1995), however our work strongly argues that phosphorylation is dispensable for Hsf1 function in general and for inactivation by the GSR. While we noted a clear correlation between Hsf1 hyperphosphorylation and low levels of Hsf1 activity, we found all but one S/T residue in Hsf1 could be simultaneously mutated to alanine without compromising Hsf1 function. Additionally, while Pka inhibition is sufficient to cause Hsf1 inhibition and hyperphosphorylation, we found that the *HSF1(152A)* mutant with only one potential phosphorylation site remained sensitive to inhibition under these conditions. Further, our data argue against phosphorylation of the one essential serine residue as a mechanism for Hsf1 inactivation, since phosphorylation of S225 would ablate Hsf1 DNA binding and we did not detect any change in Hsf1 binding in the presence of the GSR by multiple assays. Rather, we suspect that the GSR compromises Hsf1 transcriptional activation, since a chimera containing the Hsf1 DNA binding domain and the activation domain from Msn2 was able to drive Hsf1 reporter expression in the presence of the GSR. Subsequent analysis of the effect of the GSR on constitutively active Hsf1 mutants revealed that while *HSF1(F256S)* was not constitutively active in our hands, this point mutant bypassed inhibition by the GSR. Interestingly, we found that the constitutively active N-terminal truncation mutant *HSF1(147-833)* was constitutively active under basal conditions, but acutely sensitive to inhibition by the GSR. This raises the possibility that distinct mechanisms mediate repression of Hsf1 activity under basal conditions and in the

presence of the GSR. As chaperone binding, in particular by Hsp70, has also been proposed as a mechanism for Hsf1 inactivation, future biochemical analysis should explore changes in Hsf1 protein-protein interactions that are modified by the GSR and the F256S mutation to explore this as a potential mechanism of inactivation.

References

Aguilaniu, H., Gustafsson, L., Rigoulet, M., and Nyström, T. (2003). Asymmetric inheritance of oxidatively damaged proteins during cytokinesis. Science *299*, 1751–1753.

Akerfelt, M., Morimoto, R.I., and Sistonen, L. (2010). Heat shock factors: integrators of cell stress, development and lifespan. Nat Rev Mol Cell Biol *11*, 545–555.

Anckar, J., and Sistonen, L. (2011). Regulation of HSF1 function in the heat stress response: implications in aging and disease. Annu Rev Biochem *80*, 1089–1115.

Anfinsen, C.B. (1973). Principles that govern the folding of protein chains. Science *181*, 223–230.

Baird, N.A., Douglas, P.M., Simic, M.S., Grant, A.R., Moresco, J.J., Wolff, S.C., Yates, J.R.I., Manning, G., and Dillin, A. (2014). HSF-1-mediated cytoskeletal integrity determines thermotolerance and life span. Science *346*, 360–363.

Balch, W., Morimoto, R., and Dillin, A. (2008). Adapting Proteostasis for Disease Intervention. Science.

Ben-Zvi, A., Miller, E.A., and Morimoto, R.I. (2009). Collapse of proteostasis represents an early molecular event in Caenorhabditis elegans aging. Proc Natl Acad Sci USA *106*, 14914–14919.

Bishop, A.C., Ubersax, J.A., Petsch, D.T., Matheos, D.P., Gray, N.S., Blethrow, J., Shimizu, E., Tsien, J.Z., Schultz, P.G., Rose, M.D., et al. (2000). A chemical switch for inhibitor-sensitive alleles of any protein kinase. Nature *407*, 395–401.

Bonner, J.J., Heyward, S., and Fackenthal, D.L. (1992). Temperature-dependent regulation of a heterologous transcriptional activation domain fused to yeast heat shock transcription factor. Mol Cell Biol *12*, 1021–1030.

Brandman, O., Stewart-Ornstein, J., Wong, D., Larson, A., Williams, C.C., Li, G.-W., Zhou, S., King, D., Shen, P.S., Weibezahn, J., et al. (2012). A ribosome-bound quality control complex triggers degradation of nascent peptides and signals translation stress. Cell *151*, 1042–1054.

Buchberger, A., Bukau, B., and Sommer, T. (2010). Protein quality control in the cytosol and the endoplasmic reticulum: brothers in arms. Mol Cell *40*, 238–252.

Chiti, F., and Dobson, C. (2006). Protein misfolding, functional amyloid, and human disease. Annu Rev Biochem.

Colombo, S., Ronchetti, D., Thevelein, J.M., Winderickx, J., and Martegani, E. (2004). Activation state of the Ras2 protein and glucose-induced signaling in Saccharomyces cerevisiae. Journal of Biological Chemistry *279*, 46715–46722.

de Godoy, L.M.F., Olsen, J.V., Cox, J., Nielsen, M.L., Hubner, N.C., Fröhlich, F., Walther, T.C., and Mann, M. (2008). Comprehensive mass-spectrometry-based proteome quantification of haploid versus diploid yeast. Nature *455*, 1251–1254.

Dobson, C. (2003). Protein folding and misfolding. Nature.

Erjavec, N., Larsson, L., Grantham, J., and Nyström, T. (2007). Accelerated aging and failure to segregate damaged proteins in Sir2 mutants can be suppressed by overproducing the protein aggregation-remodeling factor Hsp104p. Genes & Development *21*, 2410–2421.

Gasch, A.P., Spellman, P.T., Kao, C.M., Carmel-Harel, O., Eisen, M.B., Storz, G., Botstein, D., and Brown, P.O. (2000). Genomic expression programs in the response of yeast cells to environmental changes. Mol Biol Cell *11*, 4241–4257.

Geiler-Samerotte, K.A., Dion, M.F., Budnik, B.A., Wang, S.M., Hartl, D.L., and Drummond, D.A. (2011). Misfolded proteins impose a dosage-dependent fitness cost and trigger a cytosolic unfolded protein response in yeast. Proc Natl Acad Sci USA *108*, 680–685.

Guarente, L. (1997). Link between aging and the nucleolus. Genes & Development *11*, 2449–2455.

Hao, N., and O'Shea, E.K. (2012). Signal-dependent dynamics of transcription factor translocation controls gene expression. Nat. Struct. Mol. Biol. *19*, 31–39.

Hao, N., Budnik, B.A., Gunawardena, J., and O'Shea, E.K. (2013). Tunable signal processing through modular control of transcription factor translocation. Science *339*, 460–464.

Harrison, C.J., Bohm, A.A., and Nelson, H.C. (1994). Crystal structure of the DNA binding domain of the heat shock transcription factor. Science *263*, 224–227.

Hartwell, L.H., and Unger, M.W. (1977). Unequal division in Saccharomyces cerevisiae and its implications for the control of cell division. The Journal of Cell Biology *75*, 422–435.

Henderson, K.A., and Gottschling, D.E. (2008). A mother's sacrifice: what is she keeping for herself? Curr. Opin. Cell Biol. *20*, 723–728.

Heydari, A.R., You, S., Takahashi, R., Gutsmann-Conrad, A., Sarge, K.D., and Richardson, A. (2000). Age-related alterations in the activation of heat shock transcription factor 1 in rat hepatocytes. Exp. Cell Res. *256*, 83–93.

Hsu, A.-L., Murphy, C.T., and Kenyon, C. (2003). Regulation of aging and age-related disease by DAF-16 and heat-shock factor. Science *300*, 1142–1145.

Hubl, S.T., Owens, J.C., and Nelson, H.C. (1994). Mutational analysis of the DNA-binding domain of yeast heat shock transcription factor. Nat. Struct Biol. *1*, 615–620.

Jacquet, M., Renault, G., Lallet, S., De Mey, J., and Goldbeter, A. (2003). Oscillatory nucleocytoplasmic shuttling of the general stress response transcriptional activators Msn2 and Msn4 in Saccharomyces cerevisiae. The Journal of Cell Biology *161*, 497–505.

Jakobsen, B.K., and Pelham, H.R. (1988). Constitutive binding of yeast heat shock factor to DNA in vivo. Mol Cell Biol *8*, 5040–5042.

Kennedy, B.K., and McCormick, M.A. (2011). Asymmetric segregation: the shape of things to come? Curr Biol *21*, R149–R151.

Kern, A., Ackermann, B., Clement, A.M., Duerk, H., and Behl, C. (2010a). HSF1-controlled and age-associated chaperone capacity in neurons and muscle cells of C. elegans. PLoS ONE *5*, e8568.

Kern, A., Ackermann, B., Clement, A.M., Duerk, H., and Behl, C. (2010b). HSF1-Controlled and Age-Associated Chaperone Capacity in Neurons and Muscle Cells of C. elegans. PLoS ONE *5*, e8568.

Lindner, A., and Demarez, A. (2009). Protein aggregation as a paradigm of aging. Biochimica Et Biophysica Acta (BBA)-General … 980–996.

Lindstrom, D.L., and Gottschling, D.E. (2009). The Mother Enrichment Program: A

Genetic System for Facile Replicative Life Span Analysis in Saccharomyces cerevisiae. Genetics *183*, 413–422.

McIsaac, R.S., Oakes, B.L., Wang, X., Dummit, K.A., Botstein, D., and Noyes, M.B. (2013). Synthetic gene expression perturbation systems with rapid, tunable, single-gene specificity in yeast. Nucleic Acids Research *41*, e57.

Olzscha, H., Schermann, S.M., Woerner, A.C., Pinkert, S., Hecht, M.H., Tartaglia, G.G., Vendruscolo, M., Hayer-Hartl, M., Hartl, F.U., and Vabulas, R.M. (2011). Amyloid-like aggregates sequester numerous metastable proteins with essential cellular functions. Cell *144*, 67–78.

Park, J.-I., Grant, C.M., and Dawes, I.W. (2005). The high-affinity cAMP phosphodiesterase of Saccharomyces cerevisiae is the major determinant of cAMP levels in stationary phase: involvement of different branches of the Ras-cyclic AMP pathway in stress responses. Biochem. Biophys. Res. Commun. *327*, 311–319.

Pincus, D., Aranda-Díaz, A., Zuleta, I.A., Walter, P., and El-Samad, H. (2014). Delayed Ras/PKA signaling augments the unfolded protein response. Proc Natl Acad Sci USA *111*, 14800–14805.

Pirkkala, L., Nykanen, P., and Sistonen, L. (2001). Roles of the heat shock transcription factors in regulation of the heat shock response and beyond. The FASEB Journal *15*, 1118–1131.

Richter, K., Haslbeck, M., and Buchner, J. (2010). The Heat Shock Response: Life on the Verge of Death. Mol Cell *40*, 253–266.

Sarge, K.D., Murphy, S.P., and Morimoto, R.I. (1993). Activation of heat shock gene transcription by heat shock factor 1 involves oligomerization, acquisition of DNA-binding activity, and nuclear localization and can occur in the absence of stress. Mol Cell Biol *13*, 1392–1407.

Schmitt, A.P., and McEntee, K. (1996). Msn2p, a zinc finger DNA-binding protein, is the transcriptional activator of the multistress response in Saccharomyces cerevisiae. Proc Natl Acad Sci USA *93*, 5777–5782.

Smith, A. (1998). Yeast PKA represses Msn2p/Msn4p-dependent gene expression to regulate growth, stress response and glycogen accumulation. Embo J *17*, 3556–3564.

Smith, A., Ward, M.P., and Garrett, S. (1998). Yeast PKA represses Msn2p/Msn4p-dependent gene expression to regulate growth, stress response and glycogen accumulation. Embo J *17*, 3556–3564.

Sorger, P.K., and Pelham, H.R. (1987). Purification and characterization of a heat-shock element binding protein from yeast. Embo J *6*, 3035–3041.

Trotter, E.W., Kao, C.M.-F., Berenfeld, L., Botstein, D., Petsko, G.A., and Gray, J.V. (2002). Misfolded proteins are competent to mediate a subset of the responses to heat shock in Saccharomyces cerevisiae. Journal of Biological Chemistry *277*, 44817–44825.

Tyedmers, J., Mogk, A., and Bukau, B. (2010). Cellular strategies for controlling protein aggregation. Nat Rev Mol Cell Biol *11*, 777–788.

Veatch, J.R., McMurray, M.A., Nelson, Z.W., and Gottschling, D.E. (2009). Mitochondrial dysfunction leads to nuclear genome instability via an iron-sulfur cluster defect. Cell *137*, 1247–1258.

Wu, C. (1995). Heat Shock Transcription Factors: Structure and Regulation. Annu. Rev. Cell Dev. Biol. *11*, 441–469.

Xie, Z., Zhang, Y., Zou, K., Brandman, O., Luo, C., Ouyang, Q., and Li, H. (2012). Molecular phenotyping of aging in single yeast cells using a novel microfluidic device. Aging Cell *11*, 599–606.

Zaremberg, V., and Moreno, S. (1996). Analysis of the Mechanism of Activation of cAMP-Dependent Protein Kinase Through the Study of Mutants of the Yeast Regulatory Subunit. Eur J Biochem *237*, 136–142.

Chapter 4: Future directions

In addition to the potential future studies described in the discussions of Chapter 2 and 3, our work raises a number of interesting questions regarding how Hsf has been deployed differently in yeast, mammalian cells and cancer. We pose a number of these questions below along with experimental strategies to explore them.

Our analysis clearly demonstrates that genes encoding HSPs are highly expressed in unstressed yeast and mammalian cells. In Chapter 2, we revealed that constitutive expression of HSPs in yeast is a housekeeping function assigned to Hsf1, but in mammals a distinct transcription factor, or factors, maintain HSF1-independent expression of HSPs in unstressed cells. However, in both heat shocked yeast and mammalian cells, the role of Hsf appears to be limited to driving over-expression of a similar set of HSPs, with Hsp40, Hsp70 and Hsp90 as conserved core target genes. These results raise an obvious question: Why has the role of Hsf in basal chaperone expression diverged between yeast and mammalian cells? While the precise answer is likely extremely complex, the difference clearly must be derived from the distinct evolutionary pressures that have shaped yeast and mammalian physiology. While viability of both organisms requires a sufficient supply of chaperones to maintain protein folding in diverse environment conditions, we propose a set of hypothesis and experiments to explore how differential evolutionary pressures favor distinct chaperone gene expression strategies.

A likely simple model for Hsf function in yeast and mammals is that Hsf drives expression of chaperone genes when the availability of proteostasis factors, in particular the core Hsp40/70/90 chaperones, is insufficient to meet the demand for them. However, different evolutionary selective pressures have lead to distinct utilizations of this core Hsf function. As a unicellular organism in a dynamic environment, yeast must balance countervailing pressures selecting for growth rate and robustness to environmental stresses. On the one hand, a large buffer of excess chaperones beyond their demand under ideal conditions will likely be advantageous if cells must subsequently adapt to an acute environmental change that cause the folding environment to rapidly deteriorate. However, this robustness comes with the constant cost of excess resources that must be expended to synthesize the chaperone buffer, which should confer a fitness disadvantage in terms of division rate under ideal conditions versus less well-prepared members of the population. Under this model, our strain of lab yeast appears to have balanced these two forces by tightly matching expression of Hsf1 targets to their need in the absence of stress, but also tasking Hsf1 with rapidly increasing HSP expression following stress. In support of this notion, an engineered increase in expression of Hsf1 targets in unstressed cells containing our synHDG plasmids is associated with a decrease in endogenous Hsf1 activity (see Chapter 2). Conversely, deletion of the genes encoding constitutively expressed Hsp40, Hsp70 and Hsp90 chaperones (*YDJ1*, *SSA2* and *HSC82*, respectively) causes a similar increase in Hsf1 activity in unstressed cells to heat shocked wild type cells (Brandman et al., 2012). These observations suggest that the evolutionary forces

that shaped chaperone expression in *Saccharomyces cerevisiae* favored a quick response to stress over a large buffer, however we propose that different environmental conditions could favor a strategy biased towards preparation versus a rapid response to stress.

The relative strength of the selective pressure for robustness to future stress versus the growth rate of unstressed cells likely varies as a function of the frequency, duration and magnitude of acute stress conditions, as well as the rate at which conditions degenerate. While it makes intuitive sense that an increase in stress frequency, duration, magnitude or rate of onset would increase the fitness benefit of a chaperone buffer, a more quantitative analysis of these effects alone and in combination could dramatically increase our understanding of how these features of periodic environmental stress could influence stress response evolution. A straightforward experimental approach to this problem is to perform competitive fitness assays between wild type yeast and cells constitutively expressing synHDGs above their endogenous levels under conditions that fluctuate between stressful and ideal. Cells expressing high levels of synHDGs should be more fit in conditions of periodic stress that favor a chaperone buffer, while the wild type cells should be favored under conditions where growth rate under ideal conditions dominates.

In contrast to yeast, mammalian cells exist in a multicellular organism with auto-regulated temperature and thus their environment should be generally stable. Further, unlike the competition for growth rate that unicellular yeast experience during evolution, the function

of multi-cellular tissues depends on the homogeneous function and fitness of the cells that comprise it. While the growth environment of mammalian cells is stable, stochastic protein misfolding within individual cells will induce heterogeneity in the intracellular folding environments of isogenic cells. If chaperone levels were closely matched to demand, random misfolding and subsequent activation of Hsf1 in response to it could lead to fitness variations between cells compromising tissue homogeneity. Thus, one possible explanation for the high level of HSF1-independent chaperone expression in mammalian cells is to create a chaperone buffer that dampens variability between cells in a tissue caused by random protein misfolding. To test this notion, one experimental approach is to engineer a chaperone buffer in yeast by expressing synHDGs to varying degrees above their endogenous levels and measure the fitness distribution across a clonal population using a recently developed high-throughput technique based on deep-sequencing of genetically encoded cell barcodes (Levy et al., 2015). If random fluctuations in the protein-folding environment between cells are a major driver of fitness variation, then variability should decrease as the chaperone buffer increases. However, one limitation of this approach is that fitness differences due to inherent genetic heterogeneity in the population could dominate fitness differences due to the chaperone buffer. In this case, fitness changes due to protein misfolding could be amplified by inducing a low-level of proteotoxic stress by culturing cells in the presence of a low concentration of the proline analog AZC that is insufficient to strongly induce Hsf1 activity (Trotter et al., 2002). An alternative approach would be to engineer expression of a misfolding mutant protein that has previously been demonstrated to cause a dose-

dependent decrease in fitness and induced expression of many Hsf1 target genes (Geiler-Samerotte et al., 2011). Using this system, we would expect that synHDG expression would generate a chaperone buffer that should rescue the fitness defect and Hsf1 activation induced by low expression levels for the misfolding mutant protein. However, higher levels of mutant expression should deplete the chaperone buffer, leading to concomitant Hsf1 activation and the reappearance of the fitness defect.

Finally, one prediction of the mammalian chaperone buffer model is that an engineered decrease in constitutive chaperone expression should cause mammalian HSF1 to become activated in unstressed cells. However, a large-scale RNA interference screen to identify modifiers of HSF1 activity in unstressed human cells found that surprisingly knock-down of many constitutively expressed chaperones did not induce HSF1 activity (Raychaudhuri et al., 2014). This is in stark contrast to the strong induction of Hsf1 activity in yeast associated with deletion of genes encoding constitutively expressed Hsp40, Hsp70 or Hsp90 chaperones (Brandman et al., 2012). Assuming that there were no technical issues in the mammalian study and that expression of these factors was indeed reduced, this could be cited as evidence against a mammalian chaperone buffer, or suggesting that HSF1 requires additional signals other than diminished Hsp40/70/90 levels to become activated. However, as we observed high levels of constitutive expression for multiple functionally redundant paralogs encoding members of each major chaperone family, it is possible that knock-down of any single paralog is insufficient to deplete the cumulative chaperone buffer induced by expression of all paralogous

chaperones. As the CRISPRi strategy can be used to simultaneously reduce expression of multiple genes (Qi et al., 2013), this approach should be used to test the effect on HSF1 basal activity of perturbing expression of multiple chaperone genes in combination.

While HSF1 is not essential in wild type mammalian cells, transformation during carcinogenesis is associated with a gain of yeast-like dependence on HSF1 for proliferation in the absence of stress. What changes when mammalian cells are transformed that renders viability HSF1-dependent? Previous studies favor two possibilities: One suggest that HSF1 function is expanded and its targets are diversified to include non-proteostasis factors in cancer cells and that these novel targets are the source of HSF1's essential function in cancer (Mendillo et al., 2012). Alternatively, other experiments demonstrate that cancer cells have an increased sensitivity to proteotoxic stress and suggest that the demand for proteostasis factors in unstressed cancer cells is very high, thus requiring constitutive HSF1 activity to drive sufficient chaperone expression to prevent proteotoxic collapse (Tang et al., 2015). It is also possible that both models are correct, and cancer cells require both cancer-specific HSF1 targets and proteostasis factors also regulated by HSF1 in stressed untransformed cells.

We favor first directly testing the model in which cancer cells have an increased demand for HSF1-dependent proteostasis factors. We are motivated by both our results defining the essential function of Hsf1 in yeast, and other experiments that suggest that the effects of diminished HSF1 function in cancer cells expressing an anti-HSF1 RNA-aptamer can

be rescued by Hsp70 or Hsp90 expression (Salamanca et al., 2014). The aforementioned CRISPRi strategy should also be amenable to testing whether the critical housekeeping role for HSF1 in mammalian cancers is confined to expression of the proteostasis factors we defined in untransformed cells. The 9 HSF1 targets we defined in our heat shock analysis should be tested to determine if they are individually or in combination essential for cancer cell proliferation. If they are essential, a similar CRISPR-based tool for ectopic activation of multiple genes in mammalian cells (Konermann et al., 2015) should be used to test whether engineered expression of these HSF1 targets is sufficient to rescue the proliferation of transformed *hsf1*$^{-/-}$ cells.

If the results of experiments focused on the heat shock targets of HSF1 suggest that the essential function in cancer extends beyond HSP expression, we favor a systematic analysis of HSF1-dependent gene expression in transformed cells similar to our yeast analysis. Rather than using the anchor away technique that we used in yeast (Haruki et al., 2008), we propose using a conditional degradation system that has been previously established for small-molecule mediated degradation of HSF1 mutants expressed in mammalian cells on top of endogenous HSF1 (Moore et al., 2016; Ryno et al., 2014). Using this approach, introducing wild type HSF1 fused a “destabilized domain” (DD) into our *hsf1*$^{-/-}$ cell lines will allow the HSF1-DD fusion to be degraded when a small molecule is removed from the culture media (Shoulders et al., 2013). After transforming *hsf1*$^{-/-}$ *HSF1-DD* cells into cancer cells by expression of previously defined oncogenes that induce HSF1-dependent cancers (Dai et al., 2007), NET- and RNA-seq analysis can be

used to define the immediate changes in gene expression that follow induced HSF1 degradation. Once the cancer-specific targets of HSF1 have been established by this loss-of-function analysis, similar experiments to those described above can be used to define the necessary and sufficient targets that are required for cancer cell proliferation.

These experiments should help reveal how distinct evolutionary pressures in yeast and mammalian cells, as well as in transformed cancer cells, have shaped and modified Hsf function.

References

Brandman, O., Stewart-Ornstein, J., Wong, D., Larson, A., Williams, C.C., Li, G.-W., Zhou, S., King, D., Shen, P.S., Weibezahn, J., et al. (2012). A ribosome-bound quality control complex triggers degradation of nascent peptides and signals translation stress. Cell *151*, 1042–1054.

Dai, C., Whitesell, L., Rogers, A.B., and Lindquist, S. (2007). Heat Shock Factor 1 Is a Powerful Multifaceted Modifier of Carcinogenesis. Cell *130*, 1005–1018.

Geiler-Samerotte, K.A., Dion, M.F., Budnik, B.A., Wang, S.M., Hartl, D.L., and Drummond, D.A. (2011). Misfolded proteins impose a dosage-dependent fitness cost and trigger a cytosolic unfolded protein response in yeast. Proc Natl Acad Sci USA *108*, 680–685.

Haruki, H., Nishikawa, J., and Laemmli, U.K. (2008). The Anchor-Away Technique: Rapid, Conditional Establishment of Yeast Mutant Phenotypes. Mol Cell *31*, 925–932.

Konermann, S., Brigham, M.D., Trevino, A.E., Joung, J., Abudayyeh, O.O., Barcena, C., Hsu, P.D., Habib, N., Gootenberg, J.S., Nishimasu, H., et al. (2015). Genome-scale transcriptional activation by an engineered CRISPR-Cas9 complex. Nature *517*, 583–U332.

Levy, S.F., Blundell, J.R., Venkataram, S., Petrov, D.A., Fisher, D.S., and Sherlock, G. (2015). Quantitative evolutionary dynamics using high-resolution lineage tracking. Nature *519*, 181–186.

Mendillo, M.L., Santagata, S., Koeva, M., Bell, G.W., Hu, R., Tamimi, R.M., Fraenkel, E., Ince, T.A., Whitesell, L., and Lindquist, S. (2012). HSF1 Drives a Transcriptional Program Distinct from Heat Shock to Support Highly Malignant Human Cancers. Cell *150*, 549–562.

Moore, C.L., Dewal, M.B., Nekongo, E.E., Santiago, S., Lu, N.B., Levine, S.S., and Shoulders, M.D. (2016). Transportable, Chemical Genetic Methodology for the Small Molecule-Mediated Inhibition of Heat Shock Factor 1. ACS Chem. Biol. *11*, 200–210.

Qi, L.S., Larson, M.H., Gilbert, L.A., Doudna, J.A., Weissman, J.S., Arkin, A.P., and Lim, W.A. (2013). Repurposing CRISPR as an RNA-Guided Platform for Sequence-Specific Control of Gene Expression. Cell *152*, 1173–1183.

Raychaudhuri, S., Loew, C., Körner, R., Pinkert, S., Theis, M., Hayer-Hartl, M., Buchholz, F., and Hartl, F.U. (2014). Interplay of Acetyltransferase EP300 and the Proteasome System in Regulating Heat Shock Transcription Factor 1. Cell *156*, 975–985.

Ryno, L.M., Genereux, J.C., Naito, T., Morimoto, R.I., Powers, E.T., Shoulders, M.D., and Wiseman, R.L. (2014). Characterizing the altered cellular proteome induced by the stress-independent activation of heat shock factor 1. ACS Chem. Biol. *9*, 1273–1283.

Salamanca, H.H., Antonyak, M.A., Cerione, R.A., Shi, H., and Lis, J.T. (2014). Inhibiting Heat Shock Factor 1 in Human Cancer Cells with a Potent RNA Aptamer. PLoS ONE *9*, e96330.

Shoulders, M.D., Ryno, L.M., Cooley, C.B., Kelly, J.W., and Wiseman, R.L. (2013). Broadly applicable methodology for the rapid and dosable small molecule-mediated regulation of transcription factors in human cells. J. Am. Chem. Soc. *135*, 8129–8132.

Tang, Z., Dai, S., He, Y., Doty, R.A., Shultz, L.D., Sampson, S.B., and Dai, C. (2015). MEK Guards Proteome Stability and Inhibits Tumor-Suppressive Amyloidogenesis via HSF1. Cell *160*, 729–744.

Trotter, E.W., Kao, C.M.-F., Berenfeld, L., Botstein, D., Petsko, G.A., and Gray, J.V. (2002). Misfolded proteins are competent to mediate a subset of the responses to heat shock in Saccharomyces cerevisiae. Journal of Biological Chemistry *277*, 44817–44825.

Appendix: Supplementary figures and tables for Chapter 2

Figure S2.1: Validation of Hsf1 Anchor Away as a tool for acute Hsf1 inactivation. **(A)** Representative images from confocal micrograph time sequences of Hsf1-AA cells with endogenous Hsf1-FRB-GFP treated with rapamycin at 30°C or left untreated for the indicated times. **(B)** Hsf1-AA cells with indicated plasmids and Hsf1 reporter - GFP expressed from a minimal promoter containing four engineered Hsf1-binding sites and mKate (RFP) expressed from the *TEF2* promoter - were grown logarithmically at 30°C prior to pre-treatment with rapamycin (10' at 30°C) or mock pre-treatment. This was followed by heat shock (39°C for 30') or control treatment (30°C) and, finally, cells were analyzed by flow cytometry. Shown are cell plots of Hsf1 reporter activity, which we defined as the $\log_2$ ratio of GFP to RFP fluorescence normalized to the median fluorescence of cells with empty vector after mock pre-treatment and control treatment. **(C)** Rapamycin-resistant *TOR1-1, fpr1* cells with indicated plasmids and endogenous untagged Hsf1 and Rpl13A or C-terminally tagged with FRB and FKBP12, respectively and as indicated, were spotted onto rapamycin or mock (carrier-only) plates. Shown are images of plates incubated at 30°C for 3 days. **(D)** Representative images from a epifluorescence micrograph time sequence of Hsf1-AA cells with endogenous Hsf1-FRB-GFP and Hsp104-RFP treated with rapamycin at 30°C for the indicated times. Arrows point at cells that lysed between adjacent time points.

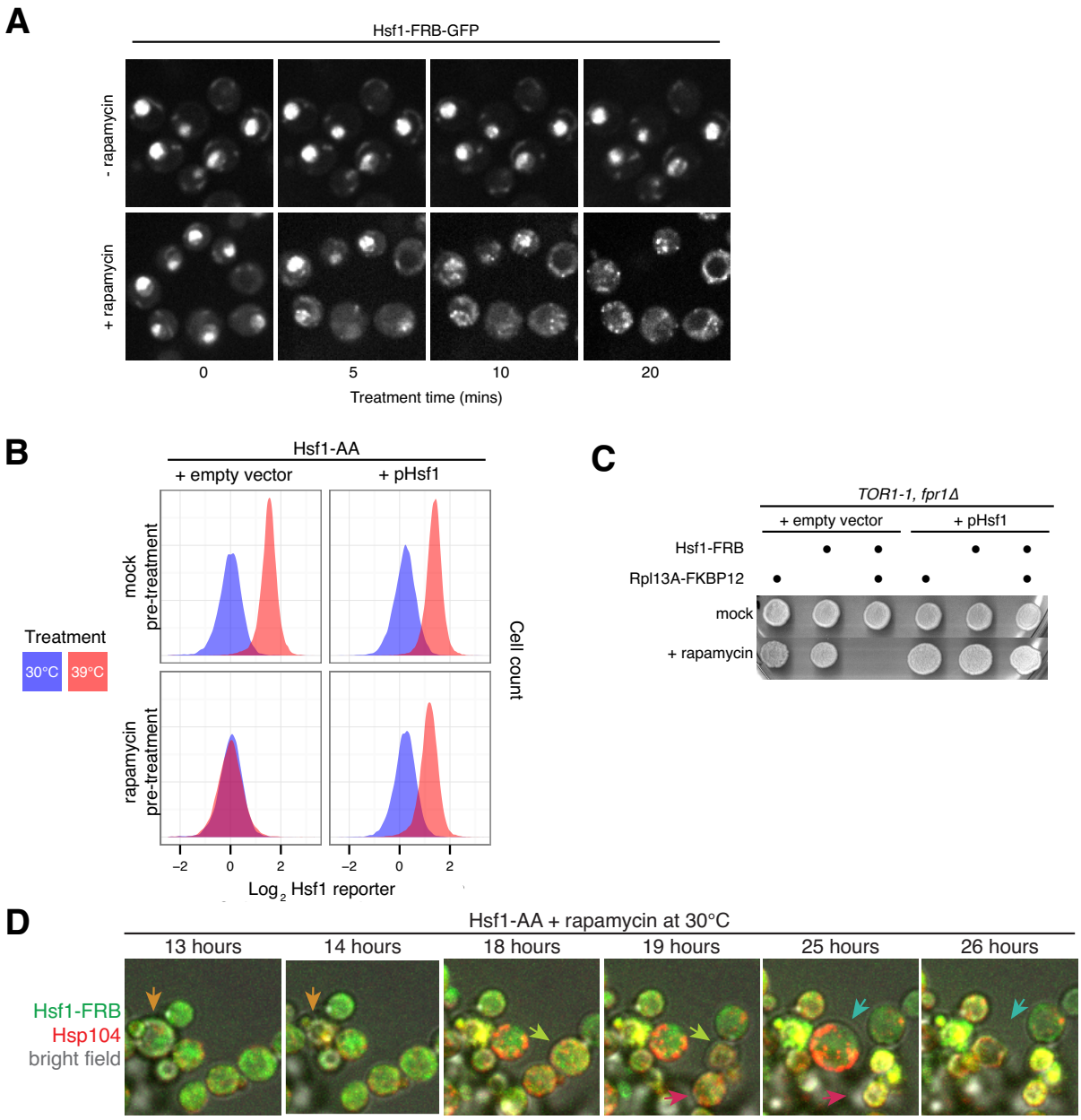

Figure S2.1: (Continued)

Figure S2.2: Defining Hsf1 targets by statistical analyses of Hsf1 promoter binding and transcription/mRNA changes induced by Hsf1 Anchor Away.

(A) Hsf1-AA cells growing logarithmically at 30°C were analyzed NET-seq immediately prior to and after 15', 30' and 60' of rapamycin treatment. Shown are gene scatter plots comparing transcription (log_2 read fragments per-kilobase per million reads, or FPKM) between adjacent time points (Left: control vs. 15'; Middle: 15' vs. 30'; Right: 30' vs. 60'). Genes defined as significantly different between control and 15' time points ($p < 10^{-4}$) are indicated in blue with 95% confidence intervals (error bars) in all three panels. Global summary statistics (top left in each panel) were computed based on transcription changes for each detected gene. **(B)** Hsf1-AA cells growing logarithmically at 30°C (control), and after treatment with rapamycin for 60', were analyzed by RNA-seq. Left: Gene ranking by mRNA abundance change induced by treatment. Genes below and above the 1st and 99th percentiles (dashed lines), respectively, were defined as significantly Hsf1-dependent. Genes defined by NET-seq analysis were color-coded blue if they were also defined by RNA-seq analysis and red if they were not. Right: Gene histogram of fold-changes induced by treatment. **(C)** Time-course of HDG transcription changes induced by rapamycin treatment at 30°C. **(D)** Gene scatter plot of transcription versus mRNA changes induced by treatment with rapamycin for 15' and 60', respectively. Linear regression fits and R^2 values are shown for genes with significant changes by NET-seq and RNA-seq, NET-seq alone, or neither, as defined by statistical tests described in Experimental Procedures. **(E)** CDF of 95% confidence interval widths for transcription of HDGs or all other genes based on NET-seq analysis of indicated samples. For each data set, the y-axis corresponds to the proportion of HDGs or all other genes with a 95% C.I. width less than or equal to the x-axis value. P-values are for the Wilcoxon rank-sum test for equal C.I. width distributions between HDGs and all other genes. ns: not significant. **(F)** CDF of standard deviations of transcription for HDGs or all other genes based on NET-seq analysis of indicated samples. The y-axis corresponds to the proportion of HDGs or all other genes with a standard deviation (SD) less than or equal to the x-axis value. P-values are for the Wilcoxon rank-sum test for equal distributions of SDs for HDGs and other genes for the same condition. **(G)** Gene scatter plot of standard deviation (SD) of transcription measurements (log_2 FPKM) for each gene after rapamycin treatment (for 15', 30' and 60') versus transcription of that gene (log_2 FPKM) in untreated cells. HDGs are indicated in blue and a local smoothed regression fit for all genes is in black. Marginal histograms for SDs and transcription of all genes are right and above, respectively. **(H)** Hsf1-FLAG-V5 cells growing logarithmically at 30°C were analyzed by ChIP-seq. Shown are distributions of ChIP-seq reads at the HDG loci. **(I)** Gene scatter plot comparing Hsf1 target transcriptional decline (defined by NET-seq fold-change after 15' rapamycin treatment relative to control for Hsf1-AA cells) with Hsf1 binding to target promoters (defined by ChIP-seq analysis of Hsf1-FLAG-V5 cells). HDGs are shown in blue, while the remaining Hsf1 targets defined by ChIP-seq are gray. Linear regression and R^2 values for each gene set are indicated. **(J)** Bioinformatic analysis of Hsf1 targets defined by ChIP-seq, NET-seq and RNA-seq, individually or the intersection of genes defined by the indicated combinations of techniques. The height of the solid bars

Figure S2.2: (Continued)

indicates the number of genes with the given annotation (GO term or promoter motif), while the height of dashed bars indicates the number of remaining genes lacking the annotation. The fill color indicates the significance of the enrichment for the annotated Hsf1 targets versus other genes (p-values for GO terms are corrected for multiple testing using the Holm–Bonferroni method). If no bar is shown for a given GO term in a particular technique category, it was not significantly enriched for Hsf1 targets (p-value > .1).

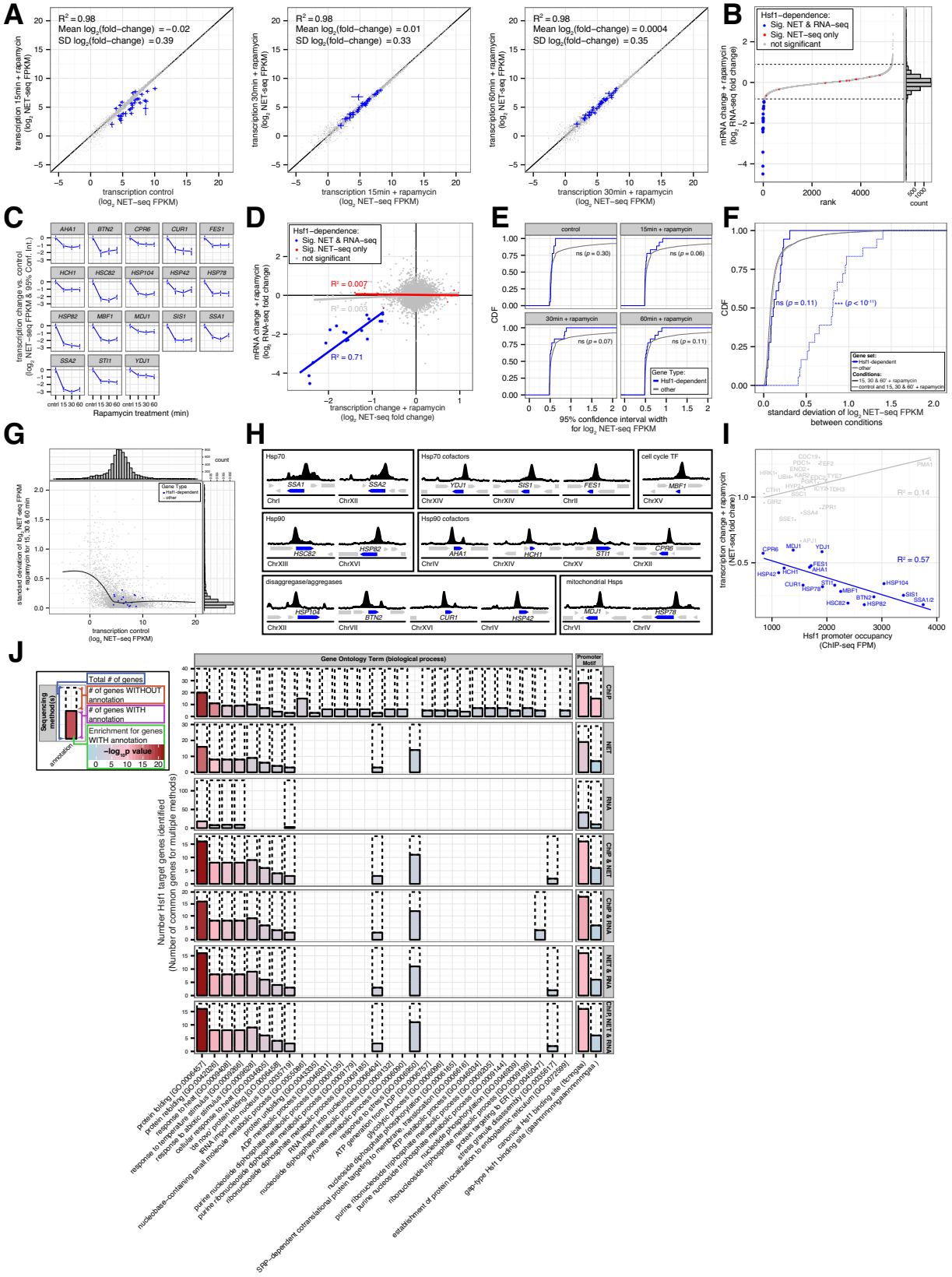

Figure S2.2: (Continued)

Figure S2.3: Msn2/4 gene targets are induced by prolonged Hsf1 inactivation, heat shock, and PKA inhibition by chemical genetics.
(A) Hsf1-AA cells were grown logarithmically at 30°C were treated with rapamycin for 60' and 240' then analyzed by RNA-seq. Left: Gene ranking by mRNA abundance change induced by treatment. Genes above the dashed line have a >4-fold increase in mRNA abundance. HDGs are indicated in blue. Right: Gene histogram of fold-changes induced by treatment. **(B)** Bioinformatic analysis of genes with > 4-fold increase in mRNA abundance induced by prolonged rapamycin treatment. Bar lengths indicate the significance level of their enrichment for the given annotation (GO term or promoter motif) (p-values for GO terms corrected for multiple testing using the Holm–Bonferroni method). **(C)** Left: HDG promoter locations of Hsf1 and Msn2/4 binding sites as in Figure 3B. Right: Hsf1-AA cells grown logarithmically at 30°C were treated with rapamycin for 60' or 240' prior to harvesting for RNA-seq analysis. Shown are HDG mRNA changes induced by prolonged rapamycin treatment. **(D)** Gene scatter plot comparing mRNA changes induced by PKA inhibition (see Figure 3D) versus prolonged rapamycin treatment (see Figure 3A). Msn2/4 targets were defined as genes with at least one Msn2/4 promoter binding site (AGGGG) that were in the top 10% of genes induced by PKA inhibition. **(E)** PKAas and PKAas *Δmsn2 Δmsn4* cells were grown logarithmically at 30°C (control) or treated with 1-NM-PP1 (120' at 30°C) prior to harvesting for RNA-seq analysis. Shown is a gene scatter plot of mRNA changes induced by PKA inhibition in each strain relative to PKAas control. **(F)** Cumulative distribution function (CDF) of mRNA abundance fold-changes induced by PKA inhibition in PKAas *Δmsn2 Δmsn4* versus PKAas cells in part (E). For each of the three gene types indicated, the y-axis corresponds to the proportion of genes within a gene type with fold-change ratios less than or equal to the corresponding value on the x-axis. P-values are for the Wilcoxon rank-sum test for equal distributions of fold-changes for the indicated gene type versus the distribution of changes for the other two types combined. **(G)** Venn diagram comparing Hsf1 target genes defined by ChIP-seq analysis of Hsf1-FLAG-V5 cells under basal (30°C) and heat shock (39°C) conditions. The names of previously defined HDGs are emphasized. **(H)** Representative confocal micrographs of PKAas cells expressing plasmid-borne mCherry-ubc9^{ts} after treatment with PKA inhibitor (1-NM-PP1) or mock (carrier-only) for 180' at 30°C. **(I)** CDF of mRNA abundance fold-changes induced by PKA inhibition after rapamycin pretreatment versus mock pretreatment in Figure 3E. For each gene set, the y-axis corresponds to the proportion of genes within a gene type with fold-change ratios less than or equal to the corresponding value on the x-axis. P-values are for the Wilcoxon rank-sum test for equal distributions of fold-changes for the indicated gene type versus the distribution of changes for the other gene types combined. **(J)** Hsf1-AA cells were pretreated with rapamycin or carrier-only (for 15' or 30' at 30°C) and then heat shock (30' at 39°C) prior to harvesting for analysis by NET-seq and RNA-seq. Shown is a gene scatter plot of transcription versus mRNA changes after heat shock induced by pre-treatment with rapamycin for 15' and 30', respectively, relative carrier pretreatment control. Colors denote gene sets and large points correspond to genes with significantly decreased transcription and mRNA abundance, as described in Experimental Procedures. **(K)** Bioinformatic analysis of

Figure S2.3: (Continued)

genes with significant decreases in heat shock transcription and mRNA abundance due to rapamycin treatment in part (J), for all significant genes (left), or other type genes (significant genes that are not HDGs, *SSA3/4*, ribosomal protein genes or Sfp1 targets), see Supplementary Discussion for details. Solid bars show the number of heat shock (HS) HDGs genes with the given annotation (GO term or promoter motif) and dashed bars show the number of remaining genes. The fill color indicates the significance level for the enrichment of the annotated HS HDGs versus all genes (p-values for GO terms are corrected for multiple testing using the Holm–Bonferroni method). Note: The CCAGC motif corresponds to the binding sites for Hac1, Swi5, and Ace2. **(L)** CDF of mRNA abundance fold-changes induced by heat shock after rapamycin pretreatment versus mock pretreatment in part (J). For each gene set, the y-axis corresponds to the proportion of genes in the set with fold-change ratios less than or equal to the corresponding value on the x-axis. P-values are for the Wilcoxon rank-sum test for equal distributions of fold-changes for that gene set versus the distribution of changes for the other gene types combined.

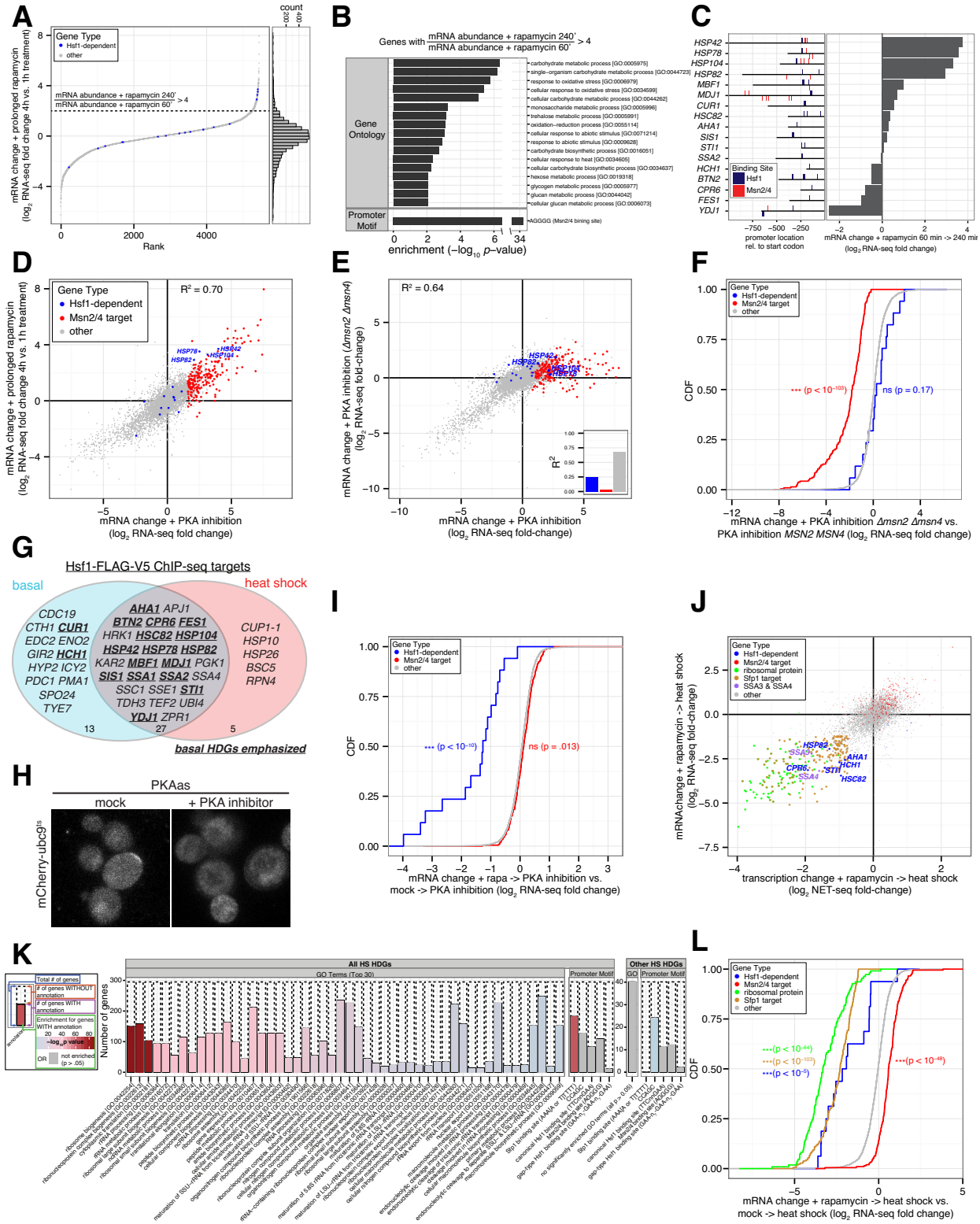

Figure S2.3: (Continued)

Figure S2.4: Validation of loss of HSF1 expression in *hsf1*$^{-/-}$ MEFs and mESCs, and analysis of HDG expression dependence on HSF1 and HSF2.
(A) Left: Whole cell lysates prepared from indicated MEFs were resolved by SDS-PAGE and analyzed by Western blotting (WB) with anti-Hsf1 and anti-ACT (Actin) antibodies**.** Right: Indicated MEFs were analyzed by immunofluorescence (IF) with anti-HSF1 antibody (red) and co-strained with DAPI (blue). **(B)** Indicated mESCs were analyzed as in (A), but with additional actin IF staining (green). **(C)** Wild-type (WT) and *hsf1*$^{-/-}$ knock out (KO) MEFs and mESCs were cultured at 37°C prior to harvesting for RNA-seq analysis. Shown is a gene scatter plot of mRNA abundances WT and KO cells for each cell type. Dark lines indicate statistical thresholds used to define genes with significant changes in expression (see Experimental Procedures) and genes with significant changes in both cell types are colored. Also indicated are gene names of HSF1-dependent genes (HDGs) defined by additional experiments and analyses (see Figures 4A-C and Experimental Procedures). **(D)** Wild-type (WT), *hsf1*$^{-/-}$, *hsf2*$^{-/-}$ and *hsf1*$^{-/-}$ *hsf2*$^{-/-}$ MEFs were cultured at 37°C and analyzed by RNA-seq. Shown is a gene scatter plot of mRNA abundances in each knock out line against the common wildtype. Dark lines indicate statistical thresholds used to define genes with significant changes in expression (see Experimental Procedures). HDGs are colored pink with only the names of HDGs with significant changes indicated. **(E)** CDF of $\log_2$ mRNA abundance differences between measured and expected KO gene expression, the latter being derived from a linear regression fit of the median KO mRNA abundance onto wild type mRNA abundance using data from (D). For each mutant, the y-axis corresponds to the proportion of genes in the set with an mRNA abundance difference less than or equal to the corresponding value on the x-axis. P-values are for the Wilcoxon rank-sum test for equal distributions of differences for HDGs versus all other genes.

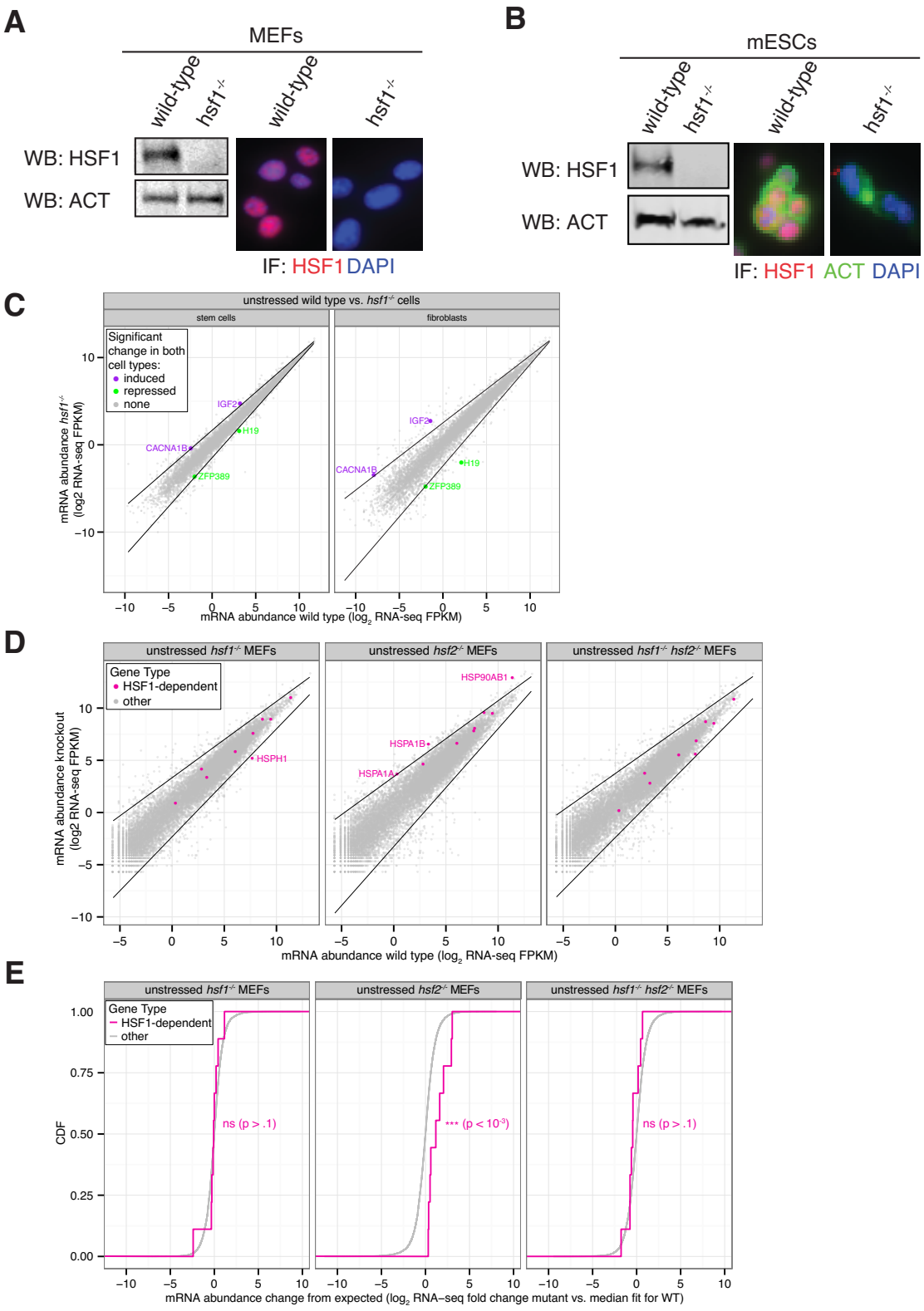

Figure S2.4: (Continued)

Figure S2.5: Defining the minimal synthetic transcriptional program that bypasses Hsf1's essential function.

(A) ORF and promoter annotation of four synHDG expression plasmids used in this study. Each plasmid is low-copy plasmid in yeast and carries a unique marker gene. **(B)** Hsf1-AA cells with Hsf1 reporter and indicated plasmids were grown logarithmically at 30°C prior to flow cytometry analysis. Shown are cell plots of Hsf1 reporter activity (see Supplementary Figure 1B for details). **(C)** Hsf1-AA cells expressing plasmid-borne mCherry-ubc9^{ts} and indicated plasmids were treated with rapamycin for indicated times at 30°C and imaged by epifluorescence microscopy. Blinded images containing at least 100 cells were scored for cells containing either 0/1-2/3+ mCherry foci and the fraction of scored cells plotted. **(D)** Top: Addition of the drug 5-FOA to *Δhsf1 ura3*$^{-}$ with *URA3*-marked *HSF1* expression plasmid kills URA^{+} cells to enable selection of cells that have spontaneously lost the *URA3*-marked plasmid. Bottom: *hsf1Δ* cells carrying a *URA3*-marked Hsf1 expression plasmid plus non-*URA3* marked expression plasmids for 15synHDGs (plasmids A-D in Figure S4A) or Hsf1 were spotted onto 5-FOA or mock plates. Shown are images of plates incubated for 3 days at 30°C. **(E)** *hsf1Δ* cells carrying expression plasmids for 15synHDGs or Hsf1 were logarithmically grown at 30°C prior to harvesting for RNA-seq analysis. Left: Gene ranking of mRNA abundance fold-changes for *Δhsf1* cells expressing plasmid-borne 15synHDGs versus Hsf1. Bioinformatic analysis of non-HDGs in the top and bottom 1% of fold-changes are indicated. Right: Gene histogram of fold-changes for all genes. **(F)** Hsf1-AA cells transformed with indicated plasmid combinations of four synHDG plasmids (plasmids A-D in Figure S4A) and four corresponding empty vectors (-) were spotted onto rapamycin or mock (carrier-only) control plates. Shown are images of plates incubated for 3 days at 30°C. **(G)** Hsf1-AA cells transformed with indicated plasmid combinations (plasmids with individual HDGs deleted are described in the Experimental Procedures) were spotted onto rapamycin or mock (carrier-only) plates. Shown are images of plates incubated for 3 days at 30°C. **(H)** Representative epifluorescence micrographs of Hsf1-AA cells expressing plasmid-borne mCherry-ubc9^{ts} and indicated synHsps or empty control were treated with β-estradiol (30') to induce Hsp expression followed by treatment with rapamycin (7 hours). Blinded images containing at least 100 cells were scored for cells containing indicated number of mCherry foci. Percentage of scored cells is shown below micrographs. **(G)** Hsf1-AA cells expressing indicated transgenes were spotted at two concentrations onto rapamycin or mock (carrier-only) plates, which also contained β-estradiol to drive synHsp expression from β-estradiol-dependent promoters (see Experimental Procedures for details). Shown are images of plates incubated at 37°C for 5 days.

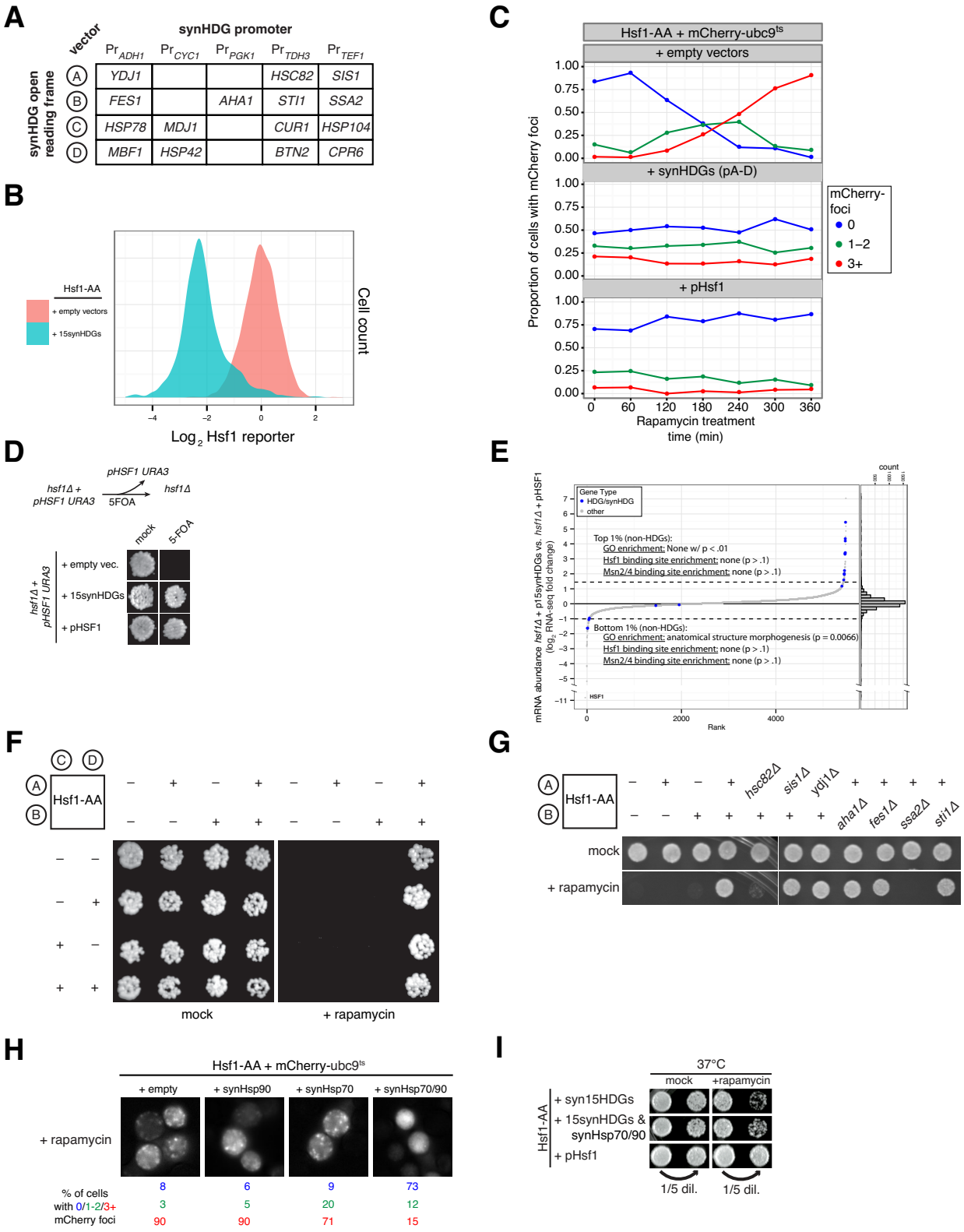

Figure S2.5: (Continued)

Table S2.1: List of strains and cell lines used.

Yeast Strain	Genotype
W303	*leu2-3,112 trp1-1 can1-100 ura3-1 ade2-1 his3-11,15*
VDY1667	W303 *MATα TPK1/2/3/as TOR1-1(S1972I)fpr1Δ::NATMXPr$_{TEF2}$-mKATE2–URA3–4xHSE-Pr$_{CYC1}$-EmGFP RPL13A-2xFKBP12–TRP1*
VDY1852	W303 *MATα TPK1/2/3/as TOR1-1(S1972I) fpr1Δ::NATMX Pr$_{TEF2}$-mKATE2–URA3–4xHSE-Pr$_{CYC1}$-EmGFP RPL13A-2xFKBP12–TRP1 HSF1-FRB–HIS3MX6*
VDY1853	W303 *MATα TPK1/2/3/as TOR1-1(S1972I) fpr1Δ::NATMX Pr$_{TEF2}$-mKATE2–URA3–4xHSE-Pr$_{CYC1}$-EmGFP HSF1-FRB–HIS3MX6*
VDY1874	W303 *MATα TPK1/2/3/as TOR1-1(S1972I)fpr1Δ::NATMX RPL13A-2xFKBP12–TRP1*
VDY1896	W303 *MATα TPK1/2/3/as TOR1-1(S1972I) fpr1Δ::NATMX RPL13A-2xFKBP12–TRP1 HSF1-FRB–HIS3MX6*
VDY1877	W303 *MATα TPK1/2/3/as TOR1-1(S1972I) fpr1Δ::NATMX RPL13A-2xFKBP12–TRP1 HSF1-FRB-GFP–HIS3MX*
VDY2130	W303 *MATα TPK1/2/3/as TOR1-1(S1972I) fpr1Δ::NATMXRPL13A-2xFKBP12–TRP1 HSF1-FRB–HIS3MX HSP104-mCLOVER–KANMX*
VDY2254	W303 *MATα TPK1/2/3/as TOR1-1(S1972I) fpr1Δ::NATMX Pr$_{TEF2}$-mKATE2–URA3–4xHSE-Pr$_{CYC1}$-EmGFP RPL13A-2xFKBP12–TRP1 HSF1-FRB–HIS3MX6RPB3-FLAG–KANMX*
VDY2367	W303 *MATα TPK1/2/3/as TOR1-1(S1972I) fpr1Δ::NATMX Pr$_{TEF2}$-mKATE2–URA3–4xHSE-Pr$_{CYC1}$-EmGFP RPL13A-2xFKBP12–TRP HSF1-FRB–KANMX*
VDY2578	*W303 MATα TPK1/2/3/as TOR1-1(S1972I) fpr1Δ::NATMX ura3-1 RPL13A-2xFKBP12–TRP1 HSF1-FRB–KANMX*
VDY2595	W303 *MATα TPK1/2/3/as TOR1-1(S1972I) fpr1Δ::NATMXPr$_{TEF2}$-mKATE2–ura3-1–4xHSE-Pr$_{CYC1}$-EmGFP RPL13A-2xFKBP12–TRP1HSF1-FRB–KANMX*
VDY2688	W303 *MATa hsf1Δ::KAN HSF1-3xFLAG-V5::TRP1*
VDY466	W303 *MATa TPK1/2/3as ADE2*
VDY488	W303 *MATa TPK1/2/3as ADE2 msn4Δ::TRP1 msn2Δ::NATMX*
DPY813	W303 *MATα TPK1/2/3/as TOR1-1(S1972I) fpr1Δ::NATMX RPL13A-2xFKBP12–TRP1 HSF1-FRB-GFP–HIS3MXPr$_{TDH3}$-NLS-mKate2::LEU2*
mDP1	CBA316 (Immortalized mEFs)
mDP4	ES Cells ES129
mDP10	mEF hsf1-/- (using CRISPR/Cas9) derrived from mDP1
mDP11	mES hsf1-/- (using CRISPR/Cas9) derrived from mDP4

Table S2.1: (Continued)

mDP12	mEF hsf2-/- (using CRISPR/Cas9) derrived from mDP1
mDP13	mEF hsf1-/- hsf2-/- (using CRISPR/Cas9) derrived from mDP10

Table S2.2: Plasmids used in this study.

Plasmids	Construct
pNH605	SfiI – $Pr_{Sc\ LEU2}$ – *Cg LEU2* – multiple cloning site – 3'-$UTR_{Sc\ LEU2}$ – SfiI
pRS412	ADE2 CEN/ARS
pRS413	HIS3 CEN/ARS
pRS415	LEU2 CEN/ARS
pRS416	URA3 CEN/ARS
pVD380	pESC Pr_{GAL1}-mCherry-UBC9wt LEU2
pVD381	pESC Pr_{GAL1}-mCherry-ubc9ts LEU2
pVD476	pRS413 HSF1 (promoter - ORF - 3'-UTR)
pVD565	pRS412 HSF1
pVD570	pRS412 Pr_{ADH1}-YDJ1 (ORF and 3'-UTR) – Pr_{TDH3}-HSC82 (ORF and 3'-UTR) – Pr_{TEF1}-SIS1 (ORF and 3'-UTR)
pVD576	pRS415 Pr_{PGK1}-AHA1 (ORF and 3'-UTR) – Pr_{ADH1}-FES1 (ORF and 3'-UTR) – Pr_{TEF1}-SSA2 (ORF and 3'-UTR) – Pr_{TDH3}-STI1 (ORF and 3'-UTR)
pVD577	pRS412 Pr_{TDH3}-CUR1 (ORF and 3'-UTR) – Pr_{ADH1}-HSP78 (ORF and 3'-UTR) – Pr_{TEF1}-HSP104 (ORF and 3'-UTR) – Pr_{CYC1}-MDJ1 (ORF and 3'-UTR)
pVD578	pRS413 Pr_{TDH3}-BTN2 (ORF and 3'-UTR) – Pr_{TEF1}-CPR6 (ORF and 3'-UTR) – Pr_{CYC1}-HSP42 (ORF and 3'-UTR) – Pr_{ADH1}-MBF1 (ORF and 3'-UTR)
pVD579	pRS412 *ade2Δ::HPHMX*
pVD580	pRS412 *ade2Δ::HPHMX* Pr_{ADH1}-YDJ1 (ORF and 3'-UTR) – Pr_{TDH3}-HSC82 (ORF and 3'-UTR) – Pr_{TEF1}-SIS1 (ORF and 3'-UTR)
pVD632	pESC Pr_{GAL1}-mCherry-ubc9ts URA3
pVD783	pRS416 Pr_{ACT1}-Z_4EV-$term_{ADH1}$ – 6xZ_4BS-Pr_{CYC1}-$term_{ADH1}$
pVD784	pRS416 Pr_{ACT1}-Z_4EV-$term_{ADH1}$ – 6xZ_4BS-Pr_{CYC1}-*SSA2* (ORF and 3'-UTR)-$term_{ADH1}$
pVD785	pRS416 Pr_{ACT1}-Z_4EV-$term_{ADH1}$ – 6xZ_4BS-Pr_{CYC1}-*HSC82* (ORF and 3'-UTR)-$term_{ADH1}$
pVD786	pRS416 6xZ_4BS-PrCYC1-HSC82 (ORF and 3'-UTR) – Pr_{ACT1}-Z_4EV-$term_{ADH1}$ – 6xZ_4BS-Pr_{CYC1}-*SSA2* (ORF and 3'-UTR)-$term_{ADH1}$
pVD787	pVD570 *hsc82Δ::URA3*
pVD788	pVD570 *sis1Δ::URA3*
pVD789	pVD570 *ydj1Δ::URA3*
pVD790	pVD576 *aha1Δ::URA3*
pVD791	pVD576 *fes1Δ::URA3*

Table S2.2: (Continued)

pVD792	pVD576 *ssa2Δ::URA3*
pVD793	pVD576 *sti1Δ::URA3*
pVD794	pNH605 Pr_{ACT1}-Z_4EV-$term_{ADH1}$ – 6xZ_4BS-Pr_{CYC1}-$term_{ADH1}$
pVD795	pNH605 Pr_{ACT1}-Z_4EV-$term_{ADH1}$ – 6xZ_4BS-Pr_{CYC1}-*HSC82* (ORF and 3'-UTR)-$term_{ADH1}$
pVD796	pNH605 Pr_{ACT1}-Z_4EV-$term_{ADH1}$ – 6xZ_4BS-Pr_{CYC1}-*SSA2* (ORF and 3'-UTR)-$term_{ADH1}$
pVD797	pNH605 6xZ_4BS-PrCYC1-HSC82 (ORF and 3'-UTR) – Pr_{ACT1}-Z_4EV-$term_{ADH1}$ – 6xZ_4BS-Pr_{CYC1}-*SSA2* (ORF and 3'-UTR)-$term_{ADH1}$
pVD902	pRS306 Pr_{ADH1}-Gal4 DBD-ER-Msn2 AD-$term_{ADH1}$ – $Pr_{Hsf1\&Gal4}$-*GFP*-$term_{ACT1}$ – Pr_{Gal4}-*mKATE2*-$term_{ADH1}$